

# TECHNISCHE UNIVERSITÄT DRESDEN

## Resource Allocation in Underlay and Overlay Spectrum Sharing

Jing Lv

geboren am 21. April 1985

von der Fakultät Elektrotechnik und Informationstechnik der Technischen  
Universität Dresden

zur Erlangung des akademischen Grades eines

Doktoringenieurs

(Dr.-Ing.)

genehmigte Dissertation

Vorsitzender: Prof. Dr.-Ing. habil. Leon Urbas

Gutachter: Prof. Dr.-Ing. Eduard A. Jorswieck

Gutachter: Prof. Dr.-Ing. habil. Tobias Weber

Tag der Einreichung: 13. Oktober 2014

Tag der Verteidigung: 16. Dezember 2014



*To my parents*



# Zusammenfassung

Aufgrund der rasanten Entwicklung im Bereich der drahtlosen Kommunikation und der ständig steigenden Nachfrage nach mobilen Anwendungen ist die Knappheit von Frequenzbändern ein entscheidender Engpass, der die Einführung neuer Funktechnologien behindert. Die gemeinsame Benutzung von Frequenzen (Spektrum-Sharing) durch primäre und sekundäre Nutzer ist eine Möglichkeit, die Effizienz bei der Verwendung des Spektrums zu verbessern.

Bei der Methode des Underlay-Spektrum-Sharing sendet der sekundäre Nutzer zeitgleich mit dem primären Nutzer unter der Einschränkung, dass für den primären Nutzer die erzeugte Interferenz unterhalb eines Schwellwertes liegt oder gewisse Anforderungen an die Datenrate erfüllt werden. In diesem Zusammenhang wird in der Arbeit insbesondere die Koexistenz von Mehrantennensystemen untersucht. Dabei wird für die primäre Funkverbindung der Fall mit mehreren Sendeantennen und einer Empfangsantenne (MISO) angenommen. Für die sekundäre Funkverbindung werden mehrere Sendeantennen und sowohl eine als auch mehrere Empfangsantennen (MISO/MIMO) betrachtet. Der primäre Sender verwendet Maximum-Ratio-Transmission (MRT) und der primäre Empfänger Einzelnutzerdecodierung. Für den sekundären Nutzer werden außerdem am Sender eine Datenratenaufteilung (rate splitting) und am Empfänger entweder eine sukzessive Decodierung – sofern sinnvoll – oder andernfalls eine Einzelnutzerdecodierung verwendet.

Im Unterschied zur Methode des Underlay-Spektrum-Sharing kann der sekundäre Nutzer beim Verfahren des Overlay-Spektrum-Sharing die Kenntnis über die Nachrichten des primären Nutzers einsetzen, um die Übertragung sowohl der eigenen als auch der primären Nachrichten zu unterstützen. Das Wissen über die Nachrichten erhält er entweder nicht-kausal, d.h. vor der Übertragung, oder kausal, d.h. während der ersten Phase einer zweistufigen Übertragung. In der Arbeit wird speziell die Koexistenz von primären MISO-Funkverbindungen und sekundären MISO/MIMO-Funkverbindungen untersucht. Bei nicht-kausaler Kenntnis über die primären Nachrichten kann der sekundäre Sender beispielsweise das Verfahren der Dirty-Paper-Codierung (DPC) verwenden, welches es ermöglicht, die Interferenz durch die primären Nachrichten bei der Decodierung der

sekundären Nachrichten am sekundären Empfänger aufzuheben. Da die Implementierung der DPC mit einer hohen Komplexität verbunden ist, kommt als Alternative auch eine lineare Vorcodierung zum Einsatz. In beiden Fällen verwendet der primäre Transmitter MRT und der primäre Empfänger Einzelnutzerdecodierung. Besitzt der sekundäre Nutzer keine nicht-kausale Kenntnis über die primären Nachrichten, so kann er als Gegenleistung für die Mitbenutzung des Spektrums dennoch die Übertragung der primären Nachrichten unterstützen. Hierfür leitet er die primären Nachrichten mit Hilfe der Amplify-And-Forward-Methode oder der Decode-And-Forward-Methode in einer zweistufigen Übertragung weiter, währenddessen er seine eigenen Nachrichten sendet. Der primäre Nutzer passt seine Sendestrategie entsprechend an und kooperiert mit dem sekundären Nutzer, um die Anforderungen an die Datenrate zu erfüllen.

Nicht nur das Spektrum sondern auch die Sendeleistung ist eine wichtige Ressource. Daher wird zusätzlich zur Effizienz bei der Verwendung des Spektrums auch die Energieeffizienz (EE) einer sekundären MIMO-Funkverbindung für das Underlay-Spektrum-Sharing-Verfahren analysiert. Wie zuvor wird für den sekundären Nutzer am Sender eine Datenratenaufteilung (rate splitting) und am Empfänger entweder eine sukzessive Decodierung oder eine Einzelnutzerdecodierung betrachtet. Weiterhin wird die EE einer sekundären MIMO-Funkverbindung für das Overlay-Spektrum-Sharing-Verfahren untersucht. Dabei nutzt der sekundäre Nutzer die nicht-kausale Kenntnis über die primären Nachrichten aus, um mittels DPC eine interferenzfreie sekundäre Funkverbindung zu erhalten.

# Abstract

As the wireless communication technologies evolve and the demand of wireless services increases, spectrum scarcity becomes a bottleneck that limits the introduction of new technologies and services. Spectrum sharing between primary and secondary users has been brought up to improve spectrum efficiency.

In underlay spectrum sharing, the secondary user transmits simultaneously with the primary user, under the constraint that the interference induced at the primary receiver is below a certain threshold, or a certain primary rate requirement has to be satisfied. Specifically, in this thesis, the coexistence of a multiple-input single-output (MISO) primary link and a MISO/multiple-input multiple-output (MIMO) secondary link is studied. The primary transmitter employs maximum ratio transmission (MRT), and single-user decoding is deployed at the primary receiver. Three scenarios are investigated, in terms of the interference from the primary transmitter to the secondary receiver, namely, weak interference, strong interference and very strong interference, or equivalently three ranges of primary rate requirement. Rate splitting and successive decoding are deployed at the secondary transmitter and receiver, respectively, when it is feasible, and otherwise single-user decoding is deployed at the secondary receiver. For each scenario, optimal beamforming/precoding and power allocation at the secondary transmitter is derived, to maximize the achievable secondary rate while satisfying the primary rate requirement and the secondary power constraint. Numerical results show that rate splitting at the secondary transmitter and successive decoding at the secondary receiver does significantly increase the achievable secondary rate if feasible, compared with single-user decoding at the secondary receiver.

In overlay spectrum sharing, different from underlay spectrum sharing, the secondary transmitter can utilize the knowledge of the primary message, which is acquired non-causally (i.e., known in advance before transmission) or causally (i.e., acquired in the first phase of a two-phase transmission), to help transmit the primary message besides its own message. Specifically, the coexistence of a MISO primary link and a MISO/MIMO secondary link is studied. When the secondary transmitter has non-causal knowledge of the primary message, dirty-paper coding (DPC) can be deployed at the secondary

transmitter to precancel the interference (when decoding the secondary message at the secondary receiver), due to the transmission of the primary message from both transmitters. Alternatively, due to the high implementation complexity of DPC, linear precoding can be deployed at the secondary transmitter. In both cases, the primary transmitter employs MRT, and single-user decoding is deployed at the primary receiver; optimal beamforming/precoding and power allocation at the secondary transmitter is obtained, to maximize the achievable secondary rate while satisfying the primary rate requirement and the secondary power constraint. Numerical results show that with non-causal knowledge of the primary message and the deployment of DPC at the secondary transmitter, overlay spectrum sharing can achieve a significantly higher secondary rate than underlay spectrum sharing, while rate loss occurs with the deployment of linear precoding instead of DPC at the secondary transmitter.

When the secondary transmitter does not have non-causal knowledge of the primary message, and still wants to help with the primary transmission in return for the access to the spectrum, it can relay the primary message in an amplify-and-forward (AF) or a decode-and-forward (DF) way in a two-phase transmission, while transmitting its own message. The primary link adapts its transmission strategy and cooperates with the secondary link to fulfill its rate requirement. To maximize the achievable secondary rate while satisfying the primary rate requirement and the primary and secondary power constraints, in the case of AF cooperative spectrum sharing, optimal relaying matrix and beamforming vector at the secondary transmitter is obtained; in the case of DF cooperative spectrum sharing, a set of parameters are optimized, including time duration of the two phases, primary transmission strategies in the two phases and secondary transmission strategy in the second phase. Numerical results show that with the cooperation from the secondary link, the primary link can avoid outage effectively, especially when the number of antennas at the secondary transceiver is large, while the secondary link can achieve a significant rate.

Power is another precious resource besides spectrum. Instead of spectrum efficiency, energy-efficient spectrum sharing focuses on the energy efficiency (EE) optimization of the secondary transmission. The EE of the secondary transmission is defined as the ratio of the achievable secondary rate and the secondary power consumption, which includes both the transmit power and the circuit power at the secondary transmitter. For simplicity, the circuit power is modeled as a constant. Specifically, the EE of a MIMO secondary link in underlay spectrum sharing is studied. Three transmission strategies are introduced based on the primary rate requirement and the channel conditions. Rate splitting and successive decoding are deployed at the secondary transmitter and receiver,



respectively, when it is feasible, and otherwise single-user decoding is deployed at the secondary receiver. For each case, optimal transmit covariance matrices at the secondary transmitter are obtained, to maximize the EE of the secondary transmission while satisfying the primary rate requirement and the secondary power constraint. Based on this, an energy-efficient resource allocation algorithm is proposed. Numerical results show that MIMO underlay spectrum sharing with EE optimization can achieve a significantly higher EE compared with MIMO underlay spectrum sharing with rate optimization, at certain SNRs and with certain circuit power, at the cost of the achievable secondary rate, while saving the transmit power. With rate splitting at the secondary transmitter and successive decoding at the secondary receiver if feasible, a significantly higher EE can be achieved compared with the case when only single-user decoding is deployed at the secondary receiver.

Moreover, the EE of a MIMO secondary link in overlay spectrum sharing is studied, where the secondary transmitter has non-causal knowledge of the primary message and employs DPC to obtain an interference-free secondary link. Energy-efficient precoding and power allocation is obtained to maximize the EE of the secondary transmission while satisfying the primary rate requirement and the secondary power constraint. Numerical results show that MIMO overlay spectrum sharing with EE optimization can achieve a significantly higher EE compared with MIMO overlay spectrum sharing with rate optimization, at certain SNRs and with certain circuit power, at the cost of the achievable secondary rate, while saving the transmit power. MIMO overlay spectrum sharing with EE optimization can achieve a higher EE compared with MIMO underlay spectrum sharing with EE optimization.



# Acknowledgements

I want to express my gratitude to Professor Eduard Jorswieck for giving me the opportunity to do research under his supervision and explore the world. I thank him for suggesting and discussing interesting and challenging research problems. His passion and diligence for research has deeply inspired me.

I want to thank Associate Professor Ragnar Thobaben from KTH Royal Institute of Technology and Dr. Ricardo Blasco-Serrano now with Ericsson in Stockholm, for the discussions and sharing of ideas during the joint work in the European project ACROPOLIS. I want to thank Dr. Alessio Zappone, Dr. Martin Mittelbach and Dr. Pin-Hsun Lin for the discussions in the research work.

I want to thank Professor Tobias Weber from Rostock University for reviewing my thesis. I want to thank Professor Eduard Jorswieck, Dr. Pin-Hsun Lin, Johannes Richter, Carsten Janda and Bho Matthiesen for proofreading parts of my thesis. I want to thank Dr. Martin Mittelbach for helping me with the German abstract. I want to thank Sybille Siegel for the administrative work and Holger Hösel for the IT work. I also want to thank all my current and previous colleagues for making life and work in Dresden easier and more colorful.

Finally, I want to thank my parents for their love and support.

Jing Lv  
Dresden, December 2014



# Contents

<b>List of Figures</b>	<b>xvii</b>
<b>Nomenclatur</b>	<b>xix</b>
<b>1. Introduction</b>	<b>1</b>
1.1. Background and Motivation . . . . .	1
1.2. Outline and Contributions . . . . .	4
1.3. Related Work . . . . .	7
1.3.1. Interference Channel . . . . .	7
1.3.2. Underlay Spectrum Sharing . . . . .	7
1.3.3. Overlay Spectrum Sharing . . . . .	9
1.3.4. Cooperative Spectrum Sharing . . . . .	11
1.3.5. Energy-efficient Spectrum Sharing . . . . .	14
<b>2. Underlay Spectrum Sharing</b>	<b>17</b>
2.1. MISO Secondary Channel . . . . .	19
2.1.1. System Model . . . . .	19
2.1.2. Weak Interference . . . . .	20
2.1.3. Strong Interference . . . . .	21
2.1.4. Very Strong Interference . . . . .	24
2.1.5. Numerical Simulations . . . . .	25
2.2. MIMO Secondary Channel . . . . .	27
2.2.1. System Model . . . . .	27
2.2.2. Optimal Precoding and Power Allocation . . . . .	29
2.2.3. Numerical Simulations . . . . .	32
2.3. Summary . . . . .	34
2.4. Proofs . . . . .	35

<b>3. Overlay Spectrum Sharing</b>	<b>39</b>
3.1. MISO Secondary Channel with Non-causal Primary Message Knowledge	41
3.1.1. System Model . . . . .	41
3.1.2. Dirty-paper Coding at the Secondary Transmitter . . . . .	42
3.1.3. Linear Precoding at the Secondary Transmitter . . . . .	44
3.1.4. Numerical Simulations . . . . .	46
3.2. MIMO Secondary Channel with Non-causal Primary Message Knowledge	50
3.2.1. System Model . . . . .	50
3.2.2. Dirty-paper Coding at the Secondary Transmitter . . . . .	51
3.2.3. Linear Precoding at the Secondary Transmitter . . . . .	53
3.2.4. Numerical Simulations . . . . .	55
3.3. Amplify-and-Forward Cooperative Spectrum Sharing . . . . .	58
3.3.1. System Model . . . . .	58
3.3.2. Optimal Relaying Matrix and Beamforming Vector . . . . .	60
3.3.3. Alternative Solution with Parametrization . . . . .	62
3.3.4. Numerical Simulations . . . . .	63
3.4. Decode-and-Forward Cooperative Spectrum Sharing . . . . .	67
3.4.1. System Model . . . . .	67
3.4.2. Optimal Transmission Strategy . . . . .	70
3.4.3. Numerical Simulations . . . . .	75
3.5. Summary . . . . .	79
3.6. Proofs . . . . .	82
<b>4. Energy-efficient Spectrum Sharing</b>	<b>89</b>
4.1. Energy-efficient Underlay Spectrum Sharing . . . . .	91
4.1.1. System Model . . . . .	91
4.1.2. Fractional Programming . . . . .	94
4.1.3. Energy-efficient Precoding and Power Allocation . . . . .	94
4.1.4. Numerical Simulations . . . . .	97
4.2. Energy-efficient Overlay Spectrum Sharing . . . . .	103
4.2.1. System Model . . . . .	103
4.2.2. Energy-efficient Precoding and Power Allocation . . . . .	105
4.2.3. Numerical Simulations . . . . .	105
4.3. Summary . . . . .	111
<b>5. Conclusions and Future Work</b>	<b>113</b>
5.1. Conclusions . . . . .	113

5.2. Future Work . . . . .	118
<b>A. Further Contributions</b>	<b>119</b>
<b>Bibliography</b>	<b>121</b>





# List of Figures

2.1. System model consisting of a MISO primary link and a MISO secondary link – single-user decoding at the secondary receiver. . . . .	19
2.2. System model consisting of a MISO primary link and a MISO secondary link – rate splitting at the secondary transmitter and successive decoding at the secondary receiver. . . . .	22
2.3. Achievable secondary rate versus SNR of the secondary link: <i>MISO USS RS</i> versus <i>MISO USS SUD</i> with different primary link loads. . . . .	26
2.4. System model consisting of a MISO primary link and a MIMO secondary link – rate splitting at the secondary transmitter and successive decoding at the secondary receiver. . . . .	27
2.5. Achievable secondary rate versus SNR of the secondary link: <i>MIMO USS RS</i> versus <i>MIMO USS SUD</i> with different primary link loads. . . . .	33
3.1. System model consisting of a MISO primary link and a MISO secondary link – non-causal primary message at the secondary transmitter. . . . .	41
3.2. Achievable secondary rate versus SNR of the secondary link: <i>MISO OSS DPC</i> versus <i>MISO USS RS</i> with different primary link loads. . . . .	48
3.3. Achievable secondary rate versus SNR of the secondary link: <i>MISO OSS DPC</i> versus <i>MISO OSS LP</i> with different primary link loads. . . . .	49
3.4. System model consisting of a MISO primary link and a MIMO secondary link – non-causal primary message at the secondary transmitter. . . . .	50
3.5. Achievable secondary rate versus SNR of the secondary link: <i>MIMO OSS DPC</i> versus <i>MIMO USS RS</i> with different primary link loads. . . . .	56
3.6. Achievable secondary rate versus SNR of the secondary link: <i>MIMO OSS DPC</i> versus <i>MIMO OSS LP</i> with different primary link loads. . . . .	57
3.7. System model consisting of a MISO primary link and a MIMO secondary link with two-phase transmission: primary transmitter ( $P_{TX}$ ), secondary transmitter ( $S_{TX}$ ), primary receiver ( $P_{RX}$ ) and secondary receiver ( $S_{RX}$ ). . . . .	58
3.8. AFCSS system setup in the simulation . . . . .	64

List of Figures

3.9. Primary outage probability versus SNR of the secondary link with different antenna configurations at the secondary transceiver. . . . .	65
3.10. Achievable secondary rate versus SNR of the secondary link with different antenna configurations at the secondary transceiver. . . . .	66
3.11. System model consisting of a MISO primary link and a MIMO secondary link with two-phase transmission: primary transmitter ( $P_{TX}$ ), secondary transmitter ( $S_{TX}$ ), primary receiver ( $P_{RX}$ ) and secondary receiver ( $S_{RX}$ ). . . . .	67
3.12. DFCSS system setup in the simulation . . . . .	75
3.13. Primary outage probability versus SNR of the secondary link with different antenna configurations at the secondary transceiver. . . . .	77
3.14. Achievable secondary rate versus SNR of the secondary link with different antenna configurations at the secondary transceiver. . . . .	78
4.1. System model consisting of a MISO primary link and a MIMO secondary link – rate splitting at the secondary transmitter and successive decoding at the secondary receiver. . . . .	91
4.2. Secondary EE versus SNR of the secondary link: <i>MIMO USS EE Opt</i> versus <i>MIMO USS Rate Opt</i> with different primary link loads. . . . .	99
4.3. Secondary rate versus SNR of the secondary link: <i>MIMO USS EE Opt</i> versus <i>MIMO USS Rate Opt</i> with different primary link loads. . . . .	100
4.4. Secondary power versus SNR of the secondary link: <i>MIMO USS EE Opt</i> versus <i>MIMO USS Rate Opt</i> with different primary link loads. . . . .	101
4.5. Secondary EE versus SNR of the secondary link: <i>MIMO USS EE Opt</i> versus <i>MIMO USS EE Opt w/o RS</i> with different primary link loads. . . . .	102
4.6. System model consisting of a MISO primary link and a MIMO secondary link – non-causal primary message at the secondary transmitter. . . . .	103
4.7. Secondary EE versus SNR of the secondary link: <i>MIMO OSS EE Opt</i> versus <i>MIMO OSS Rate Opt</i> with different primary link loads. . . . .	107
4.8. Secondary rate versus SNR of the secondary link: <i>MIMO OSS EE Opt</i> versus <i>MIMO OSS Rate Opt</i> with different primary link loads. . . . .	108
4.9. Secondary power versus SNR of the secondary link: <i>MIMO OSS EE Opt</i> versus <i>MIMO OSS Rate Opt</i> with different primary link loads. . . . .	109
4.10. Secondary EE versus SNR of the secondary link: <i>MIMO OSS EE Opt</i> versus <i>MIMO USS EE Opt</i> with different primary link loads. . . . .	110

# Nomenclatur

## List of Notations

$\mathbf{a}$	Column vectors are written in boldface lowercase letters
$\mathbf{A}$	Matrices are written in boldface uppercase letters
$\mathbb{R}_+$	Set of all nonnegative real numbers
$\mathbb{C}$	Set of all complex numbers
$\mathbb{C}^N$	Set of all $N$ -dimensional vectors of complex numbers
$\mathbf{0}$	A zero matrix
$\mathbf{I}$	An identity matrix
$\mathbf{A} \succeq \mathbf{0}$	$\mathbf{A}$ is positive semidefinite
$\mathbf{A} \succ \mathbf{0}$	$\mathbf{A}$ is positive definite
$\Pi_{\mathbf{a}}$	The orthogonal projector onto the column space of $\mathbf{a}$ is $\Pi_{\mathbf{a}} = \frac{\mathbf{a}\mathbf{a}^H}{\ \mathbf{a}\ ^2}$
$\Pi_{\mathbf{a}}^\perp$	The orthogonal projector onto the orthogonal complement of the column space of $\mathbf{a}$ is $\Pi_{\mathbf{a}}^\perp = \mathbf{I} - \Pi_{\mathbf{a}}$
$ \cdot $	The absolute value of a scalar or the determinant of a matrix
$\ \cdot\ $	Euclidean norm of a vector or Frobenius norm of a matrix
$\text{Im}(\cdot)$	Imaginary part of a complex number
$(\cdot)^H$	Hermitian transpose of a vector or matrix
$(\cdot)^{-1}$	Inverse of a matrix
$\text{tr}(\cdot)$	Trace of a matrix
$\mathbf{v}_{max}(\cdot)$	Eigenvector which corresponds to the largest eigenvalue of a matrix
$\min(\cdot, \cdot)$	The smaller one of the two real numbers

## **List of Symbols**

REM	Radio Environment Map
MIMO	Multiple-Input Multiple-Output
MISO	Multiple-Input Single-Output
DPC	Dirty-Paper Coding
AF	Amplify-and-Forward
DF	Decode-and-Forward
SISO	Single-Input Single-Output
DoFs	Degrees of Freedom
DoF	Degree of Freedom
SNR	Signal-to-Noise Ratio
ZF	Zero Forcing
MRT	Maximum Ratio Transmission
MMSE	Minimum Mean Square Error
MRC	Maximum Ratio Combining
s.t.	subject to
KKT	Karush-Kuhn-Tucker

# Chapter 1.

## Introduction

### 1.1. Background and Motivation

Use of radio frequency bands of the electromagnetic spectrum is regulated in a spectrum management process known as spectrum allocation. There are three types of spectrum allocation: reserved frequency bands; open spectrum bands such as the unlicensed ISM bands, the unlicensed ultra-wideband band, and the amateur radio frequency allocations; licensed spectrum bands. Licensed spectrum bands are fixed, static in temporal and spatial dimensions, where the licensed users have the exclusive right to transmit to maintain interference-free communication.

As the wireless communication technologies evolve and the demand of wireless services increases, spectrum scarcity becomes a bottleneck that limits the introduction of new technologies and services. In spite of this scarcity problem, measurements have shown that current fixed spectrum allocation policy results in severe underutilization of spectrum resources [Fed02]. Furthermore, the spectrum utilization varies in space, time and frequency. Therefore, the philosophy of spectrum management requires changes to speed up technological innovation and improve spectrum efficiency. Under such circumstances, spectrum sharing between primary and secondary users in licensed and unlicensed bands has been suggested. For example, the conversion from analog TV to digital TV creates the opportunity to allow unlicensed transmission in the spectrum holes or "white spaces" unused by the licensed users, i.e., dynamic spectrum access, where standardization work has been done in the IEEE 802.11af/802.22/DySPAN, ETSI-RRS and ECMA-392. FCC in the United States has adopted rules for the operation of the devices in the TV white spaces and is monitoring the development and introduction of these devices, and Ofcom in the UK is leading a pilot trial in the TV white spaces to test the devices. Another example is the Authorized/Licensed Shared Access currently under development in 3GPP LTE-Advanced, which allows the licensee to exclusively access the underutilized spectrum on a shared basis without interfering with the incumbent,

and provides a predictable quality of service to both the incumbent and the licensee. Spectrum coexistence in licensed and unlicensed bands has also been investigated, where the secondary users coexist with the primary users under the constraint that the interference induced at the primary users is below a certain threshold or a certain primary rate requirement has to be satisfied. One example is the heterogeneous networks with small cells and device-to-device communications in 3GPP LTE/LTE-Advanced in licensed bands. Another example is spectrum coexistence in IEEE 802.11ah/802.15 in unlicensed bands, and LTE in unlicensed spectrum – Licensed-Assisted Access, namely, carrier aggregation operation to aggregate a primary cell, using licensed spectrum, to deliver critical information and guaranteed Quality of Service, and a co-located secondary cell, using unlicensed spectrum, to opportunistically boost data rate.

Cognitive radio – the enabling technology of spectrum sharing – is coined by Joseph Mitola [Mit00], and later defined by Simon Haykin [Hay05] as an intelligent wireless communication system that is aware of its environment, and learns from the environment to adapt its transmission strategy to reliably and efficiently use the radio spectrum. A paper by Andrea Goldsmith [GJMS09] unifies three spectrum sharing paradigms, interweave spectrum sharing, underlay spectrum sharing and overlay spectrum sharing, where the device employing the cognitive radio technology exploits side information about its environment to improve spectrum utilization. In interweave spectrum sharing, the secondary user requires the knowledge of the primary user’s activity information, through either spectrum sensing or radio environment map (REM), to exploit the spectrum holes unused by the primary user. In sensing-based interweave spectrum sharing, the secondary user has to detect the primary transmission, and decide about its own transmission based on the sensing result. In REM-based interweave spectrum sharing, the secondary user can consult the geolocation database about the spectrum occupancy before spectrum access. In underlay spectrum sharing, the secondary user transmits simultaneously with the primary user under the constraint that the interference induced at the primary receiver is below a certain threshold or a certain primary rate requirement has to be satisfied. In overlay spectrum sharing, the secondary user utilizes the knowledge of the primary user’s message, and helps transmit the primary message to compensate for the interference induced by its own message, under the constraint that a certain primary rate requirement has to be satisfied. A rigorous comparative study for these spectrum sharing paradigms, in terms of spectrum efficiency and implementation complexity, is still open. Generally speaking, underlay and overlay spectrum sharing utilize the spectrum more efficiently, since simultaneous transmission is allowed, while orthogonal transmission is required in interweave spectrum sharing. Moreover, the in-

interference induced at the primary receiver can be controlled in underlay and overlay spectrum sharing to satisfy the primary rate requirement, while it is not guaranteed in interweave spectrum sharing due to the miss detection of the primary transmission [ZLC10].

Multiple-antenna technology has received considerable attention during the past decade. With multiple antennas at the transmitter/receiver, transmit/receive beamforming technique can be applied to increase the achievable rate or improve the link reliability. With multiple antennas at both the transmitter and receiver, multiple-input multiple-output (MIMO) techniques, e.g., precoding or spatial multiplexing, can be deployed [TV05]. With multiple antennas at the secondary transmitter (and receiver), the interference induced at the primary receiver can be controlled by beamforming (precoding) technique, while at the same time the achievable secondary rate can be maximized.

The work in this thesis focuses on underlay and overlay spectrum sharing with multiple-antenna technology.

## 1.2. Outline and Contributions

The thesis is divided into 5 chapters.

In Chapter 1, the background and motivation of this thesis and the related work are introduced.

In Chapter 2, underlay spectrum sharing between a multiple-input single-output (MISO) primary link and a MISO/MIMO secondary link is studied. The primary transmitter employs maximum ratio transmission (MRT), and single-user decoding is deployed at the primary receiver. Rate splitting and successive decoding are deployed at the secondary transmitter and receiver, respectively, when it is feasible, and otherwise single-user decoding is deployed at the secondary receiver. Three scenarios are investigated, in terms of the interference from the primary transmitter to the secondary receiver, namely, weak interference, strong interference and very strong interference, or equivalently three ranges of primary rate requirement. For each scenario, optimal beamforming/precoding and power allocation at the secondary transmitter is derived, to maximize the achievable secondary rate while satisfying the primary rate requirement and the secondary power constraint. This chapter is partly based on the results reported in [LJ11] and [BSLT<sup>+</sup>13].

In Chapter 3, overlay spectrum sharing between a MISO primary link and a MISO/MIMO secondary link is studied. When the secondary transmitter has non-causal knowledge of the primary message, dirty-paper coding (DPC) is deployed to precancel the interference (when decoding the secondary message at the secondary receiver), due to the transmission of the primary message from both transmitters; linear precoding at the secondary transmitter is also proposed. In both cases, the primary transmitter employs MRT, and single-user decoding is deployed at the primary receiver; optimal beamforming/precoding and power allocation at the secondary transmitter is obtained, to maximize the achievable secondary rate while satisfying the primary rate requirement and the secondary power constraint. When the secondary transmitter does not have non-causal knowledge of the primary message, a two-phase transmission strategy is proposed for amplify-and-forward (AF)/decode-and-forward (DF) cooperative spectrum sharing, where the secondary transmitter acts as an/a AF/DF relay to acquire the primary message in the first phase and transmit the primary message in the second phase besides its own message. The primary link adapts its transmission strategy and cooperates with the secondary link. To maximize the achievable secondary rate while satisfying the primary rate requirement and the primary and secondary power constraints, in the case of AF cooperative spectrum sharing, optimal relaying matrix and beamforming



vector at the secondary transmitter is obtained; in the case of DF cooperative spectrum sharing, a set of parameters are optimized, including relative duration of the two phases, primary transmission strategies in the two phases and secondary transmission strategy in the second phase. This chapter is partly based on the results reported in [LBSJ<sup>+</sup>12], [LJBS<sup>+</sup>12], [LJ14] and [BSLT<sup>+</sup>13].

In Chapter 4, the energy efficiency (EE) of a MIMO secondary link in underlay spectrum sharing is studied. Rate splitting and successive decoding are deployed at the secondary transmitter and receiver, respectively, when it is feasible, and otherwise single-user decoding is deployed at the secondary receiver. Three transmission strategies are introduced based on the primary rate requirement and the channel conditions. For each case, optimal transmit covariance matrices at the secondary transmitter are obtained, to maximize the EE of the secondary transmission while satisfying the primary rate requirement and the secondary power constraint. Based on this, an energy-efficient resource allocation algorithm is proposed. Moreover, the EE of a MIMO secondary link in overlay spectrum sharing is studied, where the secondary transmitter has non-causal knowledge of the primary message and employs DPC to obtain an interference-free secondary link. Energy-efficient precoding and power allocation is obtained to maximize the EE of the secondary transmission while satisfying the primary rate requirement and the secondary power constraint. This chapter is partly based on the results reported in [LZJ14].

In Chapter 5, the conclusions and future work are given.

- [BSLT<sup>+</sup>13] R. Blasco-Serrano, J. Lv, R. Thobaben, E. A. Jorswieck, and M. Skoglund, “Multi-antenna transmission for underlay and overlay cognitive radio with explicit message learning phase,” *EURASIP Journal on Wireless Communications and Networking (JWCN)*, special issue on Cooperative Cognitive Networks, 2013.
- [LBSJ<sup>+</sup>12] J. Lv, R. Blasco-Serrano, E. Jorswieck, R. Thobaben, and A. Kliks, “Optimal beamforming in MISO cognitive channels with degraded message sets,” in *IEEE Wireless Communications and Networking Conference (WCNC)*, Apr. 2012.
- [LJ11] J. Lv and E. A. Jorswieck, “Spatial shaping in cognitive system with coded legacy transmission,” in *International ITG Workshop on Smart Antennas (WSA)*, Feb. 2011.

- [LJ14] —, “Transmission strategies for MIMO overlay spectrum sharing,” in *International ITG Workshop on Smart Antennas (WSA)*, Mar. 2014.
- [LJBS<sup>+</sup>12] J. Lv, E. Jorswieck, R. Blasco-Serrano, R. Thobaben, and A. Kliks, “Linear precoding in MISO cognitive channels with degraded message sets,” in *International ITG Workshop on Smart Antennas (WSA)*, Mar. 2012.
- [LZJ14] J. Lv, A. Zappone, and E. A. Jorswieck, “Energy-efficient MIMO underlay spectrum sharing with rate splitting,” in *IEEE International Workshop on Signal Processing Advances in Wireless Communications (SPAWC)*, Jun. 2014.

## 1.3. Related Work

### 1.3.1. Interference Channel

The proper information-theoretical model for the concurrent transmissions of wireless communication links is the interference channel. One metric to characterize the interference channel is the achievable rate region, which is the set of all rates that can be achieved, where the outer boundary is the so-called Pareto-boundary. For the two-user single-input and single-output (SISO) interference channel, the Han-Kobayashi Scheme [HK81] is proved to achieve the rate region for the class of discrete memory-less channel with strong and very strong interference, where the two transmitters employ rate splitting [Car78] and superposition coding [Cov72], and the two receivers employ partial interference decoding. In [ETW08], a simpler Han-Kobayashi type scheme is proposed for the two-user Gaussian interference channel to achieve to within a single bit per second per hertz (bit/s/Hz) of the capacity for all values of the channel parameters. In [CJ08], it is shown that interference alignment can achieve the asymptotic sum capacity and  $K/2$  degrees-of-freedom (DoFs) in the  $K$ -user time-varying SISO interference channel, when both the signal-to-noise ratio (SNR) and the signal dimensions tend to infinity. Another interference alignment scheme is introduced in [CJC09] that aims to achieve a higher multiplexing gain at any given signal dimension. Other works that deal with the maximization of the sum rate in the SISO interference channel can be found in [QZH09], [DWA09], [ASW12] and [FAAEBP14].

For the two-user MISO Gaussian interference channel with single-user decoding at the two receivers, it is shown that the optimal transmit beamforming vector to achieve a Pareto-boundary rate pair can be parametrized as a linear combination of the zero-forcing (ZF) and MRT beamformers [JLD08]. Efficient computation of the Pareto boundary of the achievable rate region is proposed in [JL10], [KL10], [ZC10] and [QZLC11], and closed-form solutions of transmit beamforming vectors that achieve Pareto-boundary points are proposed in [LKL11], [MJ12] and [LWZ<sup>+</sup>12]. Efficient computation of Pareto-optimal transmit beamforming vectors is proposed in [LKL13] with possibility of single-user decoding or successive decoding at the two receivers. Computation of the Pareto boundary of the MIMO Gaussian interference channel can be found in [CJS13], [PS13] and [MCJ14].

### 1.3.2. Underlay Spectrum Sharing

From an information-theoretical point-of-view, spectrum sharing can be modeled as the interference channel with additional constraints on the transceivers. As a matter of

fact, the transmission strategy of the primary link is usually given and fixed. In underlay spectrum sharing, the secondary link has to adapt its transmission strategy to fulfill the interference constraint at the primary receiver. With only one antenna at the secondary transmitter, power control is needed to satisfy the primary interference constraint. With multiple antennas at the secondary transmitter, the interference induced at the primary receiver can be controlled through beamforming technique. One objective can be maximizing the achievable secondary rate while satisfying the primary interference constraint and the secondary power constraint. With one single-antenna primary receiver and single-user decoding at the secondary receiver, in the case of a MISO secondary link, it is proved in [ZL08] that beamforming is the optimal secondary transmission strategy, and closed-form solution is derived for the optimal beamforming vector at the secondary transmitter to be the weighted sum of two channel-related vectors, which are obtained by Gram-Schmidt orthogonalization performed on the channels from the secondary transmitter to the primary and secondary receivers.

In the case of a MIMO secondary link, a primal-dual iterative optimization is proposed in [ZLC10] to reveal the optimal structure of the secondary transmit covariance matrix, and two suboptimal algorithms are proposed in [ZL08], where one is based on the singular-value decomposition of the MIMO secondary channel directly, and the other is based on the singular value decomposition of the projection of the MIMO secondary channel into the null space of the channel from the secondary transmitter to the primary receiver. For the special case of  $2 \times 2$  MIMO secondary link, a closed-form expression for linear transceiver design is derived to meet the achievable rates and no mutual interference between primary and secondary transceivers [BOO<sup>+</sup>10].

With capability of successive decoding (successive interference cancellation) [Cov72] at the secondary receiver, a higher secondary rate can be achieved. When the interference from the primary transmitter to the secondary receiver is not strong enough for the secondary receiver to decode the primary message, in the presence of the interference due to the transmission of the secondary message, rate splitting and superposition coding can be applied at the secondary transmitter. The secondary message is split into two parts. The secondary receiver decodes the first part of the secondary message and subtracts it, then decodes the primary message and subtracts it, and finally decodes the second part of the secondary message. It is applied for spectrum shaping in [ZM10] to determine the power spectrum density of the secondary signal, such that the achievable secondary rate is maximized while a certain primary rate requirement and secondary power constraint are satisfied. The application of rate splitting and successive decoding for spatial shaping in the MISO/MIMO secondary channel is proposed in [LJ11]

and [BSLT<sup>+</sup>13], respectively. Three scenarios are investigated, in terms of the interference from the primary transmitter to the secondary receiver, namely, weak interference, strong interference and very strong interference, or equivalently three ranges of primary rate requirement. In the case of MISO secondary channel, optimal beamforming and power allocation is derived, to maximize the achievable secondary rate while satisfying the primary rate requirement and the secondary power constraint. In all the three scenarios, the beamforming vectors are parametrized with real-valued parameters, as the weighted sum of two channel-related vectors, which are the projections of the secondary channel into the space and null space of the channel from the secondary transmitter to the primary receiver, respectively; the secondary transmitter employs full power transmission. For the scenarios of weak and very strong interference, closed-form solutions are obtained; for the scenario of strong interference, a grid search is required to obtain the optimal solution. In the case of MIMO secondary channel, optimal transmit covariance matrices are obtained by solving corresponding convex optimization problems, to maximize the achievable secondary rate while satisfying the primary rate requirement and the secondary power constraint. An additional line search is required for the scenario of strong interference to obtain the optimal solution. The secondary transmitter employs full power transmission in all the three scenarios. Note that the solution for the scenario of intermediate range of primary rate requirement in [BSLT<sup>+</sup>13] is not correct which has been pointed out in [LZJ14]. The results are presented in Section 2.1 and 2.2. Note that with MRT at the primary transmitter and single-user decoding at the primary receiver, the setting of a multiple-antenna primary transmitter has no impact on the solutions discussed in this thesis as compared with those in [LJ11].

### 1.3.3. Overlay Spectrum Sharing

In overlay spectrum sharing, the secondary transmitter can utilize the knowledge of the primary message, which is acquired non-causally (i.e., known in advance before transmission) or causally (i.e., acquired in the first phase of a two-phase transmission), to help transmit the primary message besides its own message. The secondary power is split into two parts, where one is spent for the secondary message, and the other is spent for the primary message to compensate for the interference induced at the primary receiver due to the secondary transmission, such that a certain primary rate requirement is satisfied. In many scenarios the associated capacity gains over non-cooperative transmission could serve as a motivation for having the primary transmitter share its codebook and message with the secondary transmitter [HLDV09]. Overlay spectrum sharing with non-causal primary message is also known as the cognitive radio channel

or the interference channel with degraded message sets in the literature [DMT06]. With knowledge of the primary message and codebook and perfect channel state information at the secondary transmitter, the interference (when decoding the secondary message at the secondary receiver) due to the transmission of the primary message from both transmitters is known, and can be precanceled by dirty-paper coding (DPC) [Cos83]. It is shown in [WVA07] that this scheme can achieve the capacity region in the weak interference regime, namely, when the interference from the secondary transmitter to the primary receiver is weak, and the achievable secondary rate is analyzed in [JV09] under the constraint that the primary link experiences no rate degradation and uses single-user decoder. While the capacity of part of the strong interference regime with strong interference at both receivers is obtained in [MYK07] using superposition coding and interference decoding. These results are generalized by the work in [JX08] and [MGKS08]. The results from [JV09] and [WVA07] are extended in [SV08] to the MIMO case in the weak interference regime. Recent results can be found in [RTD11], [RTD12] and [RG13].

With the deployment of DPC at the secondary transmitter to obtain an interference-free secondary link, optimal beamforming and power allocation is derived, to maximize the achievable secondary rate while satisfying the primary rate requirement and the secondary power constraint, in the case of MISO secondary channel [LBSJ<sup>+</sup>12]. The beamforming vector for the primary message is MRT, and the beamforming vector for the secondary message has the same form of parametrization with one real-valued parameter as those in [LJ11]. The secondary transmitter employs full power transmission. A line search is required to obtain the optimal solution. In the case of MIMO secondary channel [LJ14], the beamforming vector for the primary message is MRT, and the transmit covariance matrix for the secondary message is obtained by a line search while solving a convex optimization problem. The secondary transmitter employs full power transmission. Due to the high complexity of DPC, linear precoding can be applied as an alternative at the secondary transmitter. In the case of MISO secondary channel [LJBS<sup>+</sup>12], the beamforming vector for the primary message is parametrized with three real-valued parameters, as the weighted sum of two channel-related vectors, which are the projections of the channel from the secondary transmitter to the primary receiver in the space and null space of the secondary channel, respectively. The beamforming vector for the secondary message has the same form of parametrization with one real-valued parameter as that when DPC is deployed at the secondary transmitter. The secondary transmitter employs full power transmission. A cubic search is required to obtain the optimal solution. In the case of MIMO secondary channel [LJ14], an iter-

ative transceiver design algorithm is proposed, where the secondary link is constrained to single-stream transmission and minimum mean square error (MMSE) receiver is deployed at the secondary receiver. In each iteration, an optimization problem is solved to obtain the optimal beamforming and power allocation at the secondary transmitter with respect to a given secondary receiver, by the results from [LJBS<sup>+</sup>12]. The iterative algorithm converges though not guaranteed to achieve the global optimum. For the simulation, a good solution can be selected by several random initializations. The secondary transmitter employs full power transmission. The results are presented in Section 3.1 and 3.2. Note that with MRT at the primary transmitter and single-user decoding at the primary receiver, the setting of a multiple-antenna primary transmitter has no impact on the solutions discussed in this thesis as compared with those in [LBSJ<sup>+</sup>12], [LJBS<sup>+</sup>12] and [LJ14].

### 1.3.4. Cooperative Spectrum Sharing

In contrast to point-to-point communications, cooperative communications allows different users to collaborate through distributed processing, where one user's transmission is aided by the collaborating user through relaying. Two popular relaying schemes are AF and DF. In AF relaying, the received signal at the relay is amplified and retransmitted to the destination, with the advantage of low complexity and disadvantage of amplified noise at the relay. In DF relaying, the relay tries to decode the received signal, and if successful, it reencodes the message and retransmits it. Cooperative communications enables capacity increase [CG79] [KGG05] or diversity gain [LTW04], which is also attractive for spectrum sharing [ZJZ09]. Overlay spectrum sharing with causal primary message is also known as the causal cognitive radio channel or cooperative spectrum sharing in the literature [DMT06], where the secondary transmitter helps relay the primary message. Due to practical constraints, the secondary transmitter is usually assumed to work in half-duplex mode, i.e., it cannot simultaneously transmit and receive. The half-duplex causal cognitive radio channel is studied in [SJXW09], [CWO10], [WV13] and [CTKS14]. The primary link may have the incentive to adapt its transmission strategy to cooperate with the secondary link to maintain certain rate and avoid outage, especially when the primary link is weak. For example, when the primary transmitter is closer to the secondary transmitter than to its intended receiver, the channel condition to the former is better than that to the latter. The secondary transmitter relays the primary message in an AF or a DF way, while transmitting its own message. The achievable primary rate can be improved through the cooperation between the primary and secondary links.

Cooperative spectrum sharing between a SISO primary link and a MISO secondary link is studied in [MLLV11], where the secondary transmitter helps relay the primary message in the AF mode. The primary receiver applies maximum ratio combining (MRC) to the received signals in the two phases. With MRC at the secondary transmitter for receiving the primary message in the first phase, zero-forcing beamforming is proposed to mitigate the mutual interference between both transceivers in the second phase. With a MISO secondary broadcast channel, beamforming at the secondary transmitter is designed to maximize the minimum of the achievable secondary rates while satisfying the primary rate requirement and the secondary power constraint [HZBLG11]. In the AF mode, the receive beamforming vector in the first phase and transmit beamforming vector in the second phase are the same for the primary message. In [ZSWO13], multiple-antenna secondary transmitters help the transmission of a MISO primary link by amplifying and forwarding the primary message while transmitting their own messages, where the primary transmitter employs MRT or certain fixed transmit beamforming in the first phase, and the primary receiver applies MRC to the received signals in the two phases. The sum power of the secondary transmitters is minimized while satisfying the primary and secondary rate requirements. It is shown that the relaying matrix performing receive and transmit beamforming for the primary message is rank one and has a certain parametrized structure. The system model is extended to a MIMO secondary link in this thesis, where the secondary transmitter employs an AF relaying matrix for the primary message and single-stream transmission for its own message, and MMSE receiver is deployed at the secondary receiver. To fulfill its rate requirement, the primary link has the incentive to adapt the transmission strategies in the two phases, namely, the primary transmitter employs MRT in the two phases, and the primary receiver applies MRC to the received signals in the two phases. An iterative transceiver design algorithm is proposed, to maximize the achievable secondary rate while satisfying the primary rate requirement and the secondary power constraint. In each iteration, an optimization problem is solved to obtain the optimal relaying matrix and beamforming vector at the secondary transmitter, with respect to a given secondary receiver, by a bisection search through a sequence of second-order cone programming feasibility problems. The iterative algorithm converges though is not guaranteed to achieve the global optimum. A good solution can be selected by several random initializations. The secondary transmitter employs full power transmission. For this setup, an alternative heuristic solution is proposed. By the results from [ZSWO13] and [JLD08], given the secondary receiver, the relaying matrix for the primary message is parametrized with two real-valued parameters, and has the structure of the outer product of two channel-



related vectors. One is the MRC receiver for the primary signal with respect to the effective channel between the two transmitters. And the other is parametrized with one real-valued parameter, as the weighted sum of two channel-related vectors, which are the projections of the channel from the secondary transmitter to the primary receiver into the space and null space of the effective secondary channel, respectively. Moreover, by the results from [LJ11], given the secondary receiver and the relaying matrix for the primary message, the beamforming vector for the secondary message is parametrized with one real-valued parameter, as the weighted sum of two channel-related vectors, which are the projections of the effective secondary channel into the space and null space of the channel from the secondary transmitter to the primary receiver, respectively. An iterative transceiver design algorithm is proposed, where in each iteration, a grid search is performed to obtain the optimal relaying matrix and beamforming vector, with respect to a given secondary receiver. The iterative algorithm converges though not guaranteed to achieve the global optimum. A good solution can be selected by several random initializations in the simulation. The secondary transmitter employs full power transmission. The results are presented in Section 3.3.

As usual, the two phases in the AF relaying protocol are treated as having the same duration. As in [HZBLG11], the works on DF cooperative spectrum sharing in [HPT09], [LKPR11] and [SHL13] do not consider the decoding time of the primary message at the secondary transmitter. In [HPT09], the secondary transmitter tries to decode the primary message in the first time slot, and if successful, relays it to the primary receiver; the primary receiver applies MRC to the received signals in the two time slots. The relative duration of the two phases is explicitly considered in [SK11], where the two-phase transmission takes place in one time slot. Optimal time and power allocation is derived, to maximize the achievable secondary rate while satisfying the primary rate requirement and the secondary power constraint, and the constraint that the secondary receiver can decode the primary message in the first phase, such that the interference due to the relayed primary message can be cancelled at the secondary receiver in the second phase. The DF cooperative spectrum sharing between a MISO primary link and a MIMO secondary link is studied in [BSLT<sup>+</sup>13], where the secondary transmitter tries to decode the primary message in the first phase, and if successful, helps transmit the primary message besides its own message in the second phase. To fulfill its rate requirement, the primary link has the incentive to adapt the transmission strategies in the two phases, namely, the primary transmitter employs multiple-stream transmission to facilitate the decoding of the primary message at the secondary transmitter in the first phase, and MRT to facilitate its own transmission in the second phase. The

secondary transmitter employs DPC to precancel the interference (when decoding the secondary message at the secondary receiver), due to the transmission of the primary message from both transmitters in the second phase. The achievable secondary rate is maximized while satisfying the decodability condition of the primary message at the secondary transmitter, the primary rate requirement and the primary and secondary power constraints. A set of parameters are optimized, including relative duration of the two phases, primary transmission strategies in the two phases and secondary transmission strategy in the second phase. Properties of the parameters are studied to reduce the computational complexity of the optimization problem. A cubic search is required to obtain the optimal transmission strategies. Given the relative duration of the first phase and the power spent in the first phase by the primary transmitter, the primary transmit covariance matrix in the first phase is obtained, by balancing between the maximization of the received SNR at the primary receiver and that of the channel capacity from the primary transmitter to the secondary transmitter. After that, the secondary transmit covariance matrix in the second phase is obtained, by a line search over the power spent for the transmission of the primary message, while solving a corresponding convex optimization problem. The primary transmitter employs full power transmission in the two phases. The secondary transmitter employs full power transmission in the second phase. The optimal choice of parameters is the one that yields the largest secondary rate. The results are presented in Section 3.4.

### 1.3.5. Energy-efficient Spectrum Sharing

Besides spectrum, power is another precious resource as energy consumption of mobile networks is growing fast with various emerging applications, which is especially problematic for mobile devices with limited battery life. Energy-efficient wireless communications not only have great ecological benefits and represent social responsibility in fighting climate change, but also have significant economic benefits in terms of electricity bill [FJL<sup>+</sup>13]. Several definitions of energy efficiency (EE) have been proposed in the literature. One approach which is gaining momentum lately is to define the EE of a communication link as the ratio of the achievable rate over the power consumption. Energy-efficient precoding is investigated for point-to-point single-user MIMO systems in [BL11], considering static, slow and fast-fading channels. However, [BL11] does not take into account the circuit power that is dissipated in the electronic circuitry of the transmitter. In [VLDE13], a new EE performance metric is proposed, which takes into account the effects of using finite blocks for transmitting and using imperfect or partial channel state information. The relation between EE and SE is investigated in [JDI<sup>+</sup>13].

A realistic power model is adopted and both independent Rayleigh fading and semicorrelated fading channels are considered. A novel and closed-form upper bound for EE as a function of SE is derived. The EE optimization problem for a MIMO broadcast channel is addressed [XQ13], where the transmit covariance matrix is optimized under fixed active transmit antenna sets, and then active transmit antenna selection is utilized. Power allocation to achieve the EE of a MIMO multiple access channel is studied in [Mia13], first with the assumption of a fixed amount of circuit power consumption, then with improved circuit management to turn off circuit operations when some antennas are not used to reduce circuit power consumption. The EE of a MIMO interference channel is maximized in [JC13], by designing the transmit covariance matrices jointly for each transceiver pair. Centralized and decentralized algorithms are developed based on global and local channel state information at each transmitter, respectively. A new criterion of weighted sum EE is considered in [HHYO14] for energy efficient multicell multiuser precoding design, which is defined as the weighted sum of the energy efficiencies of multiple cells. The sum-of-ratio form of the energy efficient precoding problem is transformed into a parameterized polynomial form optimization problem, and the user rate is formulated as a polynomial optimization problem with the test conditional probabilities to be optimized. A solution is obtained through a two-layer optimization.

The EE of a MIMO secondary link in underlay spectrum sharing is optimized in [HT13a], with the primary interference constraint and the secondary power constraint. Energy-efficient precoding for the secondary transmission is proposed, where the nonlinear optimization problem is transformed into a parametrized convex optimization problem and the solution is discussed. In [HT13b], the EE of a MIMO secondary multiple access channel is maximized with the primary interference constraint and the secondary power constraint, which is defined as the ratio of weighted sum rate and power consumption. The nonlinear EE optimization problem is transformed into a series of parametrized convex optimization problems, which are solved by a combination of bisection search method and cyclic coordinate ascent-based iterative water-filling algorithm.

In [LZJ14], the EE of a MIMO secondary link in underlay spectrum sharing is studied, where rate splitting and successive decoding are deployed at the secondary transmitter and receiver, respectively, when it is feasible, and otherwise single-user decoding is deployed at the secondary receiver. Rate splitting and successive decoding are well-established techniques to increase the achievable rate of a communication link [CT06], but their application to spectrum sharing is relatively new. They have been deployed in [ZM10] and [LJ11], where it has been shown to achieve a significantly higher secondary rate. However, both [ZM10] and [LJ11] deal with rate maximization, whereas the po-

tential of rate splitting and successive decoding for EE maximization is not investigated. An energy-efficient resource allocation algorithm is proposed in [LZJ14], to optimize the EE of the secondary transmission while satisfying the primary rate requirement and the secondary power constraint. Three transmission strategies are introduced based on the primary rate requirement and the channel conditions. For each case, the original non-convex fractional problem is reformulated into a concave fractional program, which can be efficiently solved by fractional programming, e.g., Dinkelbach's method [Din67], to obtain the optimal transmit covariance matrices. An additional line search is required for the case of intermediate primary rate requirement to obtain the optimal solution. Based on this, an energy-efficient resource allocation algorithm is proposed. Moreover, in this thesis, the EE of a MIMO secondary link in overlay spectrum sharing is maximized with the primary rate requirement and the secondary power constraint, where the secondary transmitter has non-causal knowledge of the primary message and employs DPC to obtain an interference-free secondary link. The beamforming vector for the primary message is MRT, and the transmit covariance matrix for the secondary message is obtained through solving a concave fractional program by fractional programming. The results are presented in Section 4.1 and 4.2, respectively.

## Chapter 2.

# Underlay Spectrum Sharing

This chapter focuses on underlay spectrum sharing, where the secondary user transmits simultaneously with the primary user, under the constraint that the interference induced at the primary receiver is below a certain threshold, or a certain primary rate requirement has to be satisfied. Specifically, the coexistence of a MISO primary link and a MISO/MIMO secondary link is studied. The primary transmitter employs MRT, and single-user decoding is deployed at the primary receiver. Three scenarios are investigated, in terms of the interference from the primary transmitter to the secondary receiver, namely, weak interference, strong interference and very strong interference, or equivalently three ranges of primary rate requirement. For the scenario of weak interference (high range of primary rate requirement), single-user decoding is deployed at the secondary receiver; for the scenario of strong interference (intermediate range of primary rate requirement), rate splitting is deployed at the secondary transmitter, and successive decoding is deployed at the secondary receiver; for the scenario of very strong interference (low range of primary rate requirement), successive decoding is deployed at the secondary receiver, and rate splitting is not needed at the secondary transmitter. For each scenario, optimal beamforming/precoding and power allocation at the secondary transmitter is derived, to maximize the achievable secondary rate while satisfying the primary rate requirement and the secondary power constraint.

This chapter is partly based on the results reported in [LJ11] and [BSLT<sup>+</sup>13]. Note that with MRT at the primary transmitter and single-user decoding at the primary receiver, the setting of a multiple-antenna primary transmitter has no impact on the solutions discussed in this thesis as compared with those in [LJ11], and the solution for the scenario of intermediate range of primary rate requirement in [BSLT<sup>+</sup>13] is not correct which has been pointed out in [LZJ14].



## 2.1. MISO Secondary Channel

### 2.1.1. System Model

The system considered is depicted in Figure 2.1 and consists of a MISO primary link with  $N_{T,1}$  transmit antennas and a MISO secondary link with  $N_{T,2}$  transmit antennas, assuming single-user decoding at the secondary receiver. The channels from the primary transmitter to the primary and secondary receivers are denoted as  $\mathbf{h}_{11}$  and  $\mathbf{h}_{12}$ , respectively. The channels from the secondary transmitter to the primary and secondary receivers are denoted as  $\mathbf{h}_{21}$  and  $\mathbf{h}_{22}$ , respectively. The noises at the primary and secondary receivers are denoted as  $n_1$  and  $n_2$ , respectively. The channels and noises are modeled as independent and identically distributed complex Gaussian random variables with zero mean and unit variance. Assume that the primary transmitter knows  $\mathbf{h}_{11}$ ; the secondary transmitter knows  $\mathbf{h}_{11}$ ,  $\mathbf{h}_{12}$ ,  $\mathbf{h}_{21}$  and  $\mathbf{h}_{22}$ .

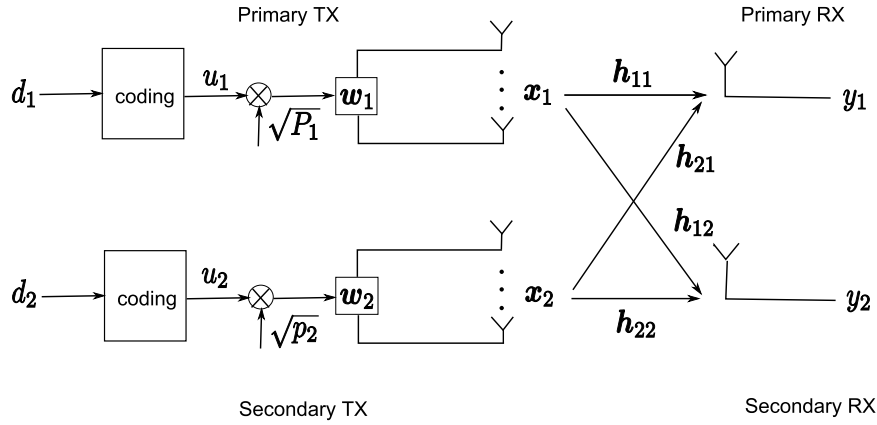


Figure 2.1.: System model consisting of a MISO primary link and a MISO secondary link – single-user decoding at the secondary receiver.

The primary transmission strategy is normally given and fixed, with a rate requirement of  $R_1^*$ , and single-user decoding is deployed at the primary receiver. The primary transmitter employs an  $N_{T,1} \times 1$  beamforming vector  $\mathbf{w}_1$  ( $\|\mathbf{w}_1\| = 1$ ) and power  $P_1$  for message  $d_1$ . With MRT, i.e.,  $\mathbf{w}_1 = \frac{\mathbf{h}_{11}}{\|\mathbf{h}_{11}\|}$ , the signal from the primary transmitter is

$$\mathbf{x}_1 = \sqrt{P_1} \frac{\mathbf{h}_{11}}{\|\mathbf{h}_{11}\|} u_1(d_1), \quad (2.1)$$

where  $d_1$  is encoded into symbol  $u_1$  with unit average power, by a random Gaussian codebook with fixed information rate  $R_1^*$ . The primary receiver has knowledge of the codebook of  $d_1$ .

Similarly, the secondary transmitter employs an  $N_{T,2} \times 1$  beamforming vector  $\mathbf{w}_2$  ( $\|\mathbf{w}_2\| = 1$ ) and power  $p_2$  for message  $d_2$ , as it has been proved that beamforming is the optimal secondary transmission strategy [ZL08]. The secondary transmitter has a power constraint of  $P_2$ . The signal from the secondary transmitter is

$$\mathbf{x}_2 = \sqrt{p_2} \mathbf{w}_2 u_2(d_2), \quad (2.2)$$

where  $d_2$  is encoded into symbol  $u_2$  with unit average power by a different Gaussian codebook. The secondary receiver has knowledge of the codebook of  $d_2$ .

The signals at the primary and secondary receivers are

$$y_1 = \sqrt{P_1} \|\mathbf{h}_{11}\| u_1(d_1) + \sqrt{p_2} \mathbf{h}_{21}^H \mathbf{w}_2 u_2(d_2) + n_1, \quad (2.3)$$

$$y_2 = \sqrt{p_2} \mathbf{h}_{22}^H \mathbf{w}_2 u_2(d_2) + \frac{\sqrt{P_1}}{\|\mathbf{h}_{11}\|} \mathbf{h}_{12}^H \mathbf{h}_{11} u_1(d_1) + n_2, \quad (2.4)$$

respectively.

### 2.1.2. Weak Interference

When the interference from the primary transmitter to the secondary receiver is weak, namely, the secondary receiver can not decode the primary message even without secondary transmission, i.e.,

$$R_1^* \geq \log_2 \left( 1 + \frac{P_1}{\|\mathbf{h}_{11}\|^2} |\mathbf{h}_{12}^H \mathbf{h}_{11}|^2 \right), \quad (2.5)$$

then single-user decoding is deployed at the secondary receiver.

The achievable rates for the primary and secondary links are

$$R_1 = \log_2 \left( 1 + \frac{P_1 \|\mathbf{h}_{11}\|^2}{1 + p_2 |\mathbf{h}_{21}^H \mathbf{w}_2|^2} \right), \quad (2.6)$$

$$R_2 = \log_2 \left( 1 + \frac{p_2 |\mathbf{h}_{22}^H \mathbf{w}_2|^2}{1 + \frac{P_1}{\|\mathbf{h}_{11}\|^2} |\mathbf{h}_{12}^H \mathbf{h}_{11}|^2} \right), \quad (2.7)$$

respectively, for any feasible choice of beamforming vector  $\mathbf{w}_2$  and power  $p_2$ .

To maximize the secondary achievable rate  $R_2$  while satisfying the primary rate requirement  $R_1^*$  and the secondary power constraint  $P_2$ , the optimization problem can be formulated as

$$\max_{\mathbf{w}_2, p_2} p_2 |\mathbf{h}_{22}^H \mathbf{w}_2|^2 \quad (2.8a)$$

$$\text{s.t. } \log_2 \left( 1 + \frac{P_1 \|\mathbf{h}_{11}\|^2}{1 + p_2 |\mathbf{h}_{21}^H \mathbf{w}_2|^2} \right) \geq R_1^*, \quad (2.8b)$$

$$\|\mathbf{w}_2\| = 1, \quad (2.8c)$$

$$0 \leq p_2 \leq P_2. \quad (2.8d)$$



**Proposition 1.** *The optimal beamforming vector that solves (2.8) can be parametrized as*

$$\mathbf{w}_2^*(\lambda) = \sqrt{\lambda} \frac{\Pi_{\mathbf{h}_{21}} \mathbf{h}_{22}}{\|\Pi_{\mathbf{h}_{21}} \mathbf{h}_{22}\|} + \sqrt{1-\lambda} \frac{\Pi_{\mathbf{h}_{21}}^\perp \mathbf{h}_{22}}{\|\Pi_{\mathbf{h}_{21}}^\perp \mathbf{h}_{22}\|}, \quad (2.9)$$

where

$$\lambda = \min \left( \lambda_{\text{MRT}}, \frac{P_{\text{int}}}{P_2 \|\mathbf{h}_{21}\|^2} \right), \quad (2.10)$$

$$\Pi_{\mathbf{h}_{21}} = \frac{\mathbf{h}_{21} \mathbf{h}_{21}^H}{\|\mathbf{h}_{21}\|^2}, \quad \Pi_{\mathbf{h}_{21}}^\perp = \mathbf{I} - \Pi_{\mathbf{h}_{21}}, \quad \lambda_{\text{MRT}} = \frac{\|\Pi_{\mathbf{h}_{21}} \mathbf{h}_{22}\|^2}{\|\mathbf{h}_{22}\|^2} \quad \text{and} \quad P_{\text{int}} = \frac{P_1 \|\mathbf{h}_{11}\|^2}{2^{R_1^*} - 1} - 1 \geq 0.$$

The optimal power is

$$p_2^* = P_2. \quad (2.11)$$

*Proof.* The proof is provided in Section 2.4.1.  $\square$

**Remark 1.** *The optimal beamforming vector is parametrized with one real-valued parameter, as the weighted sum of the projections of the channel  $\mathbf{h}_{22}$  into the space and null space of the channel  $\mathbf{h}_{21}$ , respectively. The parameter is determined as in (2.10) to allocate the power in these two directions of the beamforming vector to control the interference at the primary receiver while maximizing the achievable secondary rate.*

**Remark 2.**  $P_{\text{int}}$  can be seen as the interference constraint at the primary receiver.  $P_{\text{int}} = 0$  leads to the optimal choice of  $\lambda = 0$ , which corresponds to zero-forcing transmission.  $\lambda = \lambda_{\text{MRT}}$  corresponds to maximum ratio transmission.

**Remark 3.** *The parametrization in (2.9) has a different form than that in [ZL08], which is the weighted sum of two channel-related vectors, obtained by Gram-Schmidt orthogonalization performed on the channels  $\mathbf{h}_{21}$  and  $\mathbf{h}_{22}$ .*

**Remark 4.** *With multiple antennas at the secondary transmitter, full power transmission is allowed which maximizes the achievable secondary rate. The parametrization in (2.9) with one real-valued parameter in closed-form significantly reduces the computational complexity of finding the optimal beamforming vector.*

### 2.1.3. Strong Interference

When the interference from the primary transmitter to the secondary receiver is strong, namely, the secondary receiver can decode the primary message without secondary transmission, but can not reliably do so when the secondary signal is transmitted at its maximum allowed power, i.e.,

$$\log_2 \left( 1 + \frac{P_1}{\|\mathbf{h}_{11}\|^2} |\mathbf{h}_{12}^H \mathbf{h}_{11}|^2 \right) < R_1^* < \log_2 \left( 1 + \frac{P_1}{\|\mathbf{h}_{11}\|^2} |\mathbf{h}_{12}^H \mathbf{h}_{11}|^2 \right), \quad (2.12)$$

where  $\mathbf{w}_2^*$  is the optimal beamforming vector for (2.8) by Proposition 1, the achievable rate for the secondary link can be increased by employing rate splitting [Car78] at the secondary transmitter and successive decoding [Cov72] at the secondary receiver.

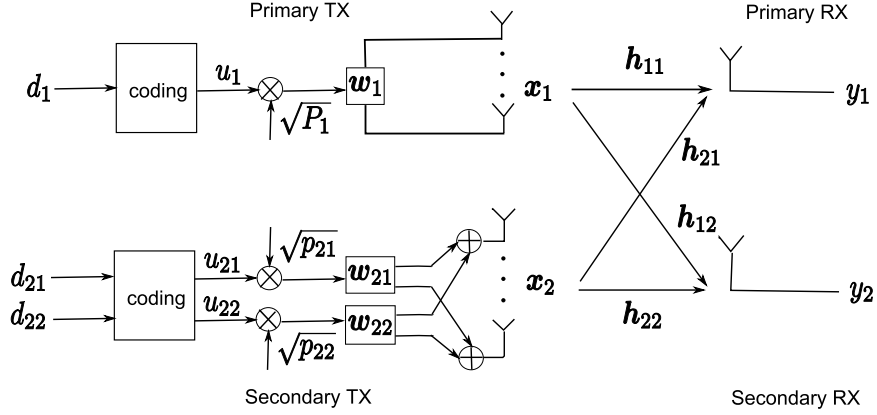


Figure 2.2.: System model consisting of a MISO primary link and a MISO secondary link – rate splitting at the secondary transmitter and successive decoding at the secondary receiver.

Rate splitting at the secondary transmitter is described as follows. As in Figure 2.2, the secondary message  $d_2$  is split into two sub-messages  $d_{21}$  and  $d_{22}$ , which can be encoded by superposition coding [Cov72]. The signal from the secondary transmitter is  $\mathbf{x}_2 = \mathbf{x}_{21} + \mathbf{x}_{22}$  with  $\mathbf{x}_{21} = \sqrt{p_{21}}\mathbf{w}_{21}u_{21}(d_{21})$  and  $\mathbf{x}_{22} = \sqrt{p_{22}}\mathbf{w}_{22}u_{22}(d_{22})$ .  $d_{21}$  and  $d_{22}$  are encoded into symbols  $u_{21}$  and  $u_{22}$  with unit average power, respectively, by two different Gaussian codebooks.  $\mathbf{w}_{21}$  ( $\|\mathbf{w}_{21}\| = 1$ ) and  $\mathbf{w}_{22}$  ( $\|\mathbf{w}_{22}\| = 1$ ) are the  $N_{T,2} \times 1$  beamforming vectors, and  $p_{21}$  and  $p_{22}$  are the powers. The secondary receiver has the knowledge of the codebooks of  $d_{21}$ ,  $d_{22}$  and  $d_1$ .

The received signals at the primary and secondary receivers are

$$y_1 = \sqrt{P_1}\|\mathbf{h}_{11}\|u_1(d_1) + \sqrt{p_{21}}\mathbf{h}_{21}^H\mathbf{w}_{21}u_{21}(d_{21}) + \sqrt{p_{22}}\mathbf{h}_{21}^H\mathbf{w}_{22}u_{22}(d_{22}) + n_1, \quad (2.13)$$

$$y_2 = \sqrt{p_{21}}\mathbf{h}_{22}^H\mathbf{w}_{21}u_{21}(d_{21}) + \sqrt{p_{22}}\mathbf{h}_{22}^H\mathbf{w}_{22}u_{22}(d_{22}) + \frac{\sqrt{P_1}}{\|\mathbf{h}_{11}\|}\mathbf{h}_{12}^H\mathbf{h}_{11}u_1(d_1) + n_2, \quad (2.14)$$

respectively.

Successive decoding at the secondary receiver is described as follows. Firstly, the secondary receiver decodes  $d_{21}$ , while treating  $\mathbf{x}_{22}$  and  $\mathbf{x}_1$  as noises, i.e.,

$$R_{21} = \log_2 \left( 1 + \frac{p_{21}|\mathbf{h}_{22}^H\mathbf{w}_{21}|^2}{1 + p_{22}|\mathbf{h}_{22}^H\mathbf{w}_{22}|^2 + \frac{P_1}{\|\mathbf{h}_{11}\|^2}|\mathbf{h}_{12}^H\mathbf{h}_{11}|^2} \right). \quad (2.15)$$

After cancelling  $\mathbf{x}_{21}$ , the secondary receiver should be able to decode  $d_1$ , while treating

$\mathbf{x}_{22}$  as noise, i.e.,

$$R_1^* \leq \log_2 \left( 1 + \frac{\frac{P_1}{\|\mathbf{h}_{11}\|^2} |\mathbf{h}_{12}^H \mathbf{h}_{11}|^2}{1 + p_{22} |\mathbf{h}_{22}^H \mathbf{w}_{22}|^2} \right). \quad (2.16)$$

Finally, after cancelling  $\mathbf{x}_1$ , the secondary receiver decodes  $d_{22}$ , i.e.,

$$R_{22} = \log_2 (1 + p_{22} |\mathbf{h}_{22}^H \mathbf{w}_{22}|^2). \quad (2.17)$$

The achievable secondary rate is

$$\begin{aligned} R_2 &= R_{21} + R_{22} \\ &= \log_2 \left( 1 + \frac{p_{21} |\mathbf{h}_{22}^H \mathbf{w}_{21}|^2}{1 + p_{22} |\mathbf{h}_{22}^H \mathbf{w}_{22}|^2 + \frac{P_1}{\|\mathbf{h}_{11}\|^2} |\mathbf{h}_{12}^H \mathbf{h}_{11}|^2} \right) + \log_2 (1 + p_{22} |\mathbf{h}_{22}^H \mathbf{w}_{22}|^2), \end{aligned} \quad (2.18)$$

for any feasible choice of beamforming vectors  $\mathbf{w}_{21}$  and  $\mathbf{w}_{22}$  and powers  $p_{21}$  and  $p_{22}$ .

To maximize the secondary achievable rate  $R_2$  while satisfying the primary rate requirement  $R_1^*$  and the secondary power constraint  $P_2$ , the optimization problem can be formulated as

$$\max_{\substack{\mathbf{w}_{21}, \mathbf{w}_{22} \\ p_{21}, p_{22}}} R_2 \quad (2.19a)$$

$$\text{s.t. } \log_2 \left( 1 + \frac{\frac{P_1}{\|\mathbf{h}_{11}\|^2} |\mathbf{h}_{12}^H \mathbf{h}_{11}|^2}{1 + p_{22} |\mathbf{h}_{22}^H \mathbf{w}_{22}|^2} \right) \geq R_1^*, \quad (2.19b)$$

$$\log_2 \left( 1 + \frac{P_1 \|\mathbf{h}_{11}\|^2}{1 + p_{21} |\mathbf{h}_{21}^H \mathbf{w}_{21}|^2 + p_{22} |\mathbf{h}_{21}^H \mathbf{w}_{22}|^2} \right) \geq R_1^*, \quad (2.19c)$$

$$\|\mathbf{w}_{21}\| = \|\mathbf{w}_{22}\| = 1, \quad (2.19d)$$

$$p_{21} + p_{22} \leq P_2, p_{21} \geq 0, p_{22} \geq 0. \quad (2.19e)$$

**Proposition 2.** *The beamforming vectors that solve (2.19) can be parametrized as*

$$\mathbf{w}_{21}(\lambda_1) = \sqrt{\lambda_1} \frac{\Pi_{\mathbf{h}_{21}} \mathbf{h}_{22}}{\|\Pi_{\mathbf{h}_{21}} \mathbf{h}_{22}\|} + \sqrt{1 - \lambda_1} \frac{\Pi_{\mathbf{h}_{21}}^\perp \mathbf{h}_{22}}{\|\Pi_{\mathbf{h}_{21}}^\perp \mathbf{h}_{22}\|}, \quad (2.20)$$

$$\mathbf{w}_{22}(\lambda_2) = \sqrt{\lambda_2} \frac{\Pi_{\mathbf{h}_{21}} \mathbf{h}_{22}}{\|\Pi_{\mathbf{h}_{21}} \mathbf{h}_{22}\|} + \sqrt{1 - \lambda_2} \frac{\Pi_{\mathbf{h}_{21}}^\perp \mathbf{h}_{22}}{\|\Pi_{\mathbf{h}_{21}}^\perp \mathbf{h}_{22}\|}, \quad (2.21)$$

where

$$\lambda_1 = \min \left( \lambda_{\text{MRT}}, \frac{P_{\text{int}}}{p_{21} \|\mathbf{h}_{21}\|^2} \right), \quad (2.22)$$

$$P_{\text{int}} = \frac{P_1 \|\mathbf{h}_{11}\|^2}{2^{R_1^*} - 1} - 1 - p_{22} |\mathbf{h}_{21}^H \mathbf{w}_{22}(\lambda_2)|^2 \geq 0, \quad (2.23)$$

$$p_{21} = P_2 - p_{22}, \quad (2.24)$$

$$\Pi_{\mathbf{h}_{21}} = \frac{\mathbf{h}_{21}\mathbf{h}_{21}^H}{\|\mathbf{h}_{21}\|^2}, \quad \Pi_{\mathbf{h}_{21}}^\perp = \mathbf{I} - \Pi_{\mathbf{h}_{21}} \quad \text{and} \quad \lambda_{\text{MRT}} = \frac{\|\Pi_{\mathbf{h}_{21}}\mathbf{h}_{22}\|^2}{\|\mathbf{h}_{22}\|^2}.$$

The optimal solution to (2.19) can be obtained by varying  $\lambda_2 \in [0, \lambda_{\text{MRT}}]$  and  $p_{22} \in [0, P_2]$  to achieve the maximum secondary rate.

*Proof.* The proof is provided in Section 2.4.2. □

**Remark 5.** The beamforming vectors have the same form of parametrization as that in the scenario of weak interference with single-user decoding, and though have different parameters. Intuitively, since the transmission of the two secondary sub-messages have the same channels, the two beamforming vectors have the same form of parametrization; however, due to the constraint (2.19b), they are not symmetrical and can have different parameters.

**Remark 6.** Full power is used for the secondary transmission. A grid search is required to find the optimal beamforming vectors and power allocation, which significantly reduces the computational complexity of solving (2.19) with two complex-valued vectors and two real-valued scalars.

#### 2.1.4. Very Strong Interference

When the interference from the primary transmitter to the secondary receiver is very strong, namely, the secondary receiver can decode the primary message by treating the received secondary signal as noise, and subtract it before decoding the secondary message, i.e.,

$$R_1^* \leq \log_2 \left( 1 + \frac{P_1}{\|\mathbf{h}_{11}\|^2} \frac{|\mathbf{h}_{12}^H \mathbf{h}_{11}|^2}{1 + P_2 |\mathbf{h}_{22}^H \mathbf{w}_2^*|^2} \right), \quad (2.25)$$

where  $\mathbf{w}_2^*$  is the optimal beamforming vector for (2.8) by Proposition 1.

After cancelling  $\mathbf{x}_1$ , the secondary receiver can decode the secondary message  $d_2$  without interference, and the achievable secondary rate is

$$R_2 = \log_2 (1 + P_2 |\mathbf{h}_{22}^H \mathbf{w}_2^*|^2). \quad (2.26)$$

**Remark 7.** Rate splitting is not required at the secondary transmitter in the scenario of very strong interference, which shares the same solution as in the scenario of weak interference.

**Remark 8.** In the scenario of strong interference from the primary transmitter to the secondary receiver as in Section 2.1.3, the special case of  $p_{22} = 0$  corresponds to the scenario of weak interference as in Section 2.1.2, and the special case of  $p_{21} = 0$  corresponds to the scenario of very strong interference as in Section 2.1.4. By comparing

the achievable secondary rate expressions in (2.7) and (2.26), it shows that rate splitting at the secondary transmitter and successive decoding at the secondary receiver does increase the achievable secondary rate if feasible, though with higher complexities at the secondary transceiver, with respect to single-user decoding at the secondary receiver.

### 2.1.5. Numerical Simulations

Numerical simulations are performed to evaluate the performance of the proposed MISO underlay spectrum sharing (*MISO USS RS*), and compare with that of MISO underlay spectrum sharing with only single-user decoding at the secondary receiver (*MISO USS SUD*), the solution of which is as in the scenario of weak interference in Section 2.1.2, in terms of achievable secondary rate (in bit/s/Hz) versus SNR of the secondary link (in dB). The SNR is defined as the ratio of the transmit power and the noise power at the receiver, and since the noise power is normalized, the SNR is equivalent to the transmit power.

The primary rate requirement is set as a fraction of its instantaneous point-to-point channel capacity without secondary transmission, i.e.,

$$R_1^* = \rho \log_2 (1 + P_1 \|\mathbf{h}_{11}\|^2), \quad (2.27)$$

where  $0 < \rho \leq 1$  is the load factor of the primary link.

The system configuration is as follows. The primary and secondary transmitters have 2 antennas each. The SNR of the primary link is fixed at 10 dB, and the SNR of the secondary link is varied from 0 dB to 20 dB. The load factor of the primary link is varied from 25% to 100%. The simulation results are averaged over 1000 channel realizations. As in Figure 2.3, at the load factor of 25% and SNR of 10 dB, the rate gain of *MISO USS RS* over *MISO USS SUD* is about 1.7 bits/s/Hz, and becomes less significant as the load factor increases. The variation of the load factor has a significant impact on the achievable secondary rate of *MISO USS RS*, since it changes the primary rate requirement based on which *MISO USS RS* decides which of the three scenarios to work in. With smaller primary rate requirement, it is with higher probability that *MISO USS RS* works in the scenarios of strong interference and very strong interference, where a higher secondary rate can be achieved compared with the scenario of weak interference.

Numerical results show that rate splitting at the secondary transmitter and successive decoding at the secondary receiver does significantly increase the achievable secondary rate if feasible, compared with single-user decoding at the secondary receiver.

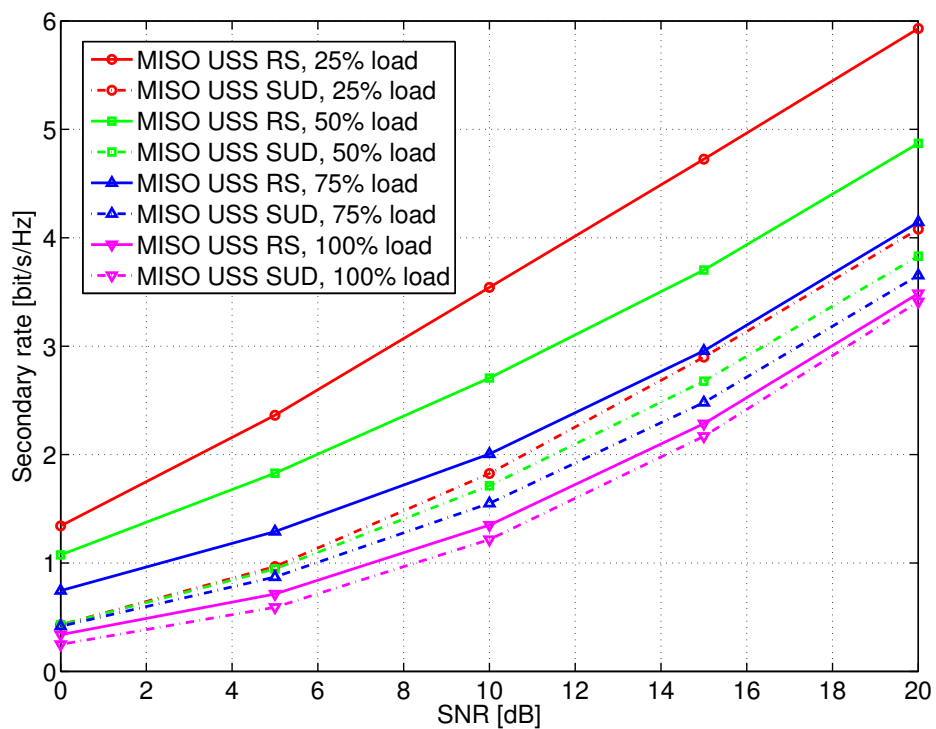


Figure 2.3.: Achievable secondary rate versus SNR of the secondary link: *MISO USS RS* versus *MISO USS SUD* with different primary link loads.

## 2.2. MIMO Secondary Channel

### 2.2.1. System Model

The system considered is depicted in Figure 2.4 and consists of a MISO primary link with  $N_{T,1}$  transmit antennas and a MIMO secondary link with  $N_{T,2}$  transmit antennas and  $N_{R,2}$  receive antennas, assuming rate splitting at the secondary transmitter and successive decoding at the secondary receiver. The channels from the primary transmitter to the primary and secondary receivers are denoted as  $\mathbf{h}_{11}$  and  $\mathbf{H}_{12}$ , respectively. The channels from the secondary transmitter to the primary and secondary receivers are denoted as  $\mathbf{h}_{21}$  and  $\mathbf{H}_{22}$ , respectively. The noises at the primary and secondary receivers are denoted as  $n_1$  and  $\mathbf{n}_2$ , respectively. The channels and noises are modeled as independent and identically distributed complex Gaussian random variables with zero mean and unit variance. Assume that the primary transmitter knows  $\mathbf{h}_{11}$ ; the secondary transmitter knows  $\mathbf{h}_{11}$ ,  $\mathbf{H}_{12}$ ,  $\mathbf{h}_{21}$  and  $\mathbf{H}_{22}$ .

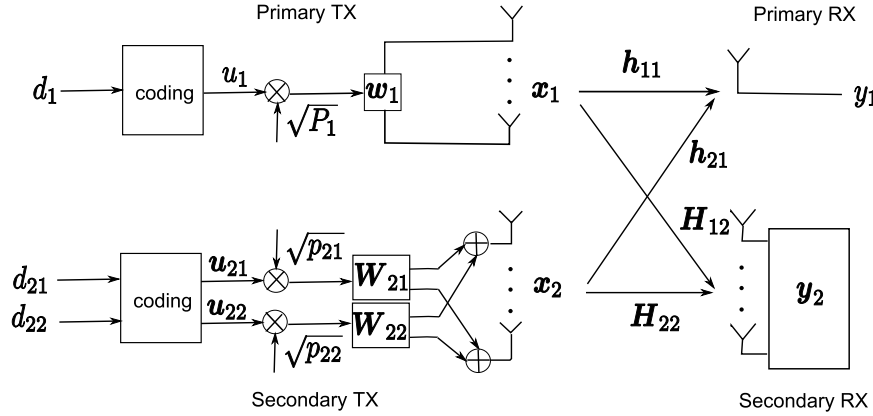


Figure 2.4.: System model consisting of a MISO primary link and a MIMO secondary link – rate splitting at the secondary transmitter and successive decoding at the secondary receiver.

The primary transmission strategy is normally given and fixed, with a rate requirement of  $R_1^*$ , and single-user decoding is deployed at the primary receiver. The primary transmitter employs an  $N_{T,1} \times 1$  beamforming vector  $\mathbf{w}_1$  ( $\|\mathbf{w}_1\| = 1$ ) and power  $P_1$  for message  $d_1$ . With MRT, i.e.,  $\mathbf{w}_1 = \frac{\mathbf{h}_{11}}{\|\mathbf{h}_{11}\|}$ , the signal from the primary transmitter is

$$\mathbf{x}_1 = \sqrt{P_1} \frac{\mathbf{h}_{11}}{\|\mathbf{h}_{11}\|} u_1(d_1), \quad (2.28)$$

where  $d_1$  is encoded into symbol  $u_1$  with unit average power, by a random Gaussian codebook with fixed information rate  $R_1^*$ . The transmit covariance matrix for  $d_1$  is

$\mathbf{K}_1 = \frac{P_1}{\|\mathbf{h}_{11}\|^2} \mathbf{h}_{11} \mathbf{h}_{11}^H$ . The primary receiver has knowledge of the codebook of  $d_1$ .

Assume that the interference from the primary transmitter to the secondary receiver is strong, and rate splitting and successive decoding are deployed at the secondary transmitter and receiver, respectively. At the secondary transmitter, the secondary message  $d_2$  is split into two sub-messages  $d_{21}$  and  $d_{22}$ .  $d_{21}$  ( $d_{22}$ ) is encoded into an  $M_1 \times 1$  ( $M_2 \times 1$ ) vector  $\mathbf{u}_{21}$  ( $\mathbf{u}_{22}$ ) of symbols with unit average power by a random Gaussian codebook.  $\mathbf{W}_{21}$  ( $\mathbf{W}_{22}$ ) is the normalized  $N_{T,2} \times M_1$  ( $N_{T,2} \times M_2$ ) precoding matrix and  $p_{21}$  ( $p_{22}$ ) is the power for  $d_{21}$  ( $d_{22}$ ), where  $1 \leq M_1, M_2 \leq \min(N_{R,2}, N_{T,2})$ . The signal from the secondary transmitter is

$$\mathbf{x}_2 = \sqrt{p_{21}} \mathbf{W}_{21} \mathbf{u}_{21}(d_{21}) + \sqrt{p_{22}} \mathbf{W}_{22} \mathbf{u}_{22}(d_{22}). \quad (2.29)$$

The transmit covariance matrices for  $d_{21}$  and  $d_{22}$  are  $\mathbf{K}_{21} = p_{21} \mathbf{W}_{21} \mathbf{W}_{21}^H$  and  $\mathbf{K}_{22} = p_{22} \mathbf{W}_{22} \mathbf{W}_{22}^H$ , respectively. The secondary receiver has knowledge of the codebooks of  $d_{21}$ ,  $d_{22}$  and  $d_1$ .

The signals at the primary and secondary receivers are

$$y_1 = \sqrt{P_1} \|\mathbf{h}_{11}\| u_1(d_1) + \sqrt{p_{21}} \mathbf{h}_{21}^H \mathbf{W}_{21} \mathbf{u}_{21}(d_{21}) + \sqrt{p_{22}} \mathbf{h}_{21}^H \mathbf{W}_{22} \mathbf{u}_{22}(d_{22}) + n_1, \quad (2.30)$$

$$y_2 = \sqrt{p_{21}} \mathbf{H}_{22} \mathbf{W}_{21} \mathbf{u}_{21}(d_{21}) + \sqrt{p_{22}} \mathbf{H}_{22} \mathbf{W}_{22} \mathbf{u}_{22}(d_{22}) + \frac{\sqrt{P_1}}{\|\mathbf{h}_{11}\|} \mathbf{H}_{12} \mathbf{h}_{11} u_1(d_1) + \mathbf{n}_2, \quad (2.31)$$

respectively.

At the secondary receiver,  $d_{21}$  is first decoded, then  $d_1$  (i.e., the interference), and finally  $d_{22}$ . This adds the constraint that the achievable rate of the primary message at the secondary receiver must be no less than  $R_1^*$  for the secondary receiver to successfully decode the primary message, i.e.,  $R_{12} \geq R_1^*$ , where

$$\begin{aligned} R_{12}(\mathbf{K}_{22}) &= \log_2 \frac{|\mathbf{I} + \mathbf{H}_{22} \mathbf{K}_{22} \mathbf{H}_{22}^H + \mathbf{H}_{12} \mathbf{K}_1 \mathbf{H}_{12}^H|}{|\mathbf{I} + \mathbf{H}_{22} \mathbf{K}_{22} \mathbf{H}_{22}^H|} \\ &= \log_2 \left| \mathbf{I} + (\mathbf{I} + \mathbf{H}_{22} \mathbf{K}_{22} \mathbf{H}_{22}^H)^{-1} \mathbf{M} \right| \end{aligned} \quad (2.32)$$

with  $\mathbf{M} = \mathbf{H}_{12} \mathbf{K}_1 \mathbf{H}_{12}^H$ , which is convex in  $\mathbf{K}_{22}$  [DC01, Lemma II.3] and matrix-decreasing in  $\mathbf{K}_{22}$  [MOA11, Ch 16, E.3.b.].

The achievable primary rate is

$$R_1(\mathbf{K}_{21}, \mathbf{K}_{22}) = \log_2 \left( 1 + \frac{\mathbf{h}_{11}^H \mathbf{K}_1 \mathbf{h}_{11}}{1 + \mathbf{h}_{21}^H (\mathbf{K}_{21} + \mathbf{K}_{22}) \mathbf{h}_{21}} \right), \quad (2.33)$$



and the achievable secondary rate is

$$\begin{aligned} R_2(\mathbf{K}_{21}, \mathbf{K}_{22}) &= \log_2 \frac{|\mathbf{I} + \mathbf{H}_{22}(\mathbf{K}_{21} + \mathbf{K}_{22})\mathbf{H}_{22}^H + \mathbf{M}|}{|\mathbf{I} + \mathbf{H}_{22}\mathbf{K}_{22}\mathbf{H}_{22}^H + \mathbf{M}|} + \log_2 |\mathbf{I} + \mathbf{H}_{22}\mathbf{K}_{22}\mathbf{H}_{22}^H| \\ &= \log_2 |\mathbf{I} + \mathbf{H}_{22}(\mathbf{K}_{21} + \mathbf{K}_{22})\mathbf{H}_{22}^H + \mathbf{M}| - R_{12}(\mathbf{K}_{22}), \end{aligned} \quad (2.34)$$

which is jointly concave in  $\mathbf{K}_{21}$  and  $\mathbf{K}_{22}$ . The first term in (2.34) corresponds to the part of the secondary message decoded in the presence of the interference (both from primary transmitter and self-interference). The second term in (2.34) corresponds to the part of the secondary message recovered after decoding and subtracting the primary message.

The two special cases, where the secondary receiver decodes the primary message at first (very strong interference) or does not decode it at all (weak interference), are included by setting  $\mathbf{K}_{21}$  and  $\mathbf{K}_{22}$  to the zero matrix, respectively.

To maximize the achievable secondary rate  $R_2$  while satisfying the primary rate requirement  $R_1^*$  and the secondary power constraint  $P_2$ , the optimization problem can be formulated as

$$\max_{\mathbf{K}_{21}, \mathbf{K}_{22}} R_2(\mathbf{K}_{21}, \mathbf{K}_{22}) \quad (2.35a)$$

$$\text{s.t. } R_1(\mathbf{K}_{21}, \mathbf{K}_{22}) \geq R_1^*, \quad (2.35b)$$

$$R_{12}(\mathbf{K}_{22}) \geq R_1^*, \quad (2.35c)$$

$$\text{tr}(\mathbf{K}_{21} + \mathbf{K}_{22}) \leq P_2, \quad (2.35d)$$

$$\mathbf{K}_{21} \succeq \mathbf{0}, \mathbf{K}_{22} \succeq \mathbf{0}, \quad (2.35e)$$

where it is implicitly assumed that (2.35c) applies only if  $\mathbf{K}_{22} \neq \mathbf{0}$ . (2.35b) and (2.35d) are jointly linear in  $\mathbf{K}_{21}$  and  $\mathbf{K}_{22}$ , respectively. Since  $R_{12}$  is convex in  $\mathbf{K}_{22}$ , (2.35c) is not convex. Overall, (2.35) is not convex. However, it is possible to solve it with limited computational complexity, as shown in the following section.

### 2.2.2. Optimal Precoding and Power Allocation

The two extreme cases in which either  $\mathbf{K}_{22} = \mathbf{0}$  or  $\mathbf{K}_{21} = \mathbf{0}$  and the intermediate case in which both  $\mathbf{K}_{21}$  and  $\mathbf{K}_{22}$  are non-zero matrices are treated separately. These three cases correspond to three distinct ranges of the primary rate requirement  $R_1^*$ .

**Case 1:**  $\mathbf{K}_{22} = \mathbf{0}$ . This case is obtained when  $R_1^* \geq \log_2 |\mathbf{I} + \mathbf{M}|$ , i.e., decoding the primary message at the secondary receiver is not possible at all. The secondary message

is decoded in the presence of the interference due to the primary message. The optimal  $\mathbf{K}_{21}$  is the solution to the problem

$$\max_{\mathbf{K}_{21}} \log_2 \left| \mathbf{I} + \mathbf{H}_{22} \mathbf{K}_{21} \mathbf{H}_{22}^H (\mathbf{I} + \mathbf{M})^{-1} \right| \quad (2.36a)$$

$$\text{s.t. } \mathbf{h}_{21}^H \mathbf{K}_{21} \mathbf{h}_{21} \leq P_{\text{int}}, \quad (2.36b)$$

$$\text{tr}(\mathbf{K}_{21}) \leq P_2, \quad (2.36c)$$

$$\mathbf{K}_{21} \succeq \mathbf{0}, \quad (2.36d)$$

where

$$P_{\text{int}} = \frac{\mathbf{h}_{11}^H \mathbf{K}_1 \mathbf{h}_{11}}{2R_1^* - 1} - 1 \geq 0. \quad (2.37)$$

The objective function in (2.36a) is concave in  $\mathbf{K}_{21}$ , and the constraints (2.36b) and (2.36c) are linear in  $\mathbf{K}_{21}$ , respectively. Overall, the optimization problem (2.36) is convex in  $\mathbf{K}_{21}$ .

**Case 2:  $\mathbf{K}_{21} = \mathbf{0}$ .** Proposition 3 shows that this case is obtained when

$$R_1^* \leq \log_2 \left| \mathbf{I} + (\mathbf{I} + \mathbf{H}_{22} \mathbf{\Sigma}^* \mathbf{H}_{22}^H)^{-1} \mathbf{M} \right|, \quad (2.38)$$

where  $\mathbf{\Sigma}^*$  is the solution to the problem

$$\max_{\mathbf{\Sigma}} \log_2 \left| \mathbf{I} + \mathbf{H}_{22} \mathbf{\Sigma} \mathbf{H}_{22}^H \right| \quad (2.39a)$$

$$\text{s.t. } \mathbf{h}_{21}^H \mathbf{\Sigma} \mathbf{h}_{21} \leq P_{\text{int}}, \quad (2.39b)$$

$$\text{tr}(\mathbf{\Sigma}) \leq P_2, \quad (2.39c)$$

$$\mathbf{\Sigma} \succeq \mathbf{0}, \quad (2.39d)$$

and  $P_{\text{int}}$  is defined as in (2.37).

**Proposition 3.** Denote by  $(\mathbf{K}_{21}^*, \mathbf{K}_{22}^*)$  a solution of (2.35). If (2.38) holds, then  $\mathbf{K}_{21}^* = \mathbf{0}$ .

*Proof.* The proof is provided in Section 2.4.3. □

The primary message is decoded and subtracted before decoding the secondary message, and rate splitting is not required at the secondary transmitter. The optimal  $\mathbf{K}_{22} = \mathbf{\Sigma}^*$ .

The objective function in (2.39a) is concave in  $\mathbf{\Sigma}$ , and the constraints (2.39b) and (2.39c) are linear in  $\mathbf{\Sigma}$ , respectively. Overall, the optimization problem (2.39) is convex in  $\mathbf{\Sigma}$ .

**Case 3:**  $\mathbf{K}_{21} \neq \mathbf{0}$  and  $\mathbf{K}_{22} \neq \mathbf{0}$ . This case corresponds to the intermediate range of  $R_1^*$ , i.e.,

$$\log_2 \left| \mathbf{I} + (\mathbf{I} + \mathbf{H}_{22} \boldsymbol{\Sigma}^* \mathbf{H}_{22}^H)^{-1} \mathbf{M} \right| < R_1^* < \log_2 |\mathbf{I} + \mathbf{M}|. \quad (2.40)$$

In this case, the solution of (2.35) is given by Proposition 4.

**Proposition 4.** *If (2.40) holds, then (2.35) is solved by  $\mathbf{K}_{21} = \widehat{\mathbf{K}}_{21} + (1 - \gamma) \widehat{\mathbf{K}}_{22}$  and  $\mathbf{K}_{22} = \gamma \widehat{\mathbf{K}}_{22}$ , where  $\gamma \in [0, 1]$  is chosen such that  $R_{12}(\mathbf{K}_{22}) = R_1^*$ , and  $\widehat{\mathbf{K}}_{21}$  and  $\widehat{\mathbf{K}}_{22}$  are the solution to the problem*

$$\max_{\mathbf{K}_{21}, \mathbf{K}_{22}} \log_2 \left| \mathbf{I} + \mathbf{H}_{22} (\mathbf{K}_{21} + \mathbf{K}_{22}) \mathbf{H}_{22}^H + \mathbf{M} \right| - R_1^* \quad (2.41a)$$

$$\text{s.t. } \mathbf{h}_{21}^H (\mathbf{K}_{21} + \mathbf{K}_{22}) \mathbf{h}_{21} \leq P_{\text{int}}, \quad (2.41b)$$

$$\log_2 \left| \mathbf{I} + (\mathbf{I} + \mathbf{H}_{22} \mathbf{K}_{22} \mathbf{H}_{22}^H)^{-1} \mathbf{M} \right| \leq R_1^* \quad (2.41c)$$

$$\text{tr}(\mathbf{K}_{21} + \mathbf{K}_{22}) \leq P_2, \quad (2.41d)$$

$$\mathbf{K}_{21} \succeq \mathbf{0}, \mathbf{K}_{22} \succeq \mathbf{0}, \quad (2.41e)$$

where  $P_{\text{int}}$  is defined as in (2.37).

*Proof.* The proof is provided in Section 2.4.4. □

The objective function in (2.41a) is jointly concave in  $\mathbf{K}_{21}$  and  $\mathbf{K}_{22}$ , the constraints (2.41b) and (2.41d) are jointly linear in  $\mathbf{K}_{21}$  and  $\mathbf{K}_{22}$ , respectively, and the constraint (2.41c) is convex in  $\mathbf{K}_{22}$ . Overall, the optimization problem (2.41) is jointly convex in  $\mathbf{K}_{21}$  and  $\mathbf{K}_{22}$ .

**Remark 9.** *The whole range of  $R_1^*$  is covered by these three cases, where in each case a corresponding convex optimization problem is solved to obtain the optimal transmit covariance matrices, e.g., by interior point methods [BV04]. An additional line search is required in Case 3. The secondary transmitter employs full power transmission in all cases, since otherwise the remaining power can be accommodated into the transmit covariance matrix in the null space of the channel  $\mathbf{h}_{21}$ , such that the objective value is nondecreased and the constraints are still satisfied in each optimization problem.*

**Remark 10.** *Comparing the two special cases, specifically (2.36) in Case 1 and (2.39) in Case 2, the solution to (2.36) is feasible for (2.39) and achieves a higher objective value for (2.39). It shows that rate splitting at the secondary transmitter and successive decoding at the secondary receiver does increase the achievable secondary rate when it is feasible, though with higher complexities at the secondary transceiver, compared with single-user decoding at the secondary receiver.*

### 2.2.3. Numerical Simulations

Numerical simulations are performed to evaluate the performance of the proposed MIMO underlay spectrum sharing (*MIMO USS RS*), and compare with that of MIMO underlay spectrum sharing with only single-user decoding at the secondary receiver (*MIMO USS SUD*), the solution of which is as in Case 1 in Section 2.2.2, in terms of achievable secondary rate (in bit/s/Hz) versus SNR of the secondary link (in dB). The SNR is defined as the ratio of the transmit power and the noise power at the receiver, and since the noise power is normalized, the SNR is equivalent to the transmit power.

The primary rate requirement is set as a fraction of its instantaneous point-to-point channel capacity without secondary transmission, i.e.,

$$R_1^* = \rho \log_2 (1 + P_1 \|\mathbf{h}_{11}\|^2), \quad (2.42)$$

where  $0 < \rho \leq 1$  is the load factor of the primary link.

The system configuration is as follows. The primary transmitter has 2 antennas, and the secondary transmitter and receiver have 2 antennas each. The SNR of the primary link is fixed at 10 dB, and the SNR of the secondary link is varied from 0 dB to 20 dB. The load factor of the primary link is varied from 25% to 100%. The simulation results are averaged over 1000 channel realizations. As in Figure 2.5, at the load factor of 25% and SNR of 10 dB, the rate gain of *MIMO USS RS* over *MIMO USS SUD* is about 1.2 bits/s/Hz, and becomes less significant as the load factor increases. The variation of the load factor has a significant impact on the achievable secondary rate of *MIMO USS RS*, since it changes the primary rate requirement based on which *MIMO USS RS* decides which of the three cases to work in.

Numerical results show that rate splitting at the secondary transmitter and successive decoding at the secondary receiver does significantly increase the achievable secondary rate if feasible, compared with single-user decoding at the secondary receiver.

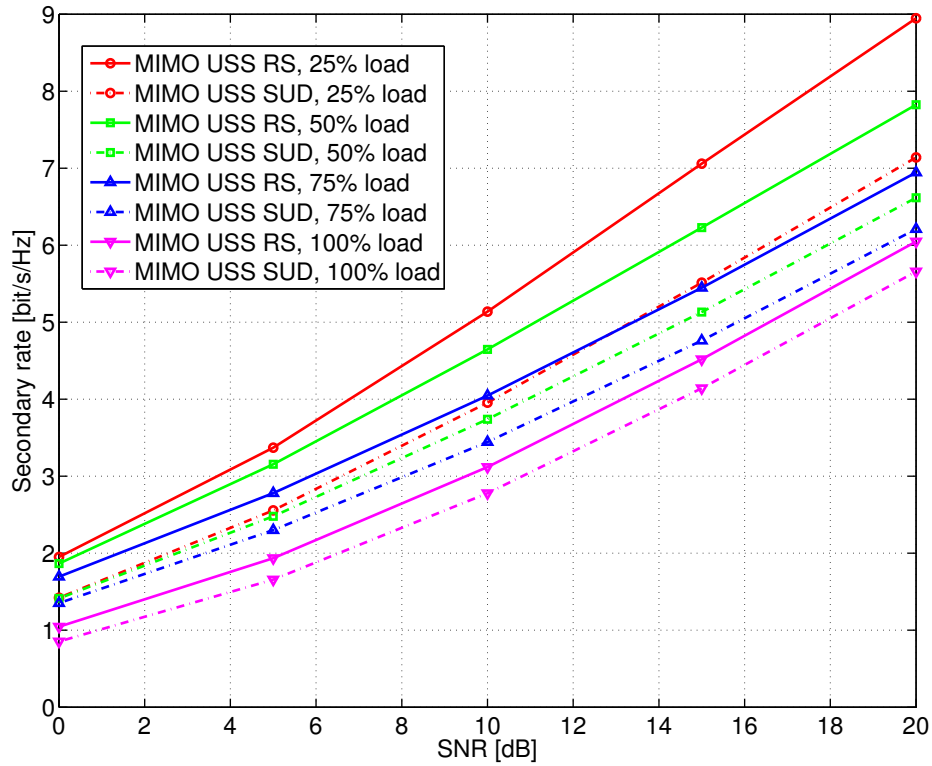


Figure 2.5.: Achievable secondary rate versus SNR of the secondary link: *MIMO USS RS* versus *MIMO USS SUD* with different primary link loads.

### 2.3. Summary

Underlay spectrum sharing between a MISO primary link and a MISO/MIMO secondary link is studied. Three scenarios are investigated, in terms of the interference from the primary transmitter to the secondary receiver, namely, weak interference, strong interference and very strong interference, or equivalently three ranges of primary rate requirement. Rate splitting and successive decoding are deployed at the secondary transmitter and receiver, respectively, when it is feasible, and otherwise single-user decoding is deployed at the secondary receiver. For each scenario, the achievable secondary rate is maximized while satisfying the primary rate requirement and the secondary power constraint. In the case of MISO secondary channel, optimal beamforming and power allocation is derived, where the beamforming vectors are parametrized with real-valued parameters. For the scenarios of weak and very strong interference, closed-form solutions are obtained; for the scenario of strong interference, a grid search is required to obtain the optimal solution. In the case of MIMO secondary channel, optimal transmit covariance matrices are obtained by solving corresponding convex optimization problems. An additional line search is required for the scenario of strong interference to obtain the optimal solution. In both cases, full power transmission is used at the secondary transmitter. Numerical results show that rate splitting at the secondary transmitter and successive decoding at the secondary receiver does significantly increase the achievable secondary rate if feasible, compared with single-user decoding at the secondary receiver.

## 2.4. Proofs

### 2.4.1. Proof of Proposition 1

The optimization problem (2.8) is equivalent to

$$\max_{\mathbf{w}_2, p_2} p_2 |\mathbf{h}_{22}^H \mathbf{w}_2|^2 \quad (2.43a)$$

$$\text{s.t. } p_2 \leq \frac{P_{\text{int}}}{|\mathbf{h}_{21}^H \mathbf{w}_2|^2}, \quad (2.43b)$$

$$\|\mathbf{w}_2\| = 1, \quad (2.43c)$$

$$0 \leq p_2 \leq P_2, \quad (2.43d)$$

where  $P_{\text{int}} = \frac{P_1 \|\mathbf{h}_{11}\|^2}{2^{R_1^*} - 1} - 1 \geq 0$ .

Assume  $|\mathbf{h}_{21}^H \mathbf{w}_2|^2 \neq 0$ ,  $p_2^* = \min\left(P_2, \frac{P_{\text{int}}}{|\mathbf{h}_{21}^H \mathbf{w}_2|^2}\right)$ , then (2.43) can be rewritten as

$$\max_{\mathbf{w}_2} \min\left(P_2 |\mathbf{h}_{22}^H \mathbf{w}_2|^2, P_{\text{int}} \frac{|\mathbf{h}_{22}^H \mathbf{w}_2|^2}{|\mathbf{h}_{21}^H \mathbf{w}_2|^2}\right) \quad (2.44a)$$

$$\text{s.t. } \|\mathbf{w}_2\| = 1. \quad (2.44b)$$

Since the objective function is monotonically increasing in the channel gain  $|\mathbf{h}_{22}^H \mathbf{w}_2|^2$  and monotonically decreasing in the channel gain  $|\mathbf{h}_{21}^H \mathbf{w}_2|^2$ , it follows from [MJ11, Theorem 1] that the solution is attained at the boundary of the channel gain region

$\Omega = \bigcup_{\|\mathbf{w}_2\|=1} (|\mathbf{h}_{22}^H \mathbf{w}_2|^2, |\mathbf{h}_{21}^H \mathbf{w}_2|^2)$  in the direction  $e = [+1, -1]$ . The boundary points of the set  $\Omega$  in the direction  $e = [+1, -1]$  can be achieved by

$$\mathbf{w}_2(\mu_1, \mu_2) = \mathbf{v}_{\max}(\mu_1 \mathbf{h}_{22} \mathbf{h}_{22}^H - \mu_2 \mathbf{h}_{21} \mathbf{h}_{21}^H) \quad (2.45)$$

where  $\mathbf{v}_{\max}(\cdot)$  denotes the principal eigenvector of a matrix, and  $\mu_1 + \mu_2 = 1$ ,  $0 \leq \mu_k \leq 1$ ,  $k = 1, 2$ . Then  $\mathbf{w}_2$  can be parametrized as

$$\mathbf{w}_2(\nu) = \frac{\nu \mathbf{w}_2^{MRT} + (1 - \nu) \mathbf{w}_2^{ZF}}{\|\nu \mathbf{w}_2^{MRT} + (1 - \nu) \mathbf{w}_2^{ZF}\|}, \quad (2.46)$$

where  $\mathbf{w}_2^{MRT} = \frac{\mathbf{h}_{22}}{\|\mathbf{h}_{22}\|}$  denotes maximum ratio transmission,  $\mathbf{w}_2^{ZF} = \frac{\Pi_{\mathbf{h}_{21}}^\perp \mathbf{h}_{22}}{\|\Pi_{\mathbf{h}_{21}}^\perp \mathbf{h}_{22}\|}$  denotes zero forcing (ZF), and  $0 \leq \nu \leq 1$ . (2.46) is equivalent to [JLD08, Corollary 2]

$$\mathbf{w}_2(\lambda) = \sqrt{\lambda} \frac{\Pi_{\mathbf{h}_{21}} \mathbf{h}_{22}}{\|\Pi_{\mathbf{h}_{21}} \mathbf{h}_{22}\|} + \sqrt{1 - \lambda} \frac{\Pi_{\mathbf{h}_{21}}^\perp \mathbf{h}_{22}}{\|\Pi_{\mathbf{h}_{21}}^\perp \mathbf{h}_{22}\|}, \quad (2.47)$$

where  $\Pi_{\mathbf{h}_{21}} = \frac{\mathbf{h}_{21} \mathbf{h}_{21}^H}{\|\mathbf{h}_{21}\|^2}$ ,  $\Pi_{\mathbf{h}_{21}}^\perp = \mathbf{I} - \Pi_{\mathbf{h}_{21}}$  and  $0 \leq \lambda \leq 1$ . By [JLD08, Corollary 2],

$$\mathbf{w}_2^{MRT} = \sqrt{\frac{l_1}{l_1 + l_2}} \frac{\Pi_{\mathbf{h}_{21}} \mathbf{h}_{22}}{\|\Pi_{\mathbf{h}_{21}} \mathbf{h}_{22}\|} + \sqrt{\frac{l_2}{l_1 + l_2}} \frac{\Pi_{\mathbf{h}_{21}}^\perp \mathbf{h}_{22}}{\|\Pi_{\mathbf{h}_{21}}^\perp \mathbf{h}_{22}\|}, \quad (2.48)$$

where  $l_1 = \|\Pi_{\mathbf{h}_{21}} \mathbf{h}_{22}\|$  and  $l_2 = \|\Pi_{\mathbf{h}_{21}}^\perp \mathbf{h}_{22}\|$ . Then  $\lambda_{MRT} = \frac{\|\Pi_{\mathbf{h}_{21}} \mathbf{h}_{22}\|^2}{\|\mathbf{h}_{22}\|^2}$ .

Using the parametrization in (2.47), define  $f(\lambda) = |\mathbf{h}_{22}^H \mathbf{w}_2(\lambda)|^2$ , then  $f(\lambda)$  is maximized at  $\lambda = \lambda_{MRT}$ . Since  $|\mathbf{h}_{21}^H \mathbf{w}_2(\lambda)|^2 = \lambda \|\mathbf{h}_{21}\|^2$ , (2.44) is equivalent to

$$\max_{0 \leq \lambda \leq 1} f(\lambda) \min \left( P_2, \frac{P_{\text{int}}}{\lambda \|\mathbf{h}_{21}\|^2} \right). \quad (2.49)$$

If  $\lambda_{MRT} \leq \frac{P_{\text{int}}}{P_2 \|\mathbf{h}_{21}\|^2}$ , then  $\lambda^* = \lambda_{MRT}$  which maximizes  $f(\lambda)$ . Otherwise, define

$$\varphi(\lambda) = \frac{f(\lambda)}{\lambda} = \frac{\left( \sqrt{\lambda} \|\Pi_{\mathbf{h}_{21}} \mathbf{h}_{22}\| + \sqrt{1-\lambda} \|\Pi_{\mathbf{h}_{21}}^\perp \mathbf{h}_{22}\| \right)^2}{\lambda} \quad (2.50)$$

Since  $\varphi'(\lambda) \leq 0$ ,  $\varphi(\lambda)$  is monotonically decreasing. Then  $\lambda^* = \frac{P_{\text{int}}}{P_2 \|\mathbf{h}_{21}\|^2}$  which maximizes  $\frac{f(\lambda)}{\lambda}$ . Overall  $\lambda^* = \min \left( \lambda_{MRT}, \frac{P_{\text{int}}}{P_2 \|\mathbf{h}_{21}\|^2} \right)$  and in both cases  $p_2^* = P_2$ .

Note that  $|\mathbf{h}_{21}^H \mathbf{w}_2|^2 = 0$  corresponds to  $\mathbf{w}_2^{ZF}$  with  $\lambda = 0$ .

### 2.4.2. Proof of Proposition 2

Given  $\mathbf{w}_{22}$  and  $p_{22}$ , assume the constraint (2.19b) is satisfied. Using the same approach as in the proof of Proposition 1 in Section 2.1.2,  $\mathbf{w}_{21}$  can be parametrized as in (2.20) with  $\lambda_1 \in [0, \lambda_{MRT}]$  in (2.22) and  $p_{21}$  is given by (2.24), assuming that the constraint (2.23) is satisfied. Since  $P_{\text{int}}$  is monotonically decreasing in  $|\mathbf{h}_{21}^H \mathbf{w}_{22}(\lambda_2)|^2$ ,  $\lambda_1$  is nonincreasing in  $|\mathbf{h}_{21}^H \mathbf{w}_{22}(\lambda_2)|^2$ . Since  $|\mathbf{h}_{22}^H \mathbf{w}_{21}|^2$  is monotonically increasing in  $\lambda_1$ ,  $|\mathbf{h}_{22}^H \mathbf{w}_{21}|^2$  is nonincreasing in  $|\mathbf{h}_{21}^H \mathbf{w}_{22}(\lambda_2)|^2$ .

Given  $\mathbf{w}_{22}$  and  $p_{22}$  such that the constraints (2.19b) and (2.23) are satisfied, the corresponding  $\mathbf{w}_{21}$  and  $p_{21}$  for (2.19) satisfy the constraint (2.19c). By keeping  $|\mathbf{h}_{22}^H \mathbf{w}_{22}|^2$  constant and reducing  $|\mathbf{h}_{21}^H \mathbf{w}_{22}|^2$  (the constraint (2.19c) is still satisfied), the objective value in (2.19a) can be increased. By [MJ11, Theorem 1], this corresponds to moving the point downwards to the boundary in the channel gain region, and the resulting part of the boundary corresponds to the parametrization of  $\mathbf{w}_{22}$  as in (2.21) with  $\lambda_2 \in [0, \lambda_{MRT}]$ .

The optimal solution to (2.19) can be obtained by varying  $\lambda_2 \in [0, \lambda_{MRT}]$  and  $p_{22} \in [0, P_2]$  to achieve the maximum secondary rate.



### 2.4.3. Proof of Proposition 3

First consider the following relaxed version of (2.35) without the constraint (2.35c)

$$\max_{\mathbf{K}_{21}, \mathbf{K}_{22}} \log_2 |\mathbf{I} + \mathbf{H}_{22}(\mathbf{K}_{21} + \mathbf{K}_{22})\mathbf{H}_{22}^H + \mathbf{M}| - R_{12}(\mathbf{K}_{22}) \quad (2.51a)$$

$$\text{s.t. } \mathbf{h}_{21}^H(\mathbf{K}_{21} + \mathbf{K}_{22})\mathbf{h}_{21} \leq P_{\text{int}}, \quad (2.51b)$$

$$\text{tr}(\mathbf{K}_{21} + \mathbf{K}_{22}) \leq P_2, \quad (2.51c)$$

$$\mathbf{K}_{21} \succeq \mathbf{0}, \mathbf{K}_{22} \succeq \mathbf{0}, \quad (2.51d)$$

with  $P_{\text{int}}$  as defined in (2.37).

The objective function in (2.51a) is jointly concave in  $\mathbf{K}_{21}$  and  $\mathbf{K}_{22}$ , the constraints (2.51b) and (2.51c) are jointly linear in  $\mathbf{K}_{21}$  and  $\mathbf{K}_{22}$ . Overall, the optimization problem (2.51) is jointly convex in  $\mathbf{K}_{21}$  and  $\mathbf{K}_{22}$ .

Now, denoting by  $(\widetilde{\mathbf{K}}_{21}, \widetilde{\mathbf{K}}_{22})$  the optimal solution to (2.51), and employing a contradiction argument, it can be shown that  $\widetilde{\mathbf{K}}_{21} = \mathbf{0}$  holds. Indeed, assume  $\widetilde{\mathbf{K}}_{21} \neq \mathbf{0}$ , then there exists  $\Psi \succeq \mathbf{0}$  with  $\mathbf{K}_{21} = \widetilde{\mathbf{K}}_{21} - \Psi \succeq \mathbf{0}$  and  $\mathbf{K}_{22} = \widetilde{\mathbf{K}}_{22} + \Psi \succeq \widetilde{\mathbf{K}}_{22}$  such that  $\mathbf{K}_{21} + \mathbf{K}_{22} = \widetilde{\mathbf{K}}_{21} + \widetilde{\mathbf{K}}_{22}$  and  $R_{12}(\mathbf{K}_{22}) < R_{12}(\widetilde{\mathbf{K}}_{22})$ , i.e., the objective value in (2.51a) is increased, since  $R_{12}$  is matrix-decreasing in  $\mathbf{K}_{22}$ . Therefore, a contradiction occurs and consequently  $\widetilde{\mathbf{K}}_{21} = \mathbf{0}$ . Exploiting this fact, (2.51) can be equivalently recast as (2.39). Moreover, the solution  $\Sigma^*$  of the relaxed problem (2.39) is also feasible for the original problem (2.35) because of assumption (2.38), therefore it is also the solution of the original problem.

### 2.4.4. Proof of Proposition 4

Before the proof of Proposition 4, Lemma 1 and Lemma 2 are introduced.

**Lemma 1.** *Problem (2.39) has a unique solution.*

*Proof.* Consider the objective function in (2.39a). If  $\mathbf{H}_{22}^H \mathbf{H}_{22} \succ \mathbf{0}$ , then  $\log_2 |\mathbf{I} + \mathbf{H}_{22} \Sigma \mathbf{H}_{22}^H|$  is strictly concave in  $\Sigma$  [DC01, Lemma II.4]; otherwise, in order to maximize  $\log_2 |\mathbf{I} + \mathbf{H}_{22} \Sigma \mathbf{H}_{22}^H|$ ,  $\Sigma$  should not include the null space of  $\mathbf{H}_{22}^H \mathbf{H}_{22}$ .

Without loss of generality, assume  $\mathbf{H}_{22}^H \mathbf{H}_{22} \succ \mathbf{0}$  such that the objective function in (2.39a) is strictly concave. Thus the convex optimization problem (2.39) has a unique solution [BV04].  $\square$

**Lemma 2.** *Denote by  $(\mathbf{K}_{21}^*, \mathbf{K}_{22}^*)$  and  $(\widetilde{\mathbf{K}}_{21}, \widetilde{\mathbf{K}}_{22})$  the optimal solution to (2.35) and (2.51), respectively. If  $R_{12}(\widetilde{\mathbf{K}}_{22}) < R_1^*$ , then  $R_{12}(\mathbf{K}_{22}^*) = R_1^*$ .*

*Proof.* The proof follows by contradiction. Assume  $R_{12}(\widetilde{\mathbf{K}}_{22}) < R_1^*$  but  $R_{12}(\mathbf{K}_{22}^*) > R_1^*$ . Then,  $(\mathbf{K}_{21}^*, \mathbf{K}_{22}^*)$  is also a solution of (2.51). To see this, observe that if  $R_{12}(\mathbf{K}_{22}^*) > R_1^*$  then the Lagrange multiplier associated with this constraint is zero by the complementary slackness condition. This implies that the Karush-Kuhn-Tucker (KKT) conditions that  $(\mathbf{K}_{21}^*, \mathbf{K}_{22}^*)$  satisfies become formally equal to the KKT conditions of (2.51), which are necessary and sufficient for optimality since the problem is a convex problem [BV04]. Moreover, by Proposition 3 and Lemma 1, (2.51) is equivalent to (2.39) and has the unique solution  $(\widetilde{\mathbf{K}}_{21} = \mathbf{0}, \widetilde{\mathbf{K}}_{22} = \boldsymbol{\Sigma}^*)$ . As a consequence,  $\mathbf{K}_{22}^* = \widetilde{\mathbf{K}}_{22} = \boldsymbol{\Sigma}^*$  which implies  $R_{12}(\mathbf{K}_{22}^*) = R_{12}(\widetilde{\mathbf{K}}_{22}) < R_1^*$ . This is a contradiction since it is assumed that  $R_{12}(\mathbf{K}_{22}^*) > R_1^*$ .  $\square$

Lemma 2 states that if the solution of the relaxed problem (2.51) is not feasible for the original problem, then any solution of the original problem fulfills (2.35c) with equality.

The proof of Proposition 4 follows. Given (2.40), the solution of the relaxed problem (2.51) is not feasible for (2.35), because otherwise it would fall back to Case 2. Then, by Lemma 2, problem (2.35) is equivalent to

$$\max_{\mathbf{K}_{21}, \mathbf{K}_{22}} \log_2 |\mathbf{I} + \mathbf{H}_{22}(\mathbf{K}_{2,1} + \mathbf{K}_{2,2})\mathbf{H}_{22}^H + \mathbf{M}| - R_1^* \quad (2.52a)$$

$$\text{s.t. } \mathbf{h}_{21}^H(\mathbf{K}_{21} + \mathbf{K}_{22})\mathbf{h}_{21} \leq P_{\text{int}}, \quad (2.52b)$$

$$\log_2 \left| \mathbf{I} + (\mathbf{I} + \mathbf{H}_{22}\mathbf{K}_{22}\mathbf{H}_{22}^H)^{-1} \mathbf{M} \right| = R_1^* \quad (2.52c)$$

$$\text{tr}(\mathbf{K}_{21} + \mathbf{K}_{22}) \leq P_2, \quad (2.52d)$$

$$\mathbf{K}_{21} \succeq \mathbf{0}, \mathbf{K}_{22} \succeq \mathbf{0}, \quad (2.52e)$$

with  $P_{\text{int}}$  as defined in (2.37). The next step is to observe that problem (2.41) is a relaxed version of (2.52) obtained by replacing the equality constraint (2.52c) with an inequality constraint. Denote by  $(\widehat{\mathbf{K}}_{21}, \widehat{\mathbf{K}}_{22})$  a solution of (2.41), then it is always possible to construct the matrices  $\mathbf{K}_{21} = \widehat{\mathbf{K}}_{21} + (1 - \gamma)\widehat{\mathbf{K}}_{22}$  and  $\mathbf{K}_{22} = \gamma\widehat{\mathbf{K}}_{22}$ , where  $\gamma \in [0, 1]$ . Thus, for any  $\gamma \in [0, 1]$ ,  $\mathbf{K}_{21} + \mathbf{K}_{22} = \widehat{\mathbf{K}}_{21} + \widehat{\mathbf{K}}_{22}$ , which implies that the pair  $(\mathbf{K}_{21}, \mathbf{K}_{22})$  yields the same objective value as  $(\widehat{\mathbf{K}}_{21}, \widehat{\mathbf{K}}_{22})$  and fulfills constraints (2.52b), (2.52d) and (2.52e). Moreover, when  $\gamma = 0$ ,  $R_{12} = \log_2 |\mathbf{I} + \mathbf{M}| > R_1^*$  due to (2.40); when  $\gamma = 1$ ,  $R_{12} = \log_2 \left| \mathbf{I} + (\mathbf{I} + \mathbf{H}_{22}\mathbf{K}_{22}\mathbf{H}_{22}^H)^{-1} \mathbf{M} \right| \leq R_1^*$  due to (2.41c). Then, it is always possible to find  $\gamma \in [0, 1]$  such that  $R_{12} = R_1^*$ , thus implying that the relaxation of (2.41) is tight, since the corresponding pair  $(\mathbf{K}_{21}, \mathbf{K}_{22})$  is a solution of the relaxed problem (2.41) which is also feasible for the original problem (2.52). This concludes the proof.

## Chapter 3.

# Overlay Spectrum Sharing

This chapter focuses on overlay spectrum sharing, where different from underlay spectrum sharing, the secondary transmitter can utilize the knowledge of the primary message, which is acquired non-causally (i.e., known in advance before transmission) or causally (i.e., acquired in the first phase of a two-phase transmission), to help transmit the primary message besides its own message. The secondary power is split into two parts, where one is spent for the secondary message, and the other is spent for the primary message, to compensate for the interference induced at the primary receiver due to the secondary transmission, such that a certain primary rate requirement is satisfied.

Specifically, the coexistence of a MISO primary link and a MISO/MIMO secondary link is studied. When the secondary transmitter has non-causal knowledge of the primary message, DPC can be deployed at the secondary transmitter to precancel the interference (when decoding the secondary message at the secondary receiver), due to the transmission of the primary message from both transmitters. Alternatively, due to the high implementation complexity of DPC, linear precoding can be deployed at the secondary transmitter. In both cases, the primary transmitter employs MRT, and single-user decoding is deployed at the primary receiver; optimal beamforming/precoding and power allocation at the secondary transmitter is obtained, to maximize the achievable secondary rate while satisfying the primary rate requirement and the secondary power constraint.

When the secondary transmitter does not have non-causal knowledge of the primary message, and still wants to help with the primary transmission in return for the access to the spectrum, it can relay the primary message in an amplify-and-forward (AF) or a decode-and-forward (DF) way in a two-phase transmission, while transmitting its own message. The primary link has the incentive to adapt its transmission strategy to cooperate with the secondary link to fulfill its rate requirement, especially when the primary link is weak. To maximize the achievable secondary rate while satisfying the

primary rate requirement and the primary and secondary power constraints, in the case of AF cooperative spectrum sharing, optimal relaying matrix and beamforming vector at the secondary transmitter is obtained; in the case of DF cooperative spectrum sharing, a set of parameters are optimized, including relative duration of the two phases, primary transmission strategies in the two phases and secondary transmission strategy in the second phase.

This chapter is partly based on the results reported in [LBSJ<sup>+</sup>12], [LJBS<sup>+</sup>12], [LJ14] and [BSLT<sup>+</sup>13].

### 3.1. MISO Secondary Channel with Non-causal Primary Message Knowledge

#### 3.1.1. System Model

The system considered is depicted in Figure 3.1 and consists of a MISO primary link with  $N_{T,1}$  transmit antennas and a MISO secondary link with  $N_{T,2}$  transmit antennas. Assume that the secondary transmitter has non-causal knowledge of the primary message. The channels from the primary transmitter to the primary and secondary receivers are denoted as  $\mathbf{h}_{11}$  and  $\mathbf{h}_{12}$ , respectively. The channels from the secondary transmitter to the primary and secondary receivers are denoted as  $\mathbf{h}_{21}$  and  $\mathbf{h}_{22}$ , respectively. The noises at the primary and secondary receivers are denoted as  $n_1$  and  $n_2$ , respectively. The channels and noises are modeled as independent and identically distributed complex Gaussian random variables with zero mean and unit variance. Assume that the primary transmitter knows  $\mathbf{h}_{11}$ ; the secondary transmitter knows  $\mathbf{h}_{11}$ ,  $\mathbf{h}_{12}$ ,  $\mathbf{h}_{21}$  and  $\mathbf{h}_{22}$ .

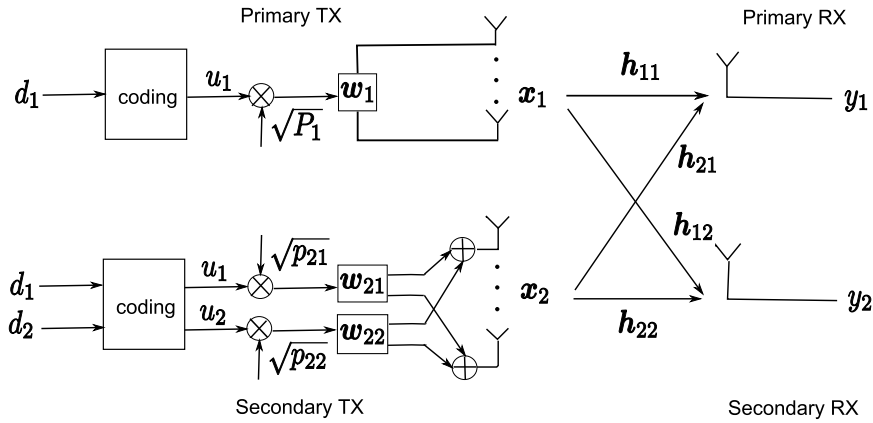


Figure 3.1.: System model consisting of a MISO primary link and a MISO secondary link – non-causal primary message at the secondary transmitter.

The primary transmission strategy is normally given and fixed, with a rate requirement of  $R_1^*$ , and single-user decoding is deployed at the primary receiver. The primary transmitter employs an  $N_{T,1} \times 1$  beamforming vector  $\mathbf{w}_1$  ( $\|\mathbf{w}_1\| = 1$ ) and power  $P_1$  for message  $d_1$ . With maximum ratio transmission, i.e.,  $\mathbf{w}_1 = \frac{\mathbf{h}_{11}}{\|\mathbf{h}_{11}\|}$ , the signal from the primary transmitter is

$$\mathbf{x}_1 = \sqrt{P_1} \frac{\mathbf{h}_{11}}{\|\mathbf{h}_{11}\|} u_1(d_1), \quad (3.1)$$

where  $d_1$  is encoded into symbol  $u_1$  with unit average power, by a random Gaussian codebook with fixed information rate  $R_1^*$ . The primary receiver has knowledge of the

codebook of  $d_1$ .

Since the secondary transmitter has non-causal knowledge of  $d_1$ , it can transmit  $d_1$  to the primary receiver as a return for the access to the spectrum. The secondary transmitter has a total power of  $P_2$ . A fraction  $p_{21}$  of it is spent in a selfless manner to help the primary link achieve its rate requirement, and the remaining power  $p_{22}$  is used for the transmission of its own message  $d_2$ .

### 3.1.2. Dirty-paper Coding at the Secondary Transmitter

With knowledge of the primary message and codebook and perfect channel state information at the secondary transmitter, the interference (when decoding  $d_2$  at the secondary receiver) due to the transmission of  $d_1$  from both transmitters is known, and can be precanceled by DPC. Specifically,  $d_1$  is encoded at first such that the interference is known before encoding of  $d_2$ . Note that it does not work to encode  $d_2$  before  $d_1$  to precancel the interference due to  $d_2$  at the primary receiver, since  $d_1$  is also present in the primary transmission which is given and fixed.

With superposition coding in combination of DPC, the signal from the secondary transmitter is

$$\mathbf{x}_2 = \sqrt{p_{21}}\mathbf{w}_{21}u_1(d_1) + \sqrt{p_{22}}\mathbf{w}_{22}u_2(d_1, d_2), \quad (3.2)$$

where  $d_1$  is encoded into symbol  $u_1$  with unit average power by the same codebook at the primary transmitter,  $d_2$  is encoded into symbol  $u_2$  with unit average power by DPC, and  $\mathbf{w}_{21}$  ( $\|\mathbf{w}_{21}\| = 1$ ) and  $\mathbf{w}_{22}$  ( $\|\mathbf{w}_{22}\| = 1$ ) are the  $N_{T,2} \times 1$  beamforming vectors. The secondary receiver has knowledge of the codebooks of  $d_1$  and  $d_2$ .

The signals at the primary and secondary receivers are

$$y_1 = \left( \sqrt{P_1}\|\mathbf{h}_{11}\| + \sqrt{p_{21}}\mathbf{h}_{21}^H\mathbf{w}_{21} \right) u_1(d_1) + \sqrt{p_{22}}\mathbf{h}_{21}^H\mathbf{w}_{22}u_2(d_1, d_2) + n_1, \quad (3.3)$$

$$y_2 = \sqrt{p_{22}}\mathbf{h}_{22}^H\mathbf{w}_{22}u_2(d_1, d_2) + \left( \frac{\sqrt{P_1}}{\|\mathbf{h}_{11}\|}\mathbf{h}_{12}^H\mathbf{h}_{11} + \sqrt{p_{21}}\mathbf{h}_{22}^H\mathbf{w}_{21} \right) u_1(d_1) + n_2, \quad (3.4)$$

respectively, which can be written as

$$\underbrace{\begin{bmatrix} y_1 \\ y_2 \end{bmatrix}}_{\mathbf{y}} = \underbrace{\begin{bmatrix} \mathbf{h}_{11}^H & \mathbf{h}_{21}^H \\ \mathbf{h}_{12}^H & \mathbf{h}_{22}^H \end{bmatrix}}_{\mathbf{H}} \underbrace{\begin{bmatrix} \sqrt{P_1} \frac{\mathbf{h}_{11}}{\|\mathbf{h}_{11}\|} & 0 \\ \sqrt{p_{21}}\mathbf{w}_{21} & \sqrt{p_{22}}\mathbf{w}_{22} \end{bmatrix}}_{\mathbf{W}} \underbrace{\begin{bmatrix} u_1(d_1) \\ u_2(d_1, d_2) \end{bmatrix}}_{\mathbf{u}} + \underbrace{\begin{bmatrix} n_1 \\ n_2 \end{bmatrix}}_{\mathbf{n}}, \quad (3.5)$$

i.e.,

$$\mathbf{y} = \mathbf{H}\mathbf{W}\mathbf{u} + \mathbf{n}, \quad (3.6)$$

where equivalently  $\mathbf{y}$  is the  $2 \times 1$  received signal vector,  $\mathbf{H}$  is the  $2 \times (N_{T,1} + N_{T,2})$  channel matrix,  $\mathbf{W}$  is the  $(N_{T,1} + N_{T,2}) \times 2$  precoding matrix,  $\mathbf{u}$  is the  $2 \times 1$  transmitted signal vector, and  $\mathbf{n}$  is the  $2 \times 1$  noise vector.

### 3.1. MISO Secondary Channel with Non-causal Primary Message Knowledge

The precoding matrix  $\mathbf{W}$  not only includes the precoding at both transmitters but also reflects the fact that the transmitters are independent and the primary transmitter has only access to  $u_1$ , while the secondary transmitter has access to both  $u_1$  and  $u_2$ . The advantage of this notation is that the achievability results derived for the single-transmitter multi-antenna broadcast channel apply directly to the two-transmitter scenario, as long as the precoding matrix is constrained to have such form [CS03] [WSS06]. Consequently, the achievable rates for the primary and secondary links are

$$R_1 = \log_2 \left( 1 + \frac{|\sqrt{P_1}|\|\mathbf{h}_{11}\| + \sqrt{p_{21}}\mathbf{h}_{21}^H\mathbf{w}_{21}|^2}{1 + p_{22}|\mathbf{h}_{21}^H\mathbf{w}_{22}|^2} \right), \quad (3.7)$$

$$R_2 = \log_2 (1 + p_{22}|\mathbf{h}_{22}^H\mathbf{w}_{22}|^2), \quad (3.8)$$

respectively, for any feasible choice of beamforming vectors  $\mathbf{w}_{21}$  and  $\mathbf{w}_{22}$  and powers  $p_{21}$  and  $p_{22}$ .

To maximize the secondary achievable rate  $R_2$  while satisfying the primary rate requirement  $R_1^*$  and the secondary power constraint  $P_2$ , the optimization problem can be formulated as

$$\max_{\substack{\mathbf{w}_{21}, \mathbf{w}_{22} \\ p_{21}, p_{22}}} p_{22}|\mathbf{h}_{22}^H\mathbf{w}_{22}|^2 \quad (3.9a)$$

$$\text{s.t. } \log_2 \left( 1 + \frac{|\sqrt{P_1}|\|\mathbf{h}_{11}\| + \sqrt{p_{21}}\mathbf{h}_{21}^H\mathbf{w}_{21}|^2}{1 + p_{22}|\mathbf{h}_{21}^H\mathbf{w}_{22}|^2} \right) \geq R_1^*, \quad (3.9b)$$

$$\|\mathbf{w}_{21}\| = \|\mathbf{w}_{22}\| = 1, \quad (3.9c)$$

$$p_{21} + p_{22} \leq P_2, p_{21} \geq 0, p_{22} \geq 0. \quad (3.9d)$$

**Proposition 5.** *To solve (3.9), the optimal beamforming vector  $\mathbf{w}_{21}$  is*

$$\mathbf{w}_{21}^* = \frac{\mathbf{h}_{21}}{\|\mathbf{h}_{21}\|}, \quad (3.10)$$

and the beamforming vector  $\mathbf{w}_{22}$  can be parametrized as

$$\mathbf{w}_{22}(\lambda) = \sqrt{\lambda} \frac{\Pi_{\mathbf{h}_{21}} \mathbf{h}_{22}}{\|\Pi_{\mathbf{h}_{21}} \mathbf{h}_{22}\|} + \sqrt{1-\lambda} \frac{\Pi_{\mathbf{h}_{21}}^\perp \mathbf{h}_{22}}{\|\Pi_{\mathbf{h}_{21}}^\perp \mathbf{h}_{22}\|}, \quad (3.11)$$

where

$$\lambda = \min \left( \lambda_{\text{MRT}}, \frac{P_{\text{int}}}{p_{22}\|\mathbf{h}_{21}\|^2} \right), \quad (3.12)$$

$$P_{\text{int}} = \frac{(\sqrt{P_1}\|\mathbf{h}_{11}\| + \sqrt{p_{21}}\|\mathbf{h}_{21}\|)^2}{2^{R_1^*} - 1} - 1 \geq 0, \quad (3.13)$$

$$p_{21} = P_2 - p_{22}, \quad (3.14)$$

$$\Pi_{\mathbf{h}_{21}} = \frac{\mathbf{h}_{21}\mathbf{h}_{21}^H}{\|\mathbf{h}_{21}\|^2}, \Pi_{\mathbf{h}_{21}}^\perp = \mathbf{I} - \Pi_{\mathbf{h}_{21}} \text{ and } \lambda_{\text{MRT}} = \frac{\|\Pi_{\mathbf{h}_{21}}\mathbf{h}_{22}\|^2}{\|\mathbf{h}_{22}\|^2}.$$

The optimal solution to (3.9) can be obtained by varying  $p_{22} \in [0, P_2]$  to achieve the maximum secondary rate.

*Proof.* The proof is provided in Section 3.6.1.  $\square$

**Remark 11.** The beamforming vector for the secondary message has the same form of parametrization with one real-valued parameter, as that in the MISO underlay spectrum sharing with weak interference as in Section 2.1.2. Full power transmission is used at the secondary transmitter. A line search is required to find the optimal beamforming vector and power allocation, which significantly reduces the computational complexity of solving (3.9) with two complex-valued vectors and two real-valued scalars.

**Remark 12.** The special case of  $p_{21} = 0$  in (3.9) corresponds to the MISO underlay spectrum sharing with very strong interference as in Section 2.1.4, with interference precancellation by DPC instead of interference cancellation by successive decoding. It shows that the proposed MISO overlay spectrum sharing can achieve a higher secondary rate than the MISO underlay spectrum sharing as proposed in Section 2.1.

### 3.1.3. Linear Precoding at the Secondary Transmitter

As in Figure 3.1, due to the high implementation complexity of DPC, linear precoding is deployed at the secondary transmitter for the primary message  $d_1$  and the secondary message  $d_2$ , i.e.,  $u_2(d_2)$  instead of  $u_2(d_1, d_2)$ , which is suboptimal compared with DPC. The signal from the secondary transmitter is

$$\mathbf{x}_2 = \sqrt{p_{21}}\mathbf{w}_{21}u_1(d_1) + \sqrt{p_{22}}\mathbf{w}_{22}u_2(d_2), \quad (3.15)$$

where  $d_1$  is encoded into symbol  $u_1$  with unit average power by the same codebook at the primary transmitter,  $d_2$  is encoded into symbol  $u_2$  with unit average power by a different Gaussian codebook, and  $\mathbf{w}_{21}$  ( $\|\mathbf{w}_{21}\| = 1$ ) and  $\mathbf{w}_{22}$  ( $\|\mathbf{w}_{22}\| = 1$ ) are the  $N_{T,2} \times 1$  beamforming vectors. The secondary receiver has knowledge of the codebook of  $d_2$ .

The signals at the primary and secondary receivers are

$$y_1 = \left( \sqrt{P_1}\|\mathbf{h}_{11}\| + \sqrt{p_{21}}\mathbf{h}_{21}^H\mathbf{w}_{21} \right) u_1(d_1) + \sqrt{p_{22}}\mathbf{h}_{21}^H\mathbf{w}_{22}u_2(d_2) + n_1, \quad (3.16)$$

$$y_2 = \sqrt{p_{22}}\mathbf{h}_{22}^H\mathbf{w}_{22}u_2(d_2) + \left( \frac{\sqrt{P_1}}{\|\mathbf{h}_{11}\|}\mathbf{h}_{12}^H\mathbf{h}_{11} + \sqrt{p_{21}}\mathbf{h}_{22}^H\mathbf{w}_{21} \right) u_1(d_1) + n_2, \quad (3.17)$$

respectively.



The achievable rates for the primary and secondary links are

$$R_1 = \log_2 \left( 1 + \frac{|\sqrt{P_1} \|\mathbf{h}_{11}\| + \sqrt{p_{21}} \mathbf{h}_{21}^H \mathbf{w}_{21}|^2}{1 + p_{22} |\mathbf{h}_{21}^H \mathbf{w}_{22}|^2} \right), \quad (3.18)$$

$$R_2 = \log_2 \left( 1 + \frac{p_{22} |\mathbf{h}_{22}^H \mathbf{w}_{22}|^2}{1 + \left| \frac{\sqrt{P_1}}{\|\mathbf{h}_{11}\|} \mathbf{h}_{12}^H \mathbf{h}_{11} + \sqrt{p_{21}} \mathbf{h}_{22}^H \mathbf{w}_{21} \right|^2} \right), \quad (3.19)$$

respectively, for any feasible choice of beamforming vectors  $\mathbf{w}_{21}$  and  $\mathbf{w}_{22}$  and powers  $p_{21}$  and  $p_{22}$ .

To maximize the secondary achievable rate  $R_2$  while satisfying the primary rate requirement  $R_1^*$  and the secondary power constraint  $P_2$ , the optimization problem can be formulated as

$$\max_{\substack{\mathbf{w}_{21}, \mathbf{w}_{22} \\ p_{21}, p_{22}}} \frac{p_{22} |\mathbf{h}_{22}^H \mathbf{w}_{22}|^2}{1 + \left| \frac{\sqrt{P_1}}{\|\mathbf{h}_{11}\|} \mathbf{h}_{12}^H \mathbf{h}_{11} + \sqrt{p_{21}} \mathbf{h}_{22}^H \mathbf{w}_{21} \right|^2} \quad (3.20a)$$

$$\text{s.t. } \log_2 \left( 1 + \frac{|\sqrt{P_1} \|\mathbf{h}_{11}\| + \sqrt{p_{21}} \mathbf{h}_{21}^H \mathbf{w}_{21}|^2}{1 + p_{22} |\mathbf{h}_{21}^H \mathbf{w}_{22}|^2} \right) \geq R_1^*, \quad (3.20b)$$

$$\|\mathbf{w}_{21}\| = \|\mathbf{w}_{22}\| = 1, \quad (3.20c)$$

$$p_{21} + p_{22} \leq P_2, p_{21} \geq 0, p_{22} \geq 0. \quad (3.20d)$$

**Proposition 6.** *The beamforming vectors that solve (3.20) can be parametrized as*

$$\mathbf{w}_{21}(\lambda_1, \psi_1, \psi_2) = e^{j\psi_1} \sqrt{\lambda_1} \frac{\Pi_{\mathbf{h}_{22}} \mathbf{h}_{21}}{\|\Pi_{\mathbf{h}_{22}} \mathbf{h}_{21}\|} + e^{j\psi_2} \sqrt{1 - \lambda_1} \frac{\Pi_{\mathbf{h}_{22}}^\perp \mathbf{h}_{21}}{\|\Pi_{\mathbf{h}_{22}}^\perp \mathbf{h}_{21}\|}, \quad (3.21)$$

$$\mathbf{w}_{22}(\lambda_2) = \sqrt{\lambda_2} \frac{\Pi_{\mathbf{h}_{21}} \mathbf{h}_{22}}{\|\Pi_{\mathbf{h}_{21}} \mathbf{h}_{22}\|} + \sqrt{1 - \lambda_2} \frac{\Pi_{\mathbf{h}_{21}}^\perp \mathbf{h}_{22}}{\|\Pi_{\mathbf{h}_{21}}^\perp \mathbf{h}_{22}\|}, \quad (3.22)$$

where

$$\psi_2 = \angle \varphi, \quad (3.23)$$

$$\varphi = \sqrt{P_1} \|\mathbf{h}_{11}\| + e^{j\psi_1} \sqrt{\lambda_1} \sqrt{p_{21}} \mathbf{h}_{21}^H \frac{\Pi_{\mathbf{h}_{22}} \mathbf{h}_{21}}{\|\Pi_{\mathbf{h}_{22}} \mathbf{h}_{21}\|}, \quad (3.24)$$

$$\lambda_2 = \min \left( \lambda_{\text{MRT}}, \frac{P_{\text{int}}}{p_{22} \|\mathbf{h}_{21}\|^2} \right), \quad (3.25)$$

$$p_{22} = P_2 - p_{21}, \quad (3.26)$$

$$P_{\text{int}} = \frac{|\sqrt{P_1} \|\mathbf{h}_{11}\| + \sqrt{p_{21}} \mathbf{h}_{21}^H \mathbf{w}_{21}(\lambda_1, \psi_1, \psi_2)|^2}{2^{R_1^*} - 1} - 1 \geq 0, \quad (3.27)$$

$$\Pi_{\mathbf{h}_{22}} = \frac{\mathbf{h}_{22} \mathbf{h}_{22}^H}{\|\mathbf{h}_{22}\|^2}, \quad \Pi_{\mathbf{h}_{22}}^\perp = \mathbf{I} - \Pi_{\mathbf{h}_{22}}, \quad \Pi_{\mathbf{h}_{21}} = \frac{\mathbf{h}_{21} \mathbf{h}_{21}^H}{\|\mathbf{h}_{21}\|^2}, \quad \Pi_{\mathbf{h}_{21}}^\perp = \mathbf{I} - \Pi_{\mathbf{h}_{21}} \quad \text{and} \quad \lambda_{\text{MRT}} = \frac{\|\Pi_{\mathbf{h}_{21}} \mathbf{h}_{22}\|^2}{\|\mathbf{h}_{22}\|^2}.$$

The optimal solution to (3.20) can be obtained by varying  $\psi_1 \in [0, 2\pi]$ ,  $\lambda_1 \in [0, 1]$  and  $p_{21} \in [0, P_2]$  to achieve the maximum secondary rate.

*Proof.* The proof is provided in Section 3.6.2.  $\square$

**Remark 13.** *The beamforming vector for the secondary message has the same form of parametrization with one real-valued parameter, as that when DPC is deployed at the secondary transmitter as in Section 3.1.2.*

**Remark 14.** *The beamforming vector for the primary message is parametrized with three real-valued parameters, as the weighted sum of the projections of the channel  $\mathbf{h}_{21}$  into the space and null space of the channel  $\mathbf{h}_{22}$ , respectively.  $\psi_1$  and  $\psi_2$  adjust the phases of these two directions in the beamforming vector to adapt to the primary message transmitted from the primary transmitter to the two receivers.*

**Remark 15.** *Full power transmission is used at the secondary transmitter. A cubic search is required to find the optimal beamforming vectors and power allocation, which significantly reduces the computational complexity of solving (3.20) with two complex-valued vectors and two real-valued scalars.*

**Remark 16.** *The optimization problems (3.9) and (3.20) have the same constraints but different objective functions in (3.9a) and (3.20a), which indicates a higher secondary rate can be achieved with the deployment of DPC than linear precoding at the secondary transmitter.*

### 3.1.4. Numerical Simulations

Numerical simulations are performed to evaluate the performance of the proposed MISO overlay spectrum sharing with DPC at the secondary transmitter (*MISO OSS DPC*), and compare with that of MISO underlay spectrum sharing (*MISO USS RS*), as proposed in Section 2.1, in terms of achievable secondary rate (in bit/s/Hz) versus SNR of the secondary link (in dB). The performance of the proposed MISO overlay spectrum sharing with linear precoding at the secondary transmitter (*MISO OSS LP*) is also evaluated and compared with that of *MISO OSS DPC*. The SNR is defined as the ratio of the transmit power and the noise power at the receiver, and since the noise power is normalized, the SNR is equivalent to the transmit power.

The primary rate requirement is set as a fraction of its instantaneous point-to-point channel capacity without secondary transmission, i.e.,

$$R_1^* = \rho \log_2 (1 + P_1 \|\mathbf{h}_{11}\|^2), \quad (3.28)$$

where  $0 < \rho \leq 1$  is the load factor of the primary link.

### 3.1. MISO Secondary Channel with Non-causal Primary Message Knowledge

The system configuration is as follows. The primary and secondary transmitters have 2 antennas each. The SNR of the primary link is fixed at 10 dB, and the SNR of the secondary link is varied from 0 dB to 20 dB. The load factor of the primary link is varied from 25% to 100%. The simulation results are averaged over 1000 channel realizations. As in Figure 3.2, at the load factor of 75% and SNR of 10 dB, the rate gain of *MISO OSS DPC* over *MISO USS RS* is about 1.7 bits/s/Hz. The variation of the load factor does not have a significant impact on the achievable secondary rate in the case of *MISO OSS DPC* compared with that of *MISO USS RS*, since *MISO OSS DPC* has the freedom to allocate power for the transmission of the primary message to compensate for the interference caused by the transmission of its own message. As in Figure 3.3, the rate loss of *MISO OSS LP* to *MISO OSS DPC* is about 0.9 bit/s/Hz at the load factor of 75% and SNR of 10 dB. As the SNR increases, the achievable secondary rate of *MISO OSS LP* approaches that of *MISO OSS DPC*, though still with gap at high SNRs.

Numerical results show that with non-causal knowledge of the primary message and the deployment of DPC at the secondary transmitter, overlay spectrum sharing can achieve a significantly higher secondary rate than underlay spectrum sharing; the rate loss due to the deployment of linear precoding instead of DPC at the secondary transmitter is less significant at high SNRs.

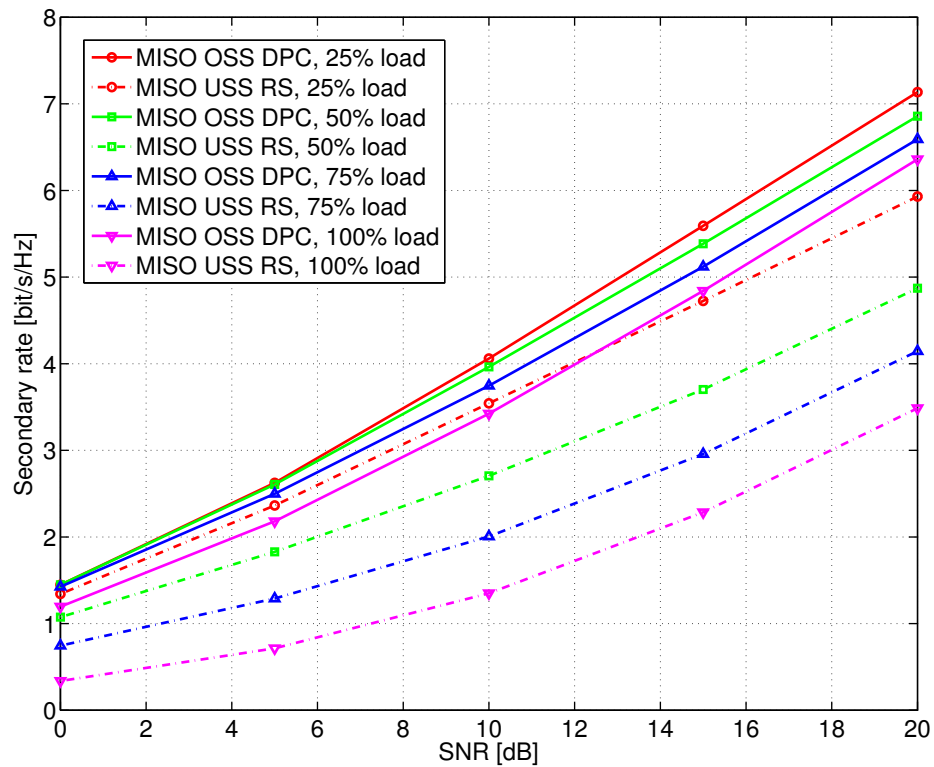


Figure 3.2.: Achievable secondary rate versus SNR of the secondary link: *MISO OSS DPC* versus *MISO USS RS* with different primary link loads.

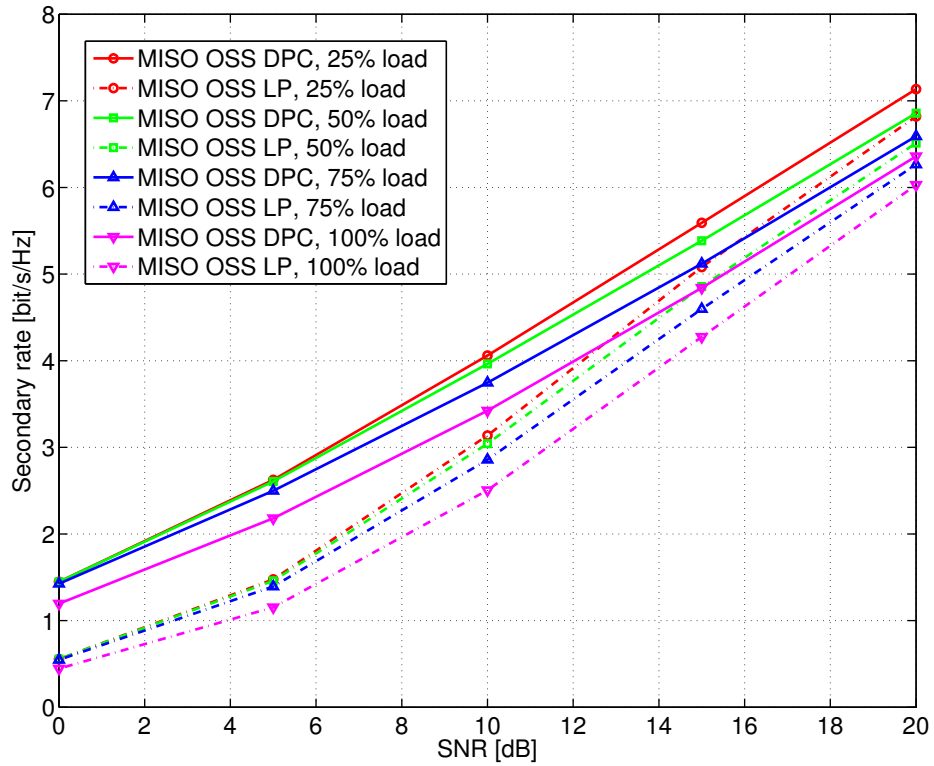


Figure 3.3.: Achievable secondary rate versus SNR of the secondary link: *MISO OSS DPC* versus *MISO OSS LP* with different primary link loads.

## 3.2. MIMO Secondary Channel with Non-causal Primary Message Knowledge

### 3.2.1. System Model

The system considered is depicted in Figure 3.4 and consists of a MISO primary link with  $N_{T,1}$  transmit antennas and a MIMO secondary link with  $N_{T,2}$  transmit antennas and  $N_{R,2}$  receive antennas. Assume that the secondary transmitter has non-causal knowledge of the primary message. The channels from the primary transmitter to the primary and secondary receivers are denoted as  $\mathbf{h}_{11}$  and  $\mathbf{H}_{12}$ , respectively. The channels from the secondary transmitter to the primary and secondary receivers are denoted as  $\mathbf{h}_{21}$  and  $\mathbf{H}_{22}$ , respectively. The noises at the primary and secondary receivers are denoted as  $n_1$  and  $n_2$ , respectively. The channels and noises are modeled as independent and identically distributed complex Gaussian random variables with zero mean and unit variance. Assume that the primary transmitter knows  $\mathbf{h}_{11}$ ; the secondary transmitter knows  $\mathbf{h}_{11}$ ,  $\mathbf{H}_{12}$ ,  $\mathbf{h}_{21}$  and  $\mathbf{H}_{22}$ .

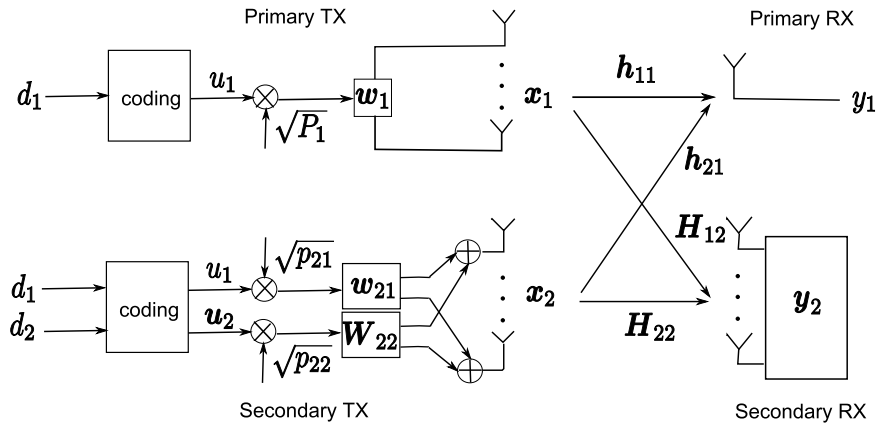


Figure 3.4.: System model consisting of a MISO primary link and a MIMO secondary link – non-causal primary message at the secondary transmitter.

The primary transmission strategy is normally given and fixed, with a rate requirement of  $R_1^*$ , and single-user decoding is deployed at the primary receiver. The primary transmitter employs an  $N_{T,1} \times 1$  beamforming vector  $\mathbf{w}_1$  ( $\|\mathbf{w}_1\| = 1$ ) and power  $P_1$  for message  $d_1$ . With maximum ratio transmission, i.e.,  $\mathbf{w}_1 = \frac{\mathbf{h}_{11}}{\|\mathbf{h}_{11}\|}$ , the signal from the primary transmitter is

$$\mathbf{x}_1 = \sqrt{P_1} \frac{\mathbf{h}_{11}}{\|\mathbf{h}_{11}\|} u_1(d_1), \quad (3.29)$$

where  $d_1$  is encoded into symbol  $u_1$  with unit average power, by a random Gaussian

codebook with fixed information rate  $R_1^*$ . The primary receiver has knowledge of the codebook of  $d_1$ .

Since the secondary transmitter has non-causal knowledge of  $d_1$ , it can transmit  $d_1$  to the primary receiver as a return for the access to the spectrum. The secondary transmitter has a total power of  $P_2$ . A fraction  $p_{21}$  of it is spent in a selfless manner to help the primary link achieve its rate requirement, and the remaining power  $p_{22}$  is used for the transmission of its own message  $d_2$ .

### 3.2.2. Dirty-paper Coding at the Secondary Transmitter

With knowledge of the primary message and codebook and perfect channel state information at the secondary transmitter, the interference (when decoding  $d_2$  at the secondary receiver) due to the transmission of  $d_1$  from both transmitters is known, and can be precanceled by DPC. With superposition coding in combination with DPC, the signal from the secondary transmitter is

$$\mathbf{x}_2 = \sqrt{p_{21}}\mathbf{w}_{21}u_1(d_1) + \sqrt{p_{22}}\mathbf{W}_{22}\mathbf{u}_2(d_1, d_2), \quad (3.30)$$

where  $d_1$  is encoded into symbol  $u_1$  with unit average power by the same codebook at the primary transmitter,  $d_2$  is encoded into  $M \times 1$  vector  $\mathbf{u}_2$  of symbols with unit average power by DPC, and  $\mathbf{w}_{21}$  ( $\|\mathbf{w}_{21}\| = 1$ ) is the  $N_{T,2} \times 1$  beamforming vector and  $\mathbf{W}_{22}$  ( $\|\mathbf{W}_{22}\| = 1$ ) is the  $N_{T,2} \times M$  precoding matrix, where  $1 \leq M \leq \min(N_{R,2}, N_{T,2})$ . The secondary receiver has knowledge of the codebooks of  $d_1$  and  $d_2$ .

By the same arguments in Section 3.1.2 and the results from [CS03] [WSS06], the achievable rates for the primary and secondary links are

$$R_1 = \log_2 \left( 1 + \frac{|\sqrt{P_1}|\|\mathbf{h}_{11}\| + \sqrt{p_{21}}\mathbf{h}_{21}^H\mathbf{w}_{21}|^2}{1 + p_{22}\|\mathbf{h}_{21}^H\mathbf{W}_{22}\|^2} \right), \quad (3.31)$$

$$R_2 = \log_2 |\mathbf{I} + p_{22}\mathbf{H}_{22}\mathbf{W}_{22}\mathbf{W}_{22}^H\mathbf{H}_{22}^H|, \quad (3.32)$$

for any feasible choice of beamforming vector  $\mathbf{w}_{21}$ , precoding matrix  $\mathbf{W}_{22}$  and powers  $p_{21}$  and  $p_{22}$ .

To maximize the secondary achievable rate  $R_2$  while satisfying the primary rate requirement  $R_1^*$  and the secondary power constraint  $P_2$ , the optimization problem can be

formulated as

$$\max_{\substack{\mathbf{w}_{21}, \mathbf{W}_{22} \\ p_{21}, p_{22}}} \log_2 |\mathbf{I} + p_{22} \mathbf{H}_{22} \mathbf{W}_{22} \mathbf{W}_{22}^H \mathbf{H}_{22}^H| \quad (3.33a)$$

$$\text{s.t. } \log_2 \left( 1 + \frac{|\sqrt{P_1} \|\mathbf{h}_{11}\| + \sqrt{p_{21}} \mathbf{h}_{21}^H \mathbf{w}_{21}|^2}{1 + p_{22} \|\mathbf{h}_{21}^H \mathbf{W}_{22}\|^2} \right) \geq R_1^*, \quad (3.33b)$$

$$\|\mathbf{w}_{21}\| = \|\mathbf{W}_{22}\| = 1, \quad (3.33c)$$

$$p_{21} + p_{22} \leq P_2, p_{21} \geq 0, p_{22} \geq 0. \quad (3.33d)$$

**Proposition 7.** For (3.33), the optimal beamforming vector  $\mathbf{w}_{21}$  is

$$\mathbf{w}_{21}^* = \frac{\mathbf{h}_{21}}{\|\mathbf{h}_{21}\|}, \quad (3.34)$$

and the optimal precoding matrix  $\mathbf{W}_{22} = \mathbf{K}^{\frac{1}{2}} / \sqrt{P_2 - p_{21}}$  to (3.33) can be obtained by a linear search over  $p_{21} \in [0, P_2]$  while solving the following convex optimization problem

$$\max_{p_{21}, \mathbf{K}} \log_2 |\mathbf{I} + \mathbf{H}_{22} \mathbf{K} \mathbf{H}_{22}^H| \quad (3.35a)$$

$$\text{s.t. } \mathbf{h}_{21}^H \mathbf{K} \mathbf{h}_{21} \leq P_{\text{int}}, \quad (3.35b)$$

$$p_{21} + \text{tr}(\mathbf{K}) \leq P_2, p_{21} \geq 0, \mathbf{K} \succeq \mathbf{0}, \quad (3.35c)$$

to achieve the maximum secondary rate, where  $P_{\text{int}} = \frac{(\sqrt{P_1} \|\mathbf{h}_{11}\| + \sqrt{p_{21}} \|\mathbf{h}_{21}\|)^2}{2^{R_1^*} - 1} - 1 \geq 0$ .

*Proof.* The proof is provided in Section 3.6.3. □

**Remark 17.** The optimal transmit covariance matrix for the secondary message and power allocation is obtained by a line search while solving the corresponding convex optimization problem, e.g., by interior point methods [BV04], which significantly reduces the computational complexity of solving (3.33) with one complex-valued vector, one complex-valued matrix and two real-valued scalars. Full power transmission is used at the secondary transmitter.

**Remark 18.** The special case of  $p_{21} = 0$  in (3.33) corresponds to Case 2 of the MIMO underlay spectrum sharing in Section 2.2, with interference precancellation by DPC instead of interference cancellation by successive decoding. It shows that the proposed MIMO overlay spectrum sharing can achieve a higher secondary rate than the MIMO underlay spectrum sharing in Section 2.2.



### 3.2.3. Linear Precoding at the Secondary Transmitter

As in Figure 3.4, due to the high implementation complexity of DPC, linear precoding is deployed at the secondary transmitter for both the primary message  $d_1$  and the secondary message  $d_2$ , and single-stream transmission is used for  $d_2$  (The problem formulation with multiple-stream transmission is intractable.), i.e.,  $\mathbf{w}_{22}$  instead of  $\mathbf{W}_{22}$  and  $u_2(d_2)$  instead of  $\mathbf{u}_2(d_1, d_2)$ , which is suboptimal compared with DPC. The signal from the secondary transmitter is

$$\mathbf{x}_2 = \sqrt{p_{21}}\mathbf{w}_{21}u_1(d_1) + \sqrt{p_{22}}\mathbf{w}_{22}u_2(d_2), \quad (3.36)$$

where  $d_1$  is encoded into symbol  $u_1$  with unit average power by the same codebook at the primary transmitter,  $d_2$  is encoded into symbol  $u_2$  with unit average power by a different Gaussian codebook, and  $\mathbf{w}_{21}$  ( $\|\mathbf{w}_{21}\| = 1$ ) and  $\mathbf{w}_{22}$  ( $\|\mathbf{w}_{22}\| = 1$ ) are the  $N_{T,2} \times 1$  beamforming vectors. The secondary receiver has knowledge of the codebook of  $d_2$ .

The achievable rates for the primary and secondary links are

$$R_1 = \log_2 \left( 1 + \frac{|\sqrt{P_1}|\|\mathbf{h}_{11}\| + \sqrt{p_{21}}\mathbf{h}_{21}^H\mathbf{w}_{21}|^2}{1 + p_{22}|\mathbf{h}_{21}^H\mathbf{w}_{22}|^2} \right), \quad (3.37a)$$

$$R_2 = \log_2 (1 + p_{22}\mathbf{w}_{22}^H\mathbf{H}_{22}^H\mathbf{Z}^{-1}\mathbf{H}_{22}\mathbf{w}_{22}), \quad (3.37b)$$

for any feasible choice of beamforming vectors  $\mathbf{w}_{21}$  and  $\mathbf{w}_{22}$  and powers  $p_{21}$  and  $p_{22}$ , where  $\mathbf{Z}$  is the interference-plus-noise covariance matrix, i.e.,

$$\mathbf{Z} = \mathbf{I} + \left( \frac{\sqrt{P_1}}{\|\mathbf{h}_{11}\|}\mathbf{H}_{12}\mathbf{h}_{11} + \sqrt{p_{21}}\mathbf{H}_{22}\mathbf{w}_{21} \right) \left( \frac{\sqrt{P_1}}{\|\mathbf{h}_{11}\|}\mathbf{H}_{12}\mathbf{h}_{11} + \sqrt{p_{21}}\mathbf{H}_{22}\mathbf{w}_{21} \right)^H. \quad (3.38)$$

To maximize the secondary achievable rate  $R_2$  while satisfying the primary rate requirement  $R_1^*$  and the secondary power constraint  $P_2$ , the optimization problem can be formulated as

$$\max_{\substack{\mathbf{w}_{21}, \mathbf{w}_{22} \\ p_{21}, p_{22}}} p_{22}\mathbf{w}_{22}^H\mathbf{H}_{22}^H\mathbf{Z}^{-1}\mathbf{H}_{22}\mathbf{w}_{22} \quad (3.39a)$$

$$\text{s.t. } \log_2 \left( 1 + \frac{|\sqrt{P_1}|\|\mathbf{h}_{11}\| + \sqrt{p_{21}}\mathbf{h}_{21}^H\mathbf{w}_{21}|^2}{1 + p_{22}|\mathbf{h}_{21}^H\mathbf{w}_{22}|^2} \right) \geq R_1^*, \quad (3.39b)$$

$$\|\mathbf{w}_{21}\| = \|\mathbf{w}_{22}\| = 1, \quad (3.39c)$$

$$p_{21} + p_{22} \leq P_2, p_{21} \geq 0, p_{22} \geq 0. \quad (3.39d)$$

The secondary transmitter employs full power transmission, since otherwise the remaining power can be accommodated into  $\mathbf{w}_{22}$  in the null space of the channel  $\mathbf{h}_{21}$ , such that the objective value is nondecreased and the constraints are still satisfied in (3.39).

(3.39) is intractable at first sight. With minimum mean square error (MMSE) receiver  $\mathbf{v} = \frac{\mathbf{Z}^{-1}\mathbf{H}_{22}\mathbf{w}_{22}}{\|\mathbf{Z}^{-1}\mathbf{H}_{22}\mathbf{w}_{22}\|}$  at the secondary receiver, (3.39) can be reformulated as

$$\max_{\substack{\mathbf{w}_{21}, \mathbf{w}_{22} \\ p_{21}, p_{22}}} \frac{p_{22}|\mathbf{v}^H \mathbf{H}_{22} \mathbf{w}_{22}|^2}{1 + \left| \mathbf{v}^H \left( \frac{\sqrt{P_1}}{\|\mathbf{h}_{11}\|} \mathbf{H}_{12} \mathbf{h}_{11} + \sqrt{p_{21}} \mathbf{H}_{22} \mathbf{w}_{21} \right) \right|^2} \quad (3.40a)$$

$$\text{s.t. } \log_2 \left( 1 + \frac{|\sqrt{P_1} \|\mathbf{h}_{11}\| + \sqrt{p_{21}} \mathbf{h}_{21}^H \mathbf{w}_{21}|^2}{1 + p_{22} |\mathbf{h}_{21}^H \mathbf{w}_{22}|^2} \right) \geq R_1^*, \quad (3.40b)$$

$$\|\mathbf{w}_{21}\| = \|\mathbf{w}_{22}\| = 1, \quad (3.40c)$$

$$p_{21} + p_{22} \leq P_2, p_{21} \geq 0, p_{22} \geq 0. \quad (3.40d)$$

Given  $\mathbf{v}$ , let  $\mathbf{g}_{22} = \mathbf{H}_{22}^H \mathbf{v}$  and  $g_{12} = \mathbf{v}^H \mathbf{H}_{12} \mathbf{h}_{11} / \|\mathbf{h}_{11}\|$  be the effective channels, (3.40) becomes

$$\max_{\substack{\mathbf{w}_{21}, \mathbf{w}_{22} \\ p_{21}, p_{22}}} \frac{p_{22}|\mathbf{g}_{22}^H \mathbf{w}_{22}|^2}{1 + |\sqrt{P_1} g_{12} + \sqrt{p_{21}} \mathbf{g}_{22}^H \mathbf{w}_{21}|^2} \quad (3.41a)$$

$$\text{s.t. } \log_2 \left( 1 + \frac{|\sqrt{P_1} \|\mathbf{h}_{11}\| + \sqrt{p_{21}} \mathbf{h}_{21}^H \mathbf{w}_{21}|^2}{1 + p_{22} |\mathbf{h}_{21}^H \mathbf{w}_{22}|^2} \right) \geq R_1^*, \quad (3.41b)$$

$$\|\mathbf{w}_{21}\| = \|\mathbf{w}_{22}\| = 1, \quad (3.41c)$$

$$p_{21} + p_{22} \leq P_2, p_{21} \geq 0, p_{22} \geq 0, \quad (3.41d)$$

which can be readily solved by [LJBS<sup>+</sup>12, Proposition 1]. By alternating optimization [BH02], specifically, iterative transmitter/receiver optimization as in [SY04], (3.39) can be solved by Algorithm 1. In each iteration, with given receiver, the optimal beamforming vectors and power allocation are obtained by solving the corresponding optimization problem; with given transmitter, the receiver is set as the MMSE receiver. The algorithm stops when the variation of the achievable secondary rate between two iterations is below certain accuracy.

---

**Algorithm 1** Algorithm to solve (3.39)

---

- 1: Initialize  $\mathbf{v}^{(0)}$ ,  $\ell = 0$ .
  - 2: **while**  $|R_2^{(\ell)} - R_2^{(\ell-1)}| > \epsilon$  **do**
  - 3:      $\ell ++$ ;
  - 4:     Obtain  $\mathbf{w}_{21}^{(\ell)}$ ,  $\mathbf{w}_{22}^{(\ell)}$ ,  $p_{21}^{(\ell)}$ ,  $p_{22}^{(\ell)}$  and  $R_2^{(\ell)}$  by solving (3.41);
  - 5:     Compute the MMSE receiver  $\mathbf{v}^{(\ell)}$ ;
  - 6: **end while**
  - 7: Output  $\mathbf{w}_{21}^{(\ell)}$ ,  $\mathbf{w}_{22}^{(\ell)}$ ,  $p_{21}^{(\ell)}$ ,  $p_{22}^{(\ell)}$  and  $\mathbf{v}^{(\ell)}$ .
- 

Since the objective value increases at each iteration and the objective function has an

upper-bound, the iterative algorithm converges. However, it is not guaranteed to achieve the global optimum. A good solution can be selected by several random initializations.

### 3.2.4. Numerical Simulations

Numerical simulations are performed to evaluate the performance of the proposed MIMO overlay spectrum sharing with DPC at the secondary transmitter (*MIMO OSS DPC*), and compare with that of MIMO underlay spectrum sharing (*MIMO USS RS*), as proposed in Section 2.2, in terms of achievable secondary rate (in bit/s/Hz) versus SNR of the secondary link (in dB). The performance of the proposed MIMO overlay spectrum sharing with linear precoding at the secondary transmitter (*MIMO OSS LP*) is also evaluated and compared with that of *MIMO OSS DPC*. The SNR is defined as the ratio of the transmit power and the noise power at the receiver, and since the noise power is normalized, the SNR is equivalent to the transmit power.

The primary rate requirement is set as a fraction of its instantaneous point-to-point channel capacity without secondary transmission, i.e.,

$$R_1^* = \rho \log_2 (1 + P_1 \|\mathbf{h}_{11}\|^2), \quad (3.42)$$

where  $0 < \rho \leq 1$  is the load factor of the primary link.

The system configuration is as follows. The primary transmitter has 2 antennas, and the secondary transmitter and receiver have 2 antennas each. The SNR of the primary link is fixed at 10 dB, and the SNR of the secondary link is varied from 0 dB to 20 dB. The load factor of the primary link is varied from 25% to 100%. The simulation results are averaged over 1000 channel realizations. As in Figure 3.5, at the load factor of 75% and SNR of 10 dB, the rate gain of *MIMO OSS DPC* over *MIMO USS RS* is about 0.9 bit/s/Hz, and the variation of the load factor does not have a significant impact on the achievable secondary rate in the case of *MIMO OSS DPC* compared with that of *MIMO USS RS*. As in Figure 3.6, the rate loss of *MIMO OSS LP* to *MIMO OSS DPC* is about 1 bit/s/Hz at the load factor of 75% and SNR of 10 dB, and the gap grows as the SNR increases, which is due to the deployment of single-stream transmission in *MIMO OSS LP*. The variation of the load factor does not have a significant impact on the achievable secondary rate in the case of *MIMO OSS LP* compared with that of *MIMO OSS DPC*. Due to the interference constraint at the primary receiver (primary rate requirement), *MIMO OSS DPC* cannot always achieve DoFs of 2 for the secondary transmission at high SNRs, resulting in a degradation on the achievable secondary rate. The degradation becomes larger with stricter interference constraint (higher load factor). While *MIMO OSS LP* always uses only 1 degree-of-freedom (DoF) with single-stream

transmission, with the extra DoF to adapt to the interference constraint at the primary receiver.

Numerical results show that with non-causal knowledge of the primary message and the deployment of DPC at the secondary transmitter, overlay spectrum sharing can achieve a significantly higher secondary rate than underlay spectrum sharing; the rate loss due to the deployment of linear precoding with single-stream transmission instead of DPC at the secondary transmitter is more significant at high SNRs.

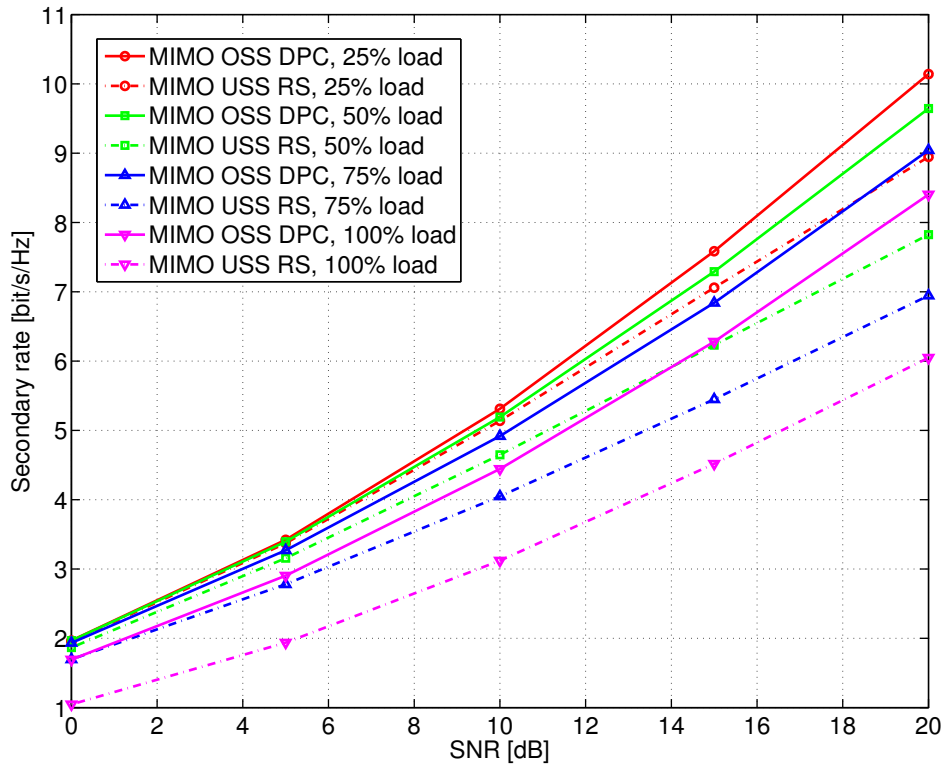


Figure 3.5.: Achievable secondary rate versus SNR of the secondary link: *MIMO OSS DPC* versus *MIMO USS RS* with different primary link loads.

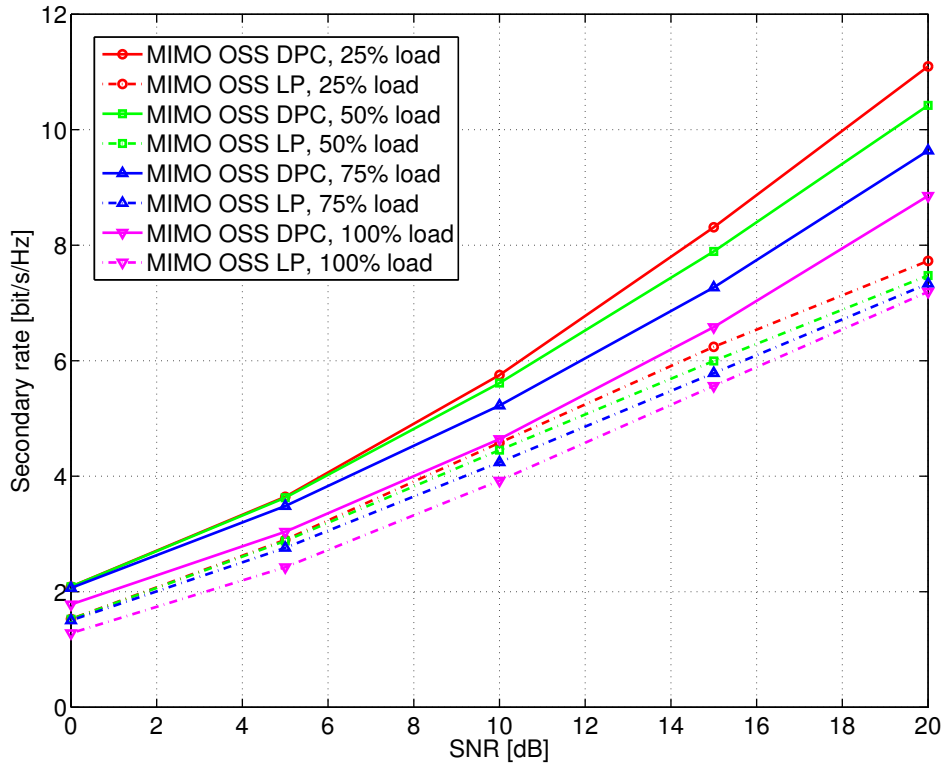


Figure 3.6.: Achievable secondary rate versus SNR of the secondary link: *MIMO OSS DPC* versus *MIMO OSS LP* with different primary link loads.

### 3.3. Amplify-and-Forward Cooperative Spectrum Sharing

#### 3.3.1. System Model

The system considered is depicted in Figure 3.7 and consists of a MISO primary link with  $N_{T,1}$  transmit antennas and a MIMO secondary link with  $N_{T,2}$  transmit antennas and  $N_{R,2}$  receive antennas, where the primary and secondary transmitters have power  $P_1$  and  $P_2$ , respectively. The primary link has a rate requirement of  $R_1^*$ . When the primary channel is good enough to achieve  $R_1^*$ , the cooperation from the secondary link is not required, thus the secondary link keeps silent; when the primary channel is in deep fading such that  $R_1^*$  cannot be fulfilled, the cooperation from the secondary link is requested to avoid outage of the primary link. Assume the secondary transmitter does not have non-causal knowledge of the primary message, and still wants to help with the primary transmission in return for the access to the spectrum. The secondary transmitter relays the primary message in an amplify-and-forward (AF) way, while transmitting its own message, where the transmission strategy of the primary link needs to be adapted. The secondary transmitter is half-duplex, i.e., it cannot transmit and receive simultaneously.

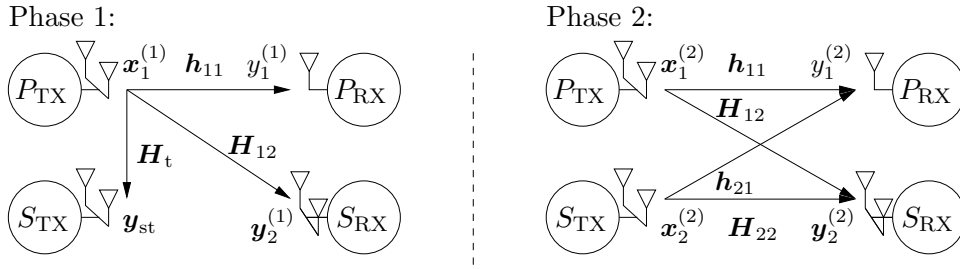


Figure 3.7.: System model consisting of a MISO primary link and a MIMO secondary link with two-phase transmission: primary transmitter ( $P_{TX}$ ), secondary transmitter ( $S_{TX}$ ), primary receiver ( $P_{RX}$ ) and secondary receiver ( $S_{RX}$ ).

The transmission consists of two phases. In the first phase, the primary transmitter employs maximum ratio transmission and power  $P_1$  for its encoded message  $d_1$ . The signal from the primary transmitter is

$$\mathbf{x}_1^{(1)} = \sqrt{P_1} \frac{\mathbf{h}_{11}}{\|\mathbf{h}_{11}\|} u_1(d_1), \quad (3.43)$$

where  $d_1$  is encoded into symbol  $u_1$  with unit average power, by a random Gaussian codebook with fixed information rate  $R_1^*$ . The primary receiver has knowledge of the codebook of  $d_1$ .

### 3.3. Amplify-and-Forward Cooperative Spectrum Sharing

The signals at the primary receiver and the secondary transmitter are

$$y_1^{(1)} = \mathbf{h}_{11}^H \mathbf{x}_1^{(1)} + n_1^{(1)}, \quad (3.44)$$

$$\mathbf{y}_{\text{st}} = \mathbf{H}_t \mathbf{x}_1^{(1)} + \mathbf{n}_{\text{st}}, \quad (3.45)$$

respectively, where  $\mathbf{x}_1^{(1)}$  is the  $N_{T,1} \times 1$  signal vector sent by the primary transmitter,  $\mathbf{h}_{11}$  is the  $N_{T,1} \times 1$  channel vector of the primary link,  $\mathbf{H}_t$  is the  $N_{T,2} \times N_{T,1}$  channel matrix between the two transmitters, and the scalar  $n_1^{(1)}$  and the  $N_{T,2} \times 1$  vector  $\mathbf{n}_{\text{st}}$  are the noises at the primary receiver and the secondary transmitter, respectively.

In the second phase, the primary transmitter transmits the same message, and employs the same transmission strategy as in the first phase, i.e.,  $\mathbf{x}_1^{(2)}$  has the same form as in (3.43). The secondary transmitter multiplies the received signal by an  $N_{T,2} \times N_{T,2}$  matrix  $\mathbf{A}$ , and employs an  $N_{T,2} \times 1$  beamforming vector  $\mathbf{w}$  for its encoded message  $d_2$ , assuming single-stream transmission (The problem formulation with multiple-stream transmission is intractable.). The signal from the secondary transmitter is

$$\mathbf{x}_2^{(2)} = \mathbf{A} \left( \mathbf{H}_t \sqrt{P_1} \frac{\mathbf{h}_{11}}{\|\mathbf{h}_{11}\|} u_1(d_1) + \mathbf{n}_{\text{st}} \right) + \mathbf{w} u_2(d_2), \quad (3.46)$$

where  $d_2$  is encoded into symbol  $u_2$  with unit average power by a different Gaussian codebook. The secondary receiver has knowledge of the codebook of  $d_2$ .

The signals at the primary and secondary receivers are

$$y_1^{(2)} = \mathbf{h}_{11}^H \mathbf{x}_1^{(2)} + \mathbf{h}_{21}^H \mathbf{x}_2^{(2)} + n_1^{(2)}, \quad (3.47)$$

$$\mathbf{y}_2^{(2)} = \mathbf{H}_{22} \mathbf{x}_2^{(2)} + \mathbf{H}_{12} \mathbf{x}_1^{(2)} + \mathbf{n}_2, \quad (3.48)$$

where  $\mathbf{x}_1^{(2)}$  and  $\mathbf{x}_2^{(2)}$  are the  $N_{T,1} \times 1$  and  $N_{T,2} \times 1$  signal vectors sent by the primary and secondary transmitters, respectively,  $\mathbf{h}_{i1}$  is the  $N_{T,i} \times 1$  channel vector between transmitter  $i \in \{1, 2\}$  and receiver 1,  $\mathbf{H}_{i2}$  is the  $N_{R,2} \times N_{T,i}$  channel matrix between transmitter  $i \in \{1, 2\}$  and receiver 2, and the scalar  $n_1^{(2)}$  and the  $N_{R,2} \times 1$  vector  $\mathbf{n}_2$  are the noises at the primary and secondary receivers, respectively.

The channels and noises are modeled as independent and identically distributed complex Gaussian random variables with zero mean and unit variance (The path-loss based channel fading is treated in the simulation.). Assume that the channels remain constant during the two phases, and the primary transmitter knows  $\mathbf{h}_{11}$ ; the secondary transmitter knows  $\mathbf{h}_{11}$ ,  $\mathbf{H}_{12}$ ,  $\mathbf{h}_{21}$ ,  $\mathbf{H}_{22}$  and  $\mathbf{H}_t$ .

The primary receiver applies maximum ratio combining (MRC) to the signals received from the two phases to maximize the received signal-to-interference-plus-noise ratio (SINR). The achievable rates for the primary and secondary links in the second phase

are

$$R_1 = \frac{1}{2} \log_2 \left( 1 + P_1 \|\mathbf{h}_{11}\|^2 + \frac{|\sqrt{P_1} \|\mathbf{h}_{11}\| + \frac{\sqrt{P_1}}{\|\mathbf{h}_{11}\|} \mathbf{h}_{21}^H \mathbf{A} \mathbf{H}_t \mathbf{h}_{11}|^2}{1 + \|\mathbf{h}_{21}^H \mathbf{A}\|^2 + |\mathbf{h}_{21}^H \mathbf{w}|^2} \right), \quad (3.49a)$$

$$R_2 = \frac{1}{2} \log_2 (1 + \mathbf{w}^H \mathbf{H}_{22}^H \mathbf{Z}^{-1} \mathbf{H}_{22} \mathbf{w}), \quad (3.49b)$$

where  $\mathbf{Z}$  is the interference-plus-noise covariance matrix, i.e.,

$$\mathbf{Z} = \mathbf{I} + \frac{P_1}{\|\mathbf{h}_{11}\|^2} (\mathbf{H}_{12} \mathbf{h}_{11} + \mathbf{H}_{22} \mathbf{A} \mathbf{H}_t \mathbf{h}_{11}) (\mathbf{H}_{12} \mathbf{h}_{11} + \mathbf{H}_{22} \mathbf{A} \mathbf{H}_t \mathbf{h}_{11})^H + \mathbf{H}_{22} \mathbf{A} \mathbf{A}^H \mathbf{H}_{22}^H. \quad (3.50)$$

To maximize the secondary achievable rate  $R_2$  while satisfying the primary rate requirement  $R_1^*$  and the secondary power constraint  $P_2$ , the optimization problem can be formulated as

$$\max_{\mathbf{A}, \mathbf{w}} R_2 \quad (3.51a)$$

$$\text{s.t. } R_1 \geq R_1^*, \quad (3.51b)$$

$$\text{tr}(\mathbf{A} \mathbf{M} \mathbf{A}^H + \mathbf{w} \mathbf{w}^H) \leq P_2, \quad (3.51c)$$

where  $\mathbf{M} = \mathbf{I} + \frac{P_1}{\|\mathbf{h}_{11}\|^2} \mathbf{H}_t \mathbf{h}_{11} \mathbf{h}_{11}^H \mathbf{H}_t^H$ .

### 3.3.2. Optimal Relaying Matrix and Beamforming Vector

(3.51) is intractable at first sight. With MMSE receiver  $\mathbf{v} = \frac{\mathbf{Z}^{-1} \mathbf{H}_{22} \mathbf{w}}{\|\mathbf{Z}^{-1} \mathbf{H}_{22} \mathbf{w}\|}$  at the secondary receiver, the achievable secondary rate in the second phase is reformulated as

$$R_2 = \frac{1}{2} \log_2 \left( 1 + \frac{|\mathbf{v}^H \mathbf{H}_{22} \mathbf{w}|^2}{1 + \frac{P_1}{\|\mathbf{h}_{11}\|^2} |\mathbf{v}^H (\mathbf{H}_{12} \mathbf{h}_{11} + \mathbf{H}_{22} \mathbf{A} \mathbf{H}_t \mathbf{h}_{11})|^2 + \|\mathbf{v}^H \mathbf{H}_{22} \mathbf{A}\|^2} \right). \quad (3.52)$$

With auxiliary variable  $t$ , (3.51) can be transformed into

$$\max_{\mathbf{A}, \mathbf{w}, t} t \quad (3.53a)$$

$$\text{s.t. } R_2 \geq t, \quad (3.53b)$$

$$R_1 \geq R_1^*, \quad (3.53c)$$

$$\text{tr}(\mathbf{A} \mathbf{M} \mathbf{A}^H + \mathbf{w} \mathbf{w}^H) \leq P_2, \quad (3.53d)$$

$$t \geq 0. \quad (3.53e)$$

Since  $\mathbf{v}^H \mathbf{H}_{22} \mathbf{w} = \frac{\mathbf{w}^H \mathbf{H}_{22}^H \mathbf{Z}^{-1} \mathbf{H}_{22} \mathbf{w}}{\|\mathbf{Z}^{-1} \mathbf{H}_{22} \mathbf{w}\|}$ , which is linear in  $\mathbf{w}$  given  $\mathbf{v}$ ,  $\text{Im}(\mathbf{v}^H \mathbf{H}_{22} \mathbf{w}) = 0$ .



Assuming  $\text{Im}(\mathbf{h}_{21}^H \mathbf{A} \mathbf{H}_t \mathbf{h}_{11}) = 0$ , which is linear in  $\mathbf{A}$ , (3.53) can be transformed into

$$\max_{\mathbf{A}, \mathbf{w}, t} t \quad (3.54a)$$

$$\text{s.t. } \mathbf{v}^H \mathbf{H}_{22} \mathbf{w} \geq \sqrt{c_1 \left( 1 + \frac{P_1}{\|\mathbf{h}_{11}\|^2} |\mathbf{v}^H (\mathbf{H}_{12} \mathbf{h}_{11} + \mathbf{H}_{22} \mathbf{A} \mathbf{H}_t \mathbf{h}_{11})|^2 + \|\mathbf{v}^H \mathbf{H}_{22} \mathbf{A}\|^2 \right)}, \quad (3.54b)$$

$$\mathbf{h}_{21}^H \mathbf{A} \mathbf{H}_t \mathbf{h}_{11} \geq \sqrt{c_2 (1 + \|\mathbf{h}_{21}^H \mathbf{A}\|^2 + |\mathbf{h}_{21}^H \mathbf{w}|^2)} - \|\mathbf{h}_{11}\|^2, \quad (3.54c)$$

$$\text{tr}(\mathbf{A} \mathbf{M} \mathbf{A}^H + \mathbf{w} \mathbf{w}^H) \leq P_2, \quad (3.54d)$$

$$\text{Im}(\mathbf{h}_{21}^H \mathbf{A} \mathbf{H}_t \mathbf{h}_{11}) = 0, \quad (3.54e)$$

$$t \geq 0, \quad (3.54f)$$

where  $c_1 = 2^{2t} - 1 \geq 0$  with  $t \geq 0$ , and  $c_2 = \frac{\|\mathbf{h}_{11}\|^2}{P_1} (2^{2R_1^*} - 1 - P_1 \|\mathbf{h}_{11}\|^2) \geq 0$  with  $R_1^* \geq \frac{1}{2} \log_2(1 + P_1 \|\mathbf{h}_{11}\|^2)$ . The feasible set of (3.54) is jointly convex in  $\mathbf{A}$  and  $\mathbf{w}$  given  $\mathbf{v}$  and  $t$ , since (3.54b) and (3.54c) are convex second-order cone constraints, and (3.54d) is convex quadratic constraint [KL10]. Given  $\mathbf{v}$ , (3.54) can be solved by a bisection search over  $t$  through a sequence of second-order cone programming feasibility problems.

By alternating optimization [BH02], i.e., iterative transmitter/receiver optimization as in [SY04], (3.51) can be solved by Algorithm 2. In each iteration, with given receiver, the optimal relaying matrix and beamforming vector are obtained by solving the corresponding optimization problem; with given transmitter, the receiver is set as the MMSE receiver. The algorithm stops when the variation of the achievable secondary rate between two iterations is below certain accuracy.

---

**Algorithm 2** Algorithm to solve (3.51)

---

- 1: Initialize  $\mathbf{v}^{(0)}$ ,  $\ell = 0$ .
  - 2: **while**  $|R_2^{(\ell)} - R_2^{(\ell-1)}| > \epsilon$  **do**
  - 3:      $\ell ++$ ;
  - 4:     Obtain  $\mathbf{A}^{(\ell)}$ ,  $\mathbf{w}^{(\ell)}$  and  $R_2^{(\ell)}$  by solving (3.54);
  - 5:     Compute the MMSE receiver  $\mathbf{v}^{(\ell)}$ ;
  - 6: **end while**
  - 7: **Output**  $\mathbf{A}^{(\ell)}$ ,  $\mathbf{w}^{(\ell)}$  and  $\mathbf{v}^{(\ell)}$ .
- 

Since the objective value increases at each iteration and the objective function has an upper-bound, the iterative algorithm converges. However, it is not guaranteed to achieve the global optimum. A good solution can be selected by several random initializations.

### 3.3.3. Alternative Solution with Parametrization

With the same approach of iterative transceiver design, an alternative heuristic solution is given as follows. Given the secondary receiver  $\mathbf{v}$ , the effective secondary channel becomes  $\mathbf{H}_{22}^H \mathbf{v}$ . As it is proved in [ZSWO13, Theorem 1], the relaying matrix  $\mathbf{A}$  is rank-one, and can be parametrized as [JLD08]

$$\mathbf{A} = \sqrt{p_A} \left( \sqrt{\lambda_A} \frac{\Pi_{\mathbf{H}_{22}^H \mathbf{v}} \mathbf{h}_{21}}{\|\Pi_{\mathbf{H}_{22}^H \mathbf{v}} \mathbf{h}_{21}\|} + \sqrt{1 - \lambda_A} \frac{\Pi_{\mathbf{H}_{22}^H \mathbf{v}}^\perp \mathbf{h}_{21}}{\|\Pi_{\mathbf{H}_{22}^H \mathbf{v}}^\perp \mathbf{h}_{21}\|} \right) \frac{\mathbf{h}_{11}^H \mathbf{H}_t^H}{\|\mathbf{H}_t \mathbf{h}_{11}\|}, \quad (3.55)$$

where  $p_A$  is the power for  $\mathbf{A}$ ,  $\lambda_A$  is the parameter within  $[0, 1]$ ,  $\Pi_{\mathbf{H}_{22}^H \mathbf{v}} = \frac{\mathbf{H}_{22}^H \mathbf{v} \mathbf{v}^H \mathbf{H}_{22}}{\|\mathbf{H}_{22}^H \mathbf{v}\|^2}$ , and  $\Pi_{\mathbf{H}_{22}^H \mathbf{v}}^\perp = \mathbf{I} - \Pi_{\mathbf{H}_{22}^H \mathbf{v}}$ .

Given  $p_A$  and  $\lambda_A$ ,  $\mathbf{A}$  is determined. Given  $\mathbf{v}$  and  $\mathbf{A}$ ,  $\mathbf{w}$  can be parametrized as [LJ11]

$$\mathbf{w} = \sqrt{p_w} \left( \sqrt{\lambda_w} \frac{\Pi_{\mathbf{h}_{21}} \mathbf{H}_{22}^H \mathbf{v}}{\|\Pi_{\mathbf{h}_{21}} \mathbf{H}_{22}^H \mathbf{v}\|} + \sqrt{1 - \lambda_w} \frac{\Pi_{\mathbf{h}_{21}}^\perp \mathbf{H}_{22}^H \mathbf{v}}{\|\Pi_{\mathbf{h}_{21}}^\perp \mathbf{H}_{22}^H \mathbf{v}\|} \right), \quad (3.56)$$

with

$$\lambda_w = \min \left( \lambda_{\text{MRT}}, \frac{P_{\text{int}}}{p_w \|\mathbf{h}_{21}\|^2} \right), \quad (3.57)$$

where  $p_w$  is the power for  $\mathbf{w}$ ,  $\lambda_w$  is the parameter within  $[0, 1]$ ,  $\Pi_{\mathbf{h}_{21}} = \frac{\mathbf{h}_{21} \mathbf{h}_{21}^H}{\|\mathbf{h}_{21}\|^2}$ ,  $\Pi_{\mathbf{h}_{21}}^\perp = \mathbf{I} - \Pi_{\mathbf{h}_{21}}$ ,  $\lambda_{\text{MRT}} = \frac{\|\Pi_{\mathbf{h}_{21}} \mathbf{H}_{22}^H \mathbf{v}\|^2}{\|\mathbf{H}_{22}^H \mathbf{v}\|^2}$ , and  $P_{\text{int}} = \frac{\left| \sqrt{P_1} \|\mathbf{h}_{11}\| + \frac{\sqrt{P_1}}{\|\mathbf{h}_{11}\|} \mathbf{h}_{21}^H \mathbf{A} \mathbf{H}_t \mathbf{h}_{11} \right|^2}{2^{2R^*} - 1 - P_1 \|\mathbf{h}_{11}\|^2} - 1 - \|\mathbf{h}_{21}^H \mathbf{A}\|^2 \geq 0$ .

**Remark 19.** *The relaying matrix  $\mathbf{A}$  is parametrized with two real-valued parameters, and has the structure of the outer product of two channel-related vectors. One is the MRC receiver for the primary signal with respect to the effective channel between the two transmitters. And the other is parametrized with one real-valued parameter, as the weighted sum of two channel-related vectors, which are the projections of the channel from the secondary transmitter to the primary receiver into the space and null space of the effective secondary channel, respectively.*

**Remark 20.** *The beamforming vector  $\mathbf{w}$  is parametrized with one real-valued parameter, as the weighted sum of two channel-related vectors, which are the projections of the effective secondary channel into the space and null space of the channel from the secondary transmitter to the primary receiver, respectively.*

Given the parametrization of  $\mathbf{A}$  and  $\mathbf{w}$ , the power constraint (3.51c) becomes

$$\left( 1 + \frac{P_1}{\|\mathbf{h}_{11}\|^2} \|\mathbf{H}_t \mathbf{h}_{11}\|^2 \right) p_A + p_w \leq P_2. \quad (3.58)$$

The secondary transmitter employs full power transmission, i.e., (3.58) with equality, since otherwise the remaining power can be accommodated into  $\mathbf{w}$  in the null space of the channel  $\mathbf{h}_{21}$ , such that the objective value is nondecreased and the constraints are still satisfied in (3.51).

The alternative solution can be found in Algorithm 3. In each iteration, with given receiver, the optimal relaying matrix and beamforming vector are obtained by a grid search while achieving the maximum secondary rate; with given transmitter, the receiver is set as the MMSE receiver. The algorithm stops when the variation of the achievable secondary rate between two iterations is below certain accuracy.

---

**Algorithm 3** Algorithm to solve (3.51)

---

```

1: Initialize  $\mathbf{v}^{(0)}$ ,  $\ell = 0$ .
2: while  $|R_2^{(\ell)} - R_2^{(\ell-1)}| > \epsilon$  do
3:    $\ell ++$ ;
4:   for  $p_A \in [0, P_2]$  do
5:     for  $\lambda_A \in [0, 1]$  do
6:       Obtain  $\mathbf{A}$  in (3.55);
7:       Obtain  $\mathbf{w}$  in (3.56);
8:       Compute  $R_2$  in (3.52), record  $\mathbf{A}^{(\ell)}$  and  $\mathbf{w}^{(\ell)}$  for maximum  $R_2^{(\ell)}$ ;
9:     end for
10:  end for
11:  Compute the MMSE receiver  $\mathbf{v}^{(\ell)}$ ;
12: end while
13: Output  $\mathbf{A}^{(\ell)}$ ,  $\mathbf{w}^{(\ell)}$  and  $\mathbf{v}^{(\ell)}$ .

```

---

Since the objective value increases at each iteration and the objective function has an upper-bound, the iterative algorithm converges. However, it is not guaranteed to achieve the global optimum. A good solution can be selected by several random initializations.

### 3.3.4. Numerical Simulations

Numerical simulations are performed to evaluate the performance of the proposed amplify-and-forward cooperative spectrum sharing (*AFCSS*), in terms of outage probability of the primary link and achievable secondary rate (in bit/s/Hz) versus SNR of the secondary link (in dB). The SNR is defined as the ratio of the transmit power and the noise power at the receiver, and since the noise power is normalized, the SNR is equivalent to the transmit power.

The system configuration is as follows. The primary transmitter has 2 antennas, and the primary link has a SNR of 10 dB and a rate requirement of 2 bits/s/Hz. The antenna configuration of the secondary link varies as  $2 \times 2$ ,  $3 \times 3$ ,  $4 \times 4$ ,  $5 \times 5$  and  $6 \times 6$ , respectively. The SNR of the secondary link is varied from 0 dB to 30 dB. To motivate and facilitate the cooperation between the primary and secondary links, i.e., when the primary link is weak, as in Figure 3.8, the distance between the primary transmitter and receiver is set as 2, and the secondary transmitter is in the middle between the primary transmitter and receiver. The distance between the secondary transmitter and receiver is set as 1, and the secondary link is perpendicular to the primary link. Then the distance between the primary transmitter and the secondary receiver is  $\sqrt{2}$ . The path loss exponent is set as 3.

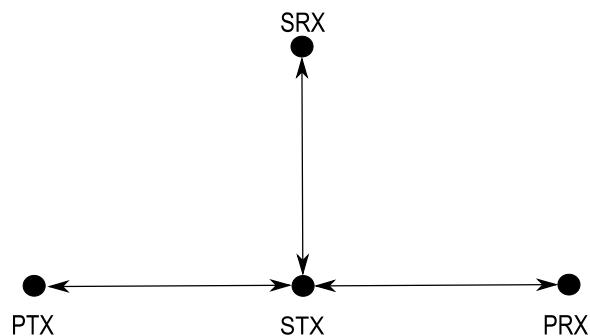


Figure 3.8.: AFCSS system setup in the simulation

In the simulation, if the primary link is good enough to support its rate requirement, there is no primary outage and the secondary link keeps silent; if the primary link experiences deep fading such that its rate requirement cannot be fulfilled, it asks for the cooperation from the secondary link with the proposed *AFCSS* strategy, if its rate requirement still cannot be achieved, then there is an primary outage, otherwise a secondary rate is achieved. The simulation results are averaged over 10000 channel realizations.

As in Figure 3.9, the primary outage probability versus SNR of the secondary link is shown in the case of the proposed *AFCSS* strategy, together with the case when there is no cooperation from the secondary link at all, which has a primary outage probability of nearly 70%. At the SNR of 10 dB and with  $2 \times 2$  secondary link, the primary outage probability decreases to about 40%, which keeps on decreasing though decelerating with more antennas at the secondary transceiver, and is about 0.3% with  $6 \times 6$  secondary link. With certain antenna configuration for the secondary link, the primary outage probability decreases as the SNR increases, and saturates at high SNRs. Since in the

second phase of the transmission, the received signal from the first phase is multiplied by the relaying matrix, including both the signal containing the primary message and the noise at the secondary transmitter, such that the achievable primary rate is limited by the noise at the secondary transmitter.

As in Figure 3.10, the achievable secondary rate versus SNR of the secondary link is shown. At the SNR of 10 dB and with  $2 \times 2$  secondary link, the achievable secondary rate is about 0.4 bit/s/Hz, which keeps on increasing though decelerating with more antennas at the secondary transceiver, and is about 2.3 bits/s/Hz with  $6 \times 6$  secondary link. With certain antenna configuration for the secondary link, the achievable secondary rate increases as the SNR increases.

Numerical results show that with the cooperation from the secondary link, the primary link can avoid outage effectively, especially when the number of antennas at the secondary transceiver is large, while the secondary link can achieve a significant rate.

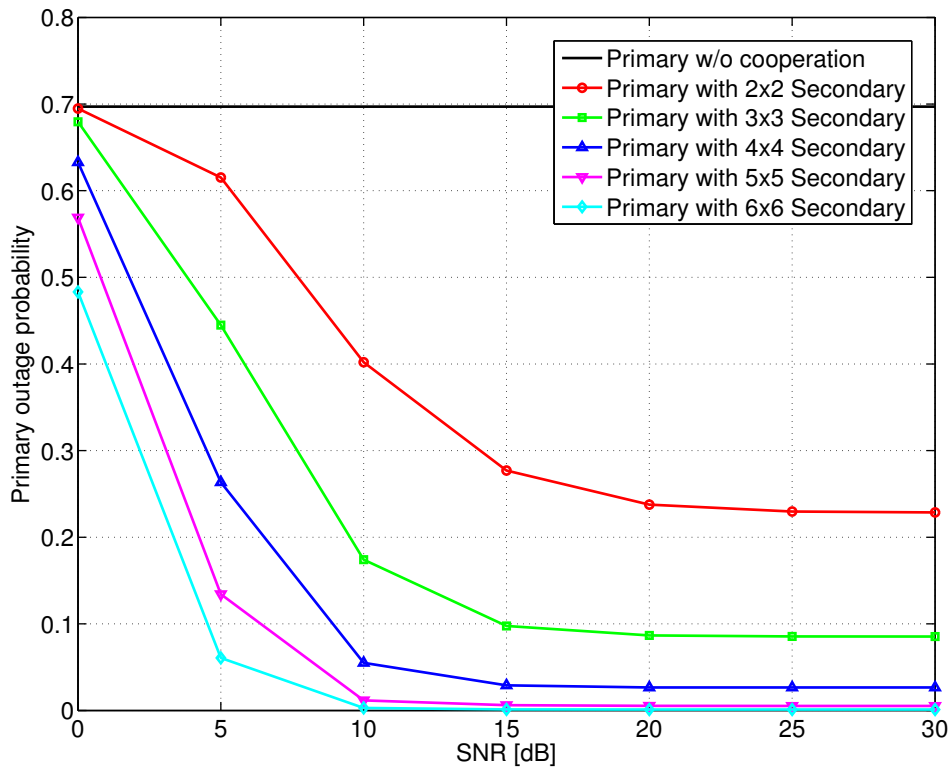


Figure 3.9.: Primary outage probability versus SNR of the secondary link with different antenna configurations at the secondary transceiver.

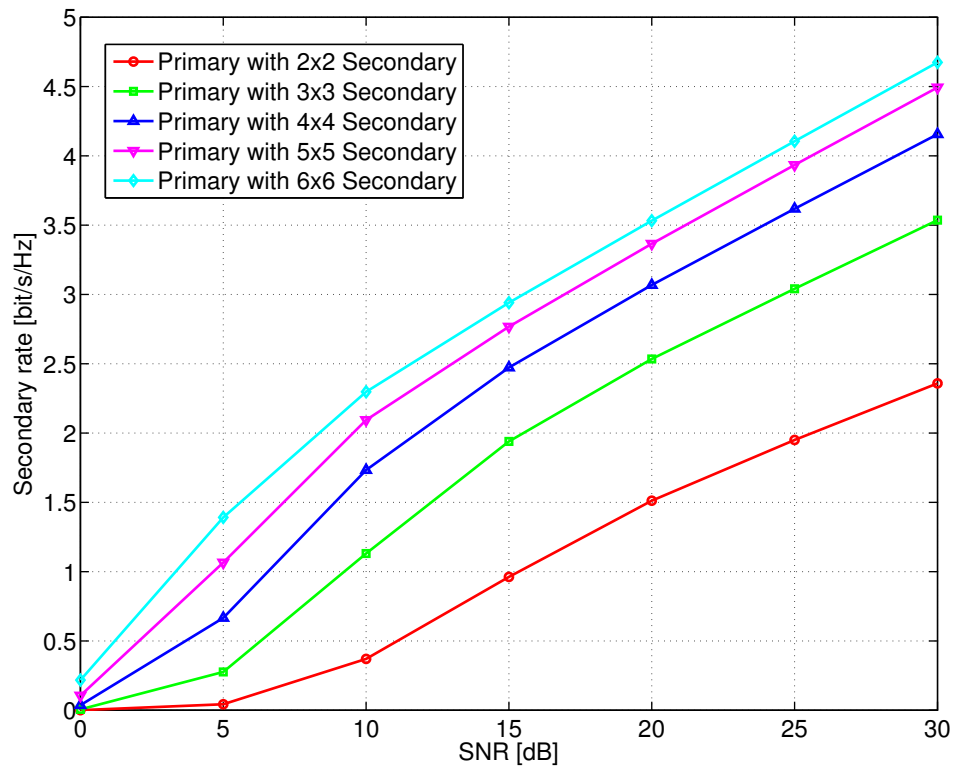


Figure 3.10.: Achievable secondary rate versus SNR of the secondary link with different antenna configurations at the secondary transceiver.

### 3.4. Decode-and-Forward Cooperative Spectrum Sharing

#### 3.4.1. System Model

The system considered is depicted in Figure 3.11 and consists of a MISO primary link with  $N_{T,1}$  transmit antennas and a MIMO secondary link with  $N_{T,2}$  transmit antennas and  $N_{R,2}$  receive antennas, where the primary and secondary transmitters have power  $P_1$  and  $P_2$ , respectively. The primary link has a rate requirement of  $R_1^*$ . When the primary channel is good enough to achieve  $R_1^*$ , the cooperation from the secondary link is not required, thus the secondary link keeps silent; when the primary channel is in deep fading such that  $R_1^*$  cannot be fulfilled, the cooperation from the secondary link is requested to avoid outage of the primary link. Assume the secondary transmitter does not have non-causal knowledge of the primary message, and still wants to help with the primary transmission in return for the access to the spectrum. The secondary transmitter relays the primary message in a decode-and-forward (DF) way, while transmitting its own message, where the transmission strategy of the primary link needs to be adapted. The secondary transmitter is half-duplex, i.e., it cannot transmit and receive simultaneously.

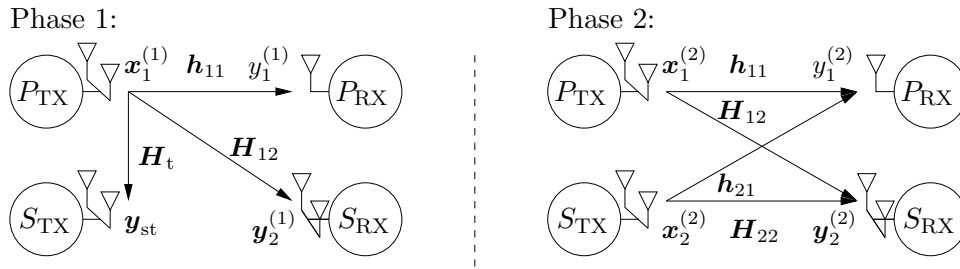


Figure 3.11.: System model consisting of a MISO primary link and a MIMO secondary link with two-phase transmission: primary transmitter ( $P_{TX}$ ), secondary transmitter ( $S_{TX}$ ), primary receiver ( $P_{RX}$ ) and secondary receiver ( $S_{RX}$ ).

The transmission consists of two phases. In the first phase with relative duration  $\alpha$ , the primary message is transmitted to both the primary receiver and the secondary transmitter. Since it is MIMO channel between the two transmitters, the primary transmitter can employ multiple-stream transmission to achieve a higher inter-transmitter rate compared with single-stream transmission and facilitate the decoding of the primary message at the secondary transmitter.

The signal from the primary transmitter is

$$\mathbf{x}_1^{(1)} = \sqrt{P_1^{(1)}} \mathbf{W}_{11} \mathbf{u}_{11}(d_1), \quad (3.59)$$

where the primary message  $d_1$  is encoded into an  $M_1 \times 1$  ( $1 \leq M_1 \leq \min(N_{T,2}, N_{T,1})$ ) vector  $\mathbf{u}_{11}$  of symbols with unit average power, by a random Gaussian codebook with fixed information rate  $R_1^{(1)}$ . With an  $N_{T,1} \times M_1$  precoding matrix  $\mathbf{W}_{11}$  ( $\|\mathbf{W}_{11}\| = 1$ ) and power  $P_1^{(1)}$ , the transmit covariance matrix  $\mathbf{K}_1^{(1)} = P_1^{(1)}\mathbf{W}_{11}\mathbf{W}_{11}^H$ , where  $\text{tr}(\mathbf{K}_1^{(1)}) = P_1^{(1)}$  and  $\mathbf{K}_1^{(1)} \succeq \mathbf{0}$ . The primary receiver and the secondary transmitter have knowledge of the codebook of  $d_1$ .

The signals at the primary receiver and the secondary transmitter are

$$y_1^{(1)} = \mathbf{h}_{11}^H \mathbf{x}_1^{(1)} + n_1^{(1)}, \quad (3.60)$$

$$\mathbf{y}_{\text{st}} = \mathbf{H}_t \mathbf{x}_1^{(1)} + \mathbf{n}_{\text{st}}, \quad (3.61)$$

respectively, where  $\mathbf{x}_1^{(1)}$  is the  $N_{T,1} \times 1$  signal vector sent by the primary transmitter,  $\mathbf{h}_{11}$  is the  $N_{T,1} \times 1$  channel vector of the primary link,  $\mathbf{H}_t$  is the  $N_{T,2} \times N_{T,1}$  channel matrix between the two transmitters, and the scalar  $n_1^{(1)}$  and the  $N_{T,2} \times 1$  vector  $\mathbf{n}_{\text{st}}$  are the noises at the primary receiver and the secondary transmitter, respectively.

The achievable rates from the primary transmitter to the primary receiver and the secondary transmitter are

$$R_1^{(1)} = \alpha \log_2 \left( 1 + \mathbf{h}_{11}^H \mathbf{K}_1^{(1)} \mathbf{h}_{11} \right), \quad (3.62)$$

$$R_t = \alpha \log_2 \left| \mathbf{I} + \mathbf{H}_t \mathbf{K}_1^{(1)} \mathbf{H}_t^H \right|, \quad (3.63)$$

respectively.

If

$$R_1^{(1)} < R_1^* \leq R_t, \quad (3.64)$$

then the secondary transmitter can decode the primary message but the primary receiver cannot, e.g., when  $\mathbf{H}_t$  has a significantly better channel quality than  $\mathbf{h}_{11}$  (e.g.,  $\text{tr}(\mathbf{H}_t^H \mathbf{H}_t) \gg \|\mathbf{h}_{11}\|^2$ ). The two-phase transmission strategy is reasonable only if the secondary transmitter can decode the primary message earlier than the primary receiver.

The transmission transits to the second phase if the decoding at the secondary transmitter is successful, otherwise an outage occurs.

The second phase with relative duration  $(1 - \alpha)$  corresponds to the set-up of the cognitive radio channel [DMT06], or overlay spectrum sharing with non-causal primary message knowledge.

The primary transmitter employs maximum ratio transmission and power  $P_1^{(2)}$  for its encoded message  $d_1$ . The signal from the primary transmitter is

$$\mathbf{x}_1^{(2)} = \sqrt{P_1^{(2)}} \frac{\mathbf{h}_{11}}{\|\mathbf{h}_{11}\|} u_{12}(d_1), \quad (3.65)$$



where  $d_1$  is encoded into symbol  $u_{12}$  with unit average power, by a different Gaussian codebook than that used in the first phase with fixed information rate  $R_1^{(2)}$ . The transmit covariance matrix  $\mathbf{K}_1^{(2)} = \frac{P_1^{(2)}}{\|\mathbf{h}_{11}\|^2} \mathbf{h}_{11} \mathbf{h}_{11}^H$ . The primary receiver has knowledge of the codebook of  $d_1$ . The power constraint at the primary transmitter in the two phases is  $\alpha P_1^{(1)} + (1 - \alpha) P_1^{(2)} \leq P_1$ , which is averaged over the two phases, taking into account the relative duration of the two phases.

The secondary transmitter helps transmit the primary message  $d_1$  with power  $p_{21}$  besides the transmission of its own message  $d_2$  with power  $p_{22}$ . DPC can be deployed to encode  $d_2$  while precanceling the interference (when decoding  $d_2$  at the secondary receiver) due to the transmission of  $d_1$  from both transmitters. The secondary transmitter employs single-stream transmission for  $d_1$  and multiple-stream transmission for  $d_2$ . The signal from the secondary transmitter is

$$\mathbf{x}_2^{(2)} = \sqrt{p_{21}} \mathbf{w}_{21} u_{12}(d_1) + \sqrt{p_{22}} \mathbf{W}_{22} \mathbf{u}_2(d_1, d_2), \quad (3.66)$$

where  $d_1$  is encoded into symbol  $u_{12}$  with unit average power by the same codebook at the primary transmitter in the second phase,  $d_2$  is encoded into an  $M_2 \times 1$  vector  $\mathbf{u}_2$  of symbols with unit average power by DPC, and  $\mathbf{w}_{21}$  ( $\|\mathbf{w}_{21}\| = 1$ ) is the  $N_{T,2} \times 1$  beamforming vector and  $\mathbf{W}_{22}$  ( $\|\mathbf{W}_{22}\| = 1$ ) is the  $N_{T,2} \times M_2$  precoding matrix, where  $1 \leq M_2 \leq \min(N_{R,2}, N_{T,2})$ . The transmit covariance matrix  $\mathbf{K}_{21} = p_{21} \mathbf{w}_{21} \mathbf{w}_{21}^H$ , where  $\text{tr}(\mathbf{K}_{21}) = p_{21}$  and  $\mathbf{K}_{21} \succeq \mathbf{0}$ , and the transmit covariance matrix  $\mathbf{K}_{22} = p_{22} \mathbf{W}_{22} \mathbf{W}_{22}^H$ , where  $\text{tr}(\mathbf{K}_{22}) = p_{22}$  and  $\mathbf{K}_{22} \succeq \mathbf{0}$ . The secondary receiver has knowledge of the codebooks of  $d_1$  and  $d_2$ . The power constraint at the secondary transmitter in the second phase is  $p_{21} + p_{22} \leq P_2$ .

The signals at the primary and secondary receivers are

$$\mathbf{y}_1^{(2)} = \mathbf{h}_{11}^H \mathbf{x}_1^{(2)} + \mathbf{h}_{21}^H \mathbf{x}_2^{(2)} + n_1^{(2)}, \quad (3.67)$$

$$\mathbf{y}_2^{(2)} = \mathbf{H}_{22} \mathbf{x}_2^{(2)} + \mathbf{H}_{12} \mathbf{x}_1^{(2)} + \mathbf{n}_2, \quad (3.68)$$

where  $\mathbf{x}_1^{(2)}$  and  $\mathbf{x}_2^{(2)}$  are the  $N_{T,1} \times 1$  and  $N_{T,2} \times 1$  signal vectors sent by the primary and secondary transmitters, respectively,  $\mathbf{h}_{i1}$  is the  $N_{T,i} \times 1$  channel vector between transmitter  $i \in \{1, 2\}$  and receiver 1,  $\mathbf{H}_{i2}$  is the  $N_{R,2} \times N_{T,i}$  channel matrix between transmitter  $i \in \{1, 2\}$  and receiver 2, and the scalar  $n_1^{(2)}$  and the  $N_{R,2} \times 1$  vector  $\mathbf{n}_2$  are the noises at the primary and secondary receivers, respectively.

The channels and noises are modeled as independent and identically distributed complex Gaussian random variables with zero mean and unit variance (The path-loss based channel fading is treated in the simulation.). Assume that the channels remain constant during the two phases, and the primary transmitter knows  $\mathbf{h}_{11}$ ; the secondary transmitter knows  $\mathbf{h}_{11}$ ,  $\mathbf{H}_{12}$ ,  $\mathbf{h}_{21}$ ,  $\mathbf{H}_{22}$  and  $\mathbf{H}_t$ .

The achievable rates for the primary and secondary links in the second phase are

$$R_1^{(2)} = (1 - \alpha) \log_2 \left( 1 + \frac{\left| \sqrt{P_1^{(2)}} \|\mathbf{h}_{11}\| + \sqrt{\frac{p_{21}}{1-\alpha}} \mathbf{h}_{21}^H \mathbf{w}_{21} \right|^2}{1 + \frac{p_{22}}{1-\alpha} \|\mathbf{h}_{21}^H \mathbf{W}_{22}\|^2} \right), \quad (3.69)$$

$$R_2 = (1 - \alpha) \log_2 \left| \mathbf{I} + \frac{p_{22}}{1-\alpha} \mathbf{H}_{22} \mathbf{W}_{22} \mathbf{W}_{22}^H \mathbf{H}_{22}^H \right|, \quad (3.70)$$

The duration of the second phase is taken into account by the scaling factor  $\frac{1}{1-\alpha}$  for  $p_{21}$  and  $p_{22}$ .

By the theory of parallel Gaussian channel [CT06], as used in the proof of [HMZ05, Proposition 2] for the decode-and-forward relay channel, the achievable primary rate is the sum of the rates in the two phases, i.e.,

$$R_1 = R_1^{(1)} + R_1^{(2)}. \quad (3.71)$$

To maximize the secondary achievable rate  $R_2$  while satisfying the primary rate requirement  $R_1^*$ , the primary power constraint  $P_1$  and the secondary power constraint  $P_2$ , the optimization problem can be formulated as

$$\max_{\alpha, \mathbf{K}_1^{(1)}, P_1^{(2)}, p_{21}, p_{22}, \mathbf{w}_{21}, \mathbf{W}_{22}} R_2 \quad (3.72a)$$

$$\text{s.t. } R_t \geq R_1^*, \quad (3.72b)$$

$$R_1 \geq R_1^*, \quad (3.72c)$$

$$\alpha \text{tr}(\mathbf{K}_1^{(1)}) + (1 - \alpha)P_1^{(2)} \leq P_1, \mathbf{K}_1^{(1)} \succeq \mathbf{0}, P_1^{(2)} \geq 0, \quad (3.72d)$$

$$p_{21} + p_{22} \leq P_2, p_{21} \geq 0, p_{22} \geq 0, \quad (3.72e)$$

$$\|\mathbf{w}_{21}\| = \|\mathbf{W}_{22}\| = 1, \quad (3.72f)$$

$$0 < \alpha < 1, \quad (3.72g)$$

where it is implicitly assumed that  $R_1^{(1)} < R_1^*$ , i.e., the transmission transits to the second phase before the primary receiver can decode the primary message.

### 3.4.2. Optimal Transmission Strategy

Since  $\mathbf{w}_{21}$  only exists in (3.72c), specifically in (3.69), the optimal  $\mathbf{w}_{21}$  is maximum ratio transmission, i.e.,  $\mathbf{w}_{21} = \frac{\mathbf{h}_{21}}{\|\mathbf{h}_{21}\|}$ . The optimization problem (3.72) is not convex; in particular, dealing with constraint (3.72c) is problematic. It seems infeasible to have an exhaustive search over the 6 variables: four real-valued parameters and two complex-valued matrices. The approach is to study the properties of the optimal parameters

through a series of propositions, which are then used to reduce the complexity of the solution.

**Proposition 8.** *The optimal transmission strategy in (3.72) makes use of all the available power at the primary and secondary transmitters, i.e.,*

1.  $\alpha \text{tr}(\mathbf{K}_1^{(1)}) + (1 - \alpha)P_1^{(2)} = P_1$ ,
2.  $p_{21} + p_{22} = P_2$ .

*Proof.* The proof is provided in Section 3.6.4. □

**Proposition 9.** *The set of parameters that solves the optimization problem in (3.72) satisfies*

$$R_1^{(1)} + R_1^{(2)} = R_1^*, \quad (3.73)$$

*i.e., constraint (3.72c) with equality.*

*Proof.* The proof is provided in Section 3.6.5. □

**Proposition 10.** *The set of parameters that solve the optimization problem in (3.72) satisfies*

$$R_t = R_1^* \quad (3.74)$$

*(i.e., constraint (3.72b) with equality) unless the optimal  $\mathbf{K}_1^{(1)}$  is proportional to the orthogonal projector onto  $\mathbf{h}_{11}$ , i.e., proportional to  $\frac{\mathbf{h}_{11}\mathbf{h}_{11}^H}{\|\mathbf{h}_{11}\|^2}$ .*

*Proof.* The proof is provided in Section 3.6.6. □

Although Proposition 10 only gives a partial characterization of  $\mathbf{K}_1^{(1)}$ , it turns out to be very useful when it comes to finding its value numerically. Combined with Proposition 8, it allows us to derive Algorithm 4 that efficiently finds  $\mathbf{K}_1^{(1)}$  given the values of the phase split  $\alpha$  and the power  $P_1^{(1)}$  ( $\text{tr}(\mathbf{K}_1^{(1)}) = P_1^{(1)}$ ) used by the primary transmitter in the first phase.

Algorithm 4 starts by verifying if MRT beamforming to the primary receiver (i.e., in the direction of  $\mathbf{h}_{11}$ , using  $\mathbf{K}_h$ ) is sufficient for decoding at the secondary transmitter (3.72b) (line 4). If MRT does not satisfy (3.72b), then the algorithm verifies (line 9) if a solution to (3.72b) exists for the given level of power  $P_1^{(1)}$  by allocating it freely, as in  $\mathbf{K}_f$ , to maximize the expression in line 8. If such solution does not exist,  $\mathbf{K}_1^{(1)}$  can not be found with given  $\alpha$  and  $P_1^{(1)}$ ; otherwise, the bisection method (Algorithm 5) is used to find the covariance matrix with largest component in the direction of  $\mathbf{h}_{11}$  that satisfies (3.72b). The search finishes when the rate achieved for this choice of covariance matrix

exceeds the target rate  $R_1^*$  by less than a predefined threshold  $\epsilon$ . The bisection search is guaranteed to converge since the objective function of the optimization problem in line 8 of Algorithm 5 is monotonically increasing in the power  $P_f$ . The maximization in Algorithm 4 (line 8) and in the bisection method (Algorithm 5, line 8) can be written as standard waterfilling problems, which can be efficiently and exactly solved [TV05]. The following corollary establishes the optimality of Algorithm 4.

**Corollary 1.** *Given the optimal values of  $\alpha$  and power  $P_1^{(1)}$  used by the primary transmitter in the first phase, Algorithm 4 finds the optimal  $\mathbf{K}_1^{(1)}$ .*

*Proof.* The proof is provided in Section 3.6.7. □

---

**Algorithm 4** Find optimal covariance matrix

---

```

1: procedure OPTIMAL-COVARIANCE( $\alpha, P_1^{(1)}$ )
2:    $P_h \leftarrow P_1^{(1)}$ ;
3:    $\mathbf{K}_h \leftarrow \frac{\mathbf{h}_{11}\mathbf{h}_{11}^H}{\|\mathbf{h}_{11}\|^2} P_h$ ;
4:   if  $\alpha \log_2 |\mathbf{I} + \mathbf{H}_t \mathbf{K}_h \mathbf{H}_t^H| \geq R_1^*$  then
5:      $\mathbf{K}_1^{(1)} \leftarrow \mathbf{K}_h$ ;
6:   else
7:      $P_f \leftarrow P_1^{(1)}$ ;
8:      $\mathbf{K}_f \leftarrow \arg \max_{\Sigma \succeq \mathbf{0}: \text{tr}(\Sigma) \leq P_f} \log_2 |\mathbf{I} + \mathbf{H}_t \Sigma \mathbf{H}_t^H|$ ;
9:     if  $\alpha \log_2 |\mathbf{I} + \mathbf{H}_t \mathbf{K}_f \mathbf{H}_t^H| < R_1^*$  then
10:       $\mathbf{K}_1^{(1)} \leftarrow \emptyset$ ;
11:    else
12:       $\mathbf{K}_1^{(1)} \leftarrow \text{BISECTION}(R_1^*, P_1^{(1)}, \epsilon)$ ;
13:    end if
14:  end if
15:  return  $\mathbf{K}_1^{(1)}$ ;
16: end procedure

```

---

---

**Algorithm 5** Bisection method
 

---

```

1: procedure BISECTION( $R_1^*$ ,  $P$ ,  $\epsilon$ )
2:    $P_{h,\text{top}} \leftarrow P$ ;
3:    $P_{h,\text{bot}} \leftarrow 0$ ;
4:   while true do
5:      $P_h \leftarrow \frac{P_{h,\text{top}} + P_{h,\text{bot}}}{2}$ ;
6:      $P_f \leftarrow P - P_h$ ;
7:      $\mathbf{K}_h \leftarrow P_h \frac{\mathbf{h}_{11} \mathbf{h}_{11}^H}{\|\mathbf{h}_{11}\|^2}$ ;
8:      $\mathbf{K}_f \leftarrow \arg \max_{\Sigma \succeq \mathbf{0}: \text{tr}(\Sigma) \leq P_f} \log_2 |\mathbf{I} + \mathbf{H}_t(\mathbf{K}_h + \Sigma) \mathbf{H}_t^H|$ ;
9:      $\text{gap} \leftarrow \alpha \log_2 |\mathbf{I} + \mathbf{H}_t(\mathbf{K}_h + \mathbf{K}_f) \mathbf{H}_t^H| - R_1^*$ ;
10:    if  $\text{gap} < 0$  then
11:       $P_{h,\text{top}} \leftarrow P_h$ ;
12:    else if  $\epsilon < \text{gap}$  then
13:       $P_{h,\text{bot}} \leftarrow P_h$ ;
14:    else
15:       $\mathbf{K}_1^{(1)} \leftarrow \mathbf{K}_h + \mathbf{K}_f$ ;
16:      break;
17:    end if
18:  end while
19:  return  $\mathbf{K}_1^{(1)}$ ;
20: end procedure

```

---



---

**Algorithm 6** Algorithm to find the optimal parameters
 

---

```

1: for  $\alpha \leftarrow [0, \dots, 1]$  do
2:   for  $P_1^{(1)} \leftarrow [0, \dots, \frac{P_1}{\alpha}]$  do
3:      $P_1^{(2)} \leftarrow \frac{P_1 - \alpha P_1^{(1)}}{1 - \alpha}$ ;
4:      $\mathbf{K}_1^{(1)} \leftarrow \text{OPTIMAL-COVARIANCE}(\alpha, P_1^{(1)})$ ;
5:     for  $p_{21} \leftarrow [0, \dots, P_2]$  do
6:        $p_{22} \leftarrow P_2 - p_{21}$ ;
7:       Obtain  $\mathbf{W}_{22}$  by solving (3.75);
8:       Record the parameters corresponding to maximum  $R_2$ ;
9:     end for
10:  end for
11: end for

```

---

Given  $\alpha$  and  $P_1^{(1)}$ ,  $P_1^{(2)} = \frac{P_1 - \alpha P_1^{(1)}}{1 - \alpha}$  and  $\mathbf{K}_1^{(1)}$  can be found by Algorithm 4. By dropping (3.72b), (3.72d) and (3.72g), and rewriting (3.72c), (3.72) can be reformulated as

$$\max_{p_{21}, p_{22}, \mathbf{W}_{22}} (1 - \alpha) \log_2 \left| \mathbf{I} + \frac{p_{22}}{1 - \alpha} \mathbf{H}_{22} \mathbf{W}_{22} \mathbf{W}_{22}^H \mathbf{H}_{22}^H \right| \quad (3.75a)$$

$$\text{s.t. } \frac{p_{22}}{1 - \alpha} \mathbf{h}_{21}^H \mathbf{W}_{22} \mathbf{W}_{22}^H \mathbf{h}_{21} \leq P_{\text{int}}, \quad (3.75b)$$

$$p_{21} + p_{22} \leq P_2, p_{21} \geq 0, p_{22} \geq 0, \quad (3.75c)$$

$$\|\mathbf{W}_{22}\| = 1, \quad (3.75d)$$

where

$$P_{\text{int}} = \frac{\left( \sqrt{P_1^{(2)}} \|\mathbf{h}_{11}\| + \sqrt{\frac{p_{21}}{1 - \alpha}} \|\mathbf{h}_{21}\| \right)^2}{2^{\frac{R_1^* - R_1^{(1)}}{1 - \alpha}} - 1} - 1 \geq 0, \quad (3.76)$$

with the assumption that  $R_1^* > R_1^{(1)}$ . (3.75) can be solved by a line search over  $p_{21} \in [0, P_2]$  ( $p_{22} = P_2 - p_{21}$ ) while solving a corresponding convex optimization problem, e.g., by interior point methods [BV04], as in Proposition 7 of Section 3.2.2 for MIMO overlay spectrum sharing with DPC at the secondary transmitter.

**Remark 21.** *When the secondary receiver has only one antenna, the second phase corresponds to MISO overlay spectrum sharing with DPC at the secondary transmitter as in Section 3.1.2, and the solution is given by Proposition 5. Due to the relative high computational complexity of the secondary transmit covariance matrix  $\mathbf{W}_{22}$ , the secondary receiver is constrained to have only one antenna in the numerical simulations, without loss of generality.*

The previous results reduce the solution to (3.72) to a search over three real-valued parameters while obtaining the two complex-valued matrices by efficient algorithms: the phase split  $\alpha$ , the power  $P_1^{(1)}$  spent by the primary transmitter in the first phase, and the power  $p_{21}$  spent for the transmission of the primary message in the second phase. In contrast, solving (3.72) directly requires search over four real-valued parameters and two complex-valued matrices.

The simplified search is summarized in Algorithm 6, which is described in the following. To find the solution, a grid search is performed over the phase split  $\alpha$  and the power  $P_1^{(1)}$  used by the primary transmitter in the first phase. Given these two values, the covariance matrix  $\mathbf{K}_1^{(1)}$  is found using Algorithm 4. Then the precoding matrix  $\mathbf{W}_{22}$  is obtained by a line search over  $p_{21}$  while solving a corresponding convex optimization problem. The optimal choice of parameters is the one that yields the largest secondary rate  $R_2$ .

### 3.4.3. Numerical Simulations

Numerical simulations are performed to evaluate the performance of the proposed decode-and-forward cooperative spectrum sharing (*DFCSS*), in terms of outage probability of the primary link and achievable secondary rate (in bit/s/Hz) versus SNR of the secondary link (in dB). The SNR is defined as the ratio of the transmit power and the noise power at the receiver, and since the noise power is normalized, the SNR is equivalent to the transmit power.

The system configuration is as follows. The primary transmitter has 2 antennas, and the primary link has a SNR of 10 dB and a rate requirement of 2 bits/s/Hz. The antenna configuration of the secondary link varies as  $2 \times 1$ ,  $3 \times 1$ ,  $4 \times 1$ ,  $5 \times 1$  and  $6 \times 1$ , respectively. The SNR of the secondary link is varied from  $-20$  dB to 20 dB. To motivate and facilitate the cooperation between the primary and secondary links, i.e., when the primary link is weak, as in Figure 3.12, the distance between the primary transmitter and receiver is set as 2, and the secondary transmitter is in the middle between the primary transmitter and receiver. The distance between the secondary transmitter and receiver is set as 1, and the secondary link is perpendicular to the primary link. Then the distance between the primary transmitter and the secondary receiver is  $\sqrt{2}$ . The path loss exponent is set as 3.

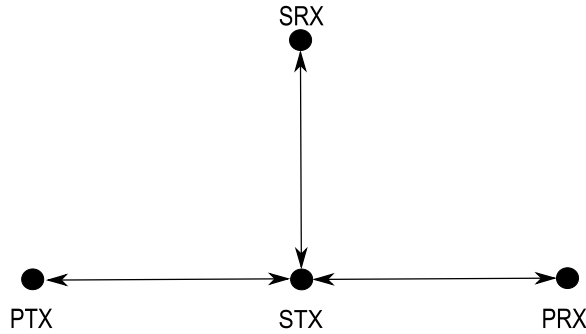


Figure 3.12.: DFCSS system setup in the simulation

In the simulation, if the primary link is good enough to support its rate requirement, there is no primary outage and the secondary link keeps silent; if the primary link experiences deep fading such that its rate requirement cannot be fulfilled, it asks for the cooperation from the secondary link with the proposed *DFCSS* strategy, if its rate requirement still cannot be achieved, then there is an primary outage, otherwise a secondary rate is achieved. The simulation results are averaged over 10000 channel realizations.

As in Figure 3.13, the primary outage probability versus SNR of the secondary link is

shown in the case of the proposed *DFCSS* strategy, together with the case when there is no cooperation from the secondary link at all, which has a primary outage probability of nearly 70%. As in Figure 3.14, the achievable secondary rate versus SNR of the secondary link is shown. As in Figure 3.13, at SNRs under  $-10$  dB, the cooperation from the secondary link can not help the primary link to minimize its outage probability, and as a result the secondary link achieves zero rate as in Figure 3.14. As in Figure 3.13, at the SNR of 0 dB and with  $2 \times 1$  secondary link, the primary outage probability decreases to about 14.5%, which keeps on decreasing though decelerating with more antennas at the secondary transmitter, and is about 0.2% with  $6 \times 1$  secondary link. With certain antenna configuration for the secondary link, the primary outage probability decreases quickly to nearly 0 as the SNR increases. Since after the secondary transmitter successfully decodes the primary message in the first phase, as the SNR increases, the achievable primary rate can be improved significantly with the transmission of the primary message by the secondary transmitter in the second phase.

As in Figure 3.14, at the SNR of 0 dB and with  $2 \times 1$  secondary link, the achievable secondary rate is about 0.4 bit/s/Hz, which keeps on increasing though decelerating with more antennas at the secondary transmitter, and is about 1.5 bits/s/Hz with  $6 \times 1$  secondary link. With certain antenna configuration for the secondary link, the achievable secondary rate increases as the SNR increases.

Numerical results show that with the cooperation from the secondary link, the primary link can avoid outage effectively, especially when the number of antennas at the secondary transmitter is large, while the secondary link can achieve a significant rate.



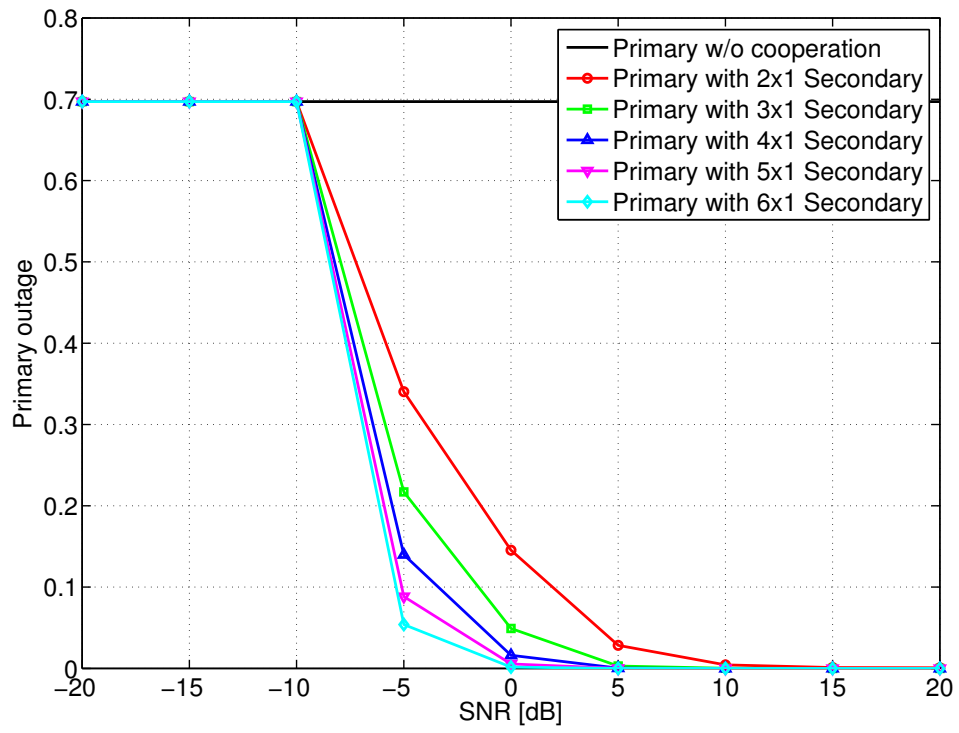


Figure 3.13.: Primary outage probability versus SNR of the secondary link with different antenna configurations at the secondary transceiver.

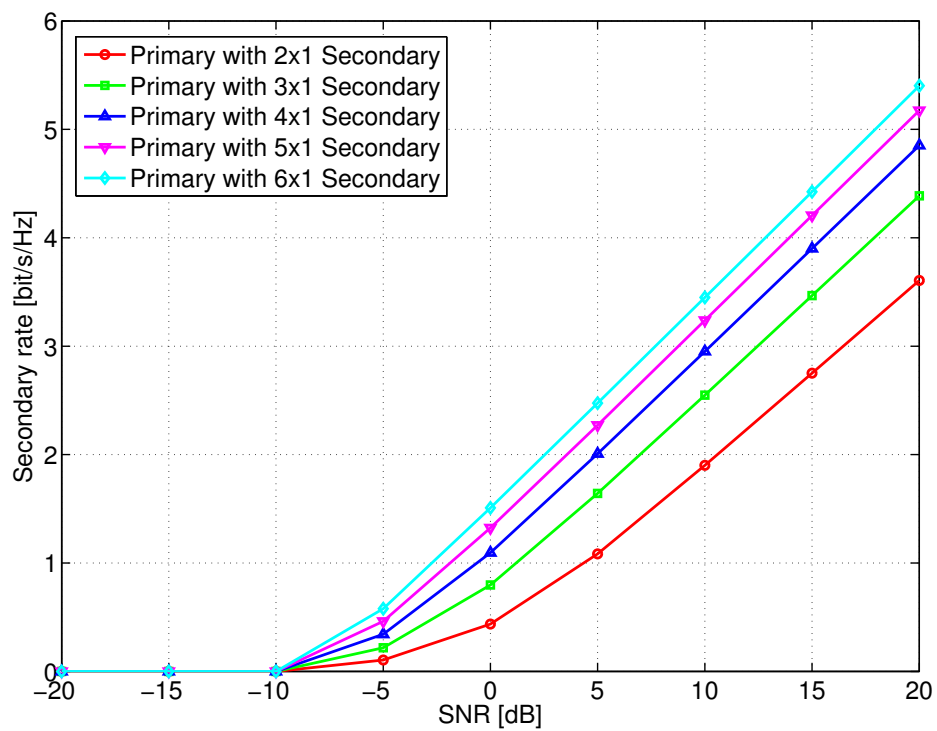


Figure 3.14.: Achievable secondary rate versus SNR of the secondary link with different antenna configurations at the secondary transceiver.

### 3.5. Summary

Overlay spectrum sharing between a MISO primary link and a MISO/MIMO secondary link is studied, where the achievable secondary rate is maximized while satisfying the primary rate requirement and the secondary power constraint. When the secondary transmitter has non-causal knowledge of the primary message and employs DPC to obtain an interference-free secondary link, optimal beamforming and power allocation is obtained in the case of MISO secondary channel, by a linear search where the beamforming vector is parametrized with one real-valued parameter; optimal transmit covariance matrix and beamforming vector is obtained in the case of MIMO secondary channel, by a linear search while solving a corresponding convex optimization problem. With linear precoding at the secondary transmitter, optimal beamforming and power allocation is obtained in the case of MISO secondary channel, by a cubic search where the beamforming vectors are parametrized with real-valued parameters; optimal beamforming and power allocation is obtained in the case of MIMO secondary channel, by the approach of iterative transceiver design, where the secondary transmitter employs single-stream transmission for its own message and MMSE receiver is deployed at the secondary receiver. In all cases, full power transmission is used at the secondary transmitter. Numerical results show that with non-causal knowledge of the primary message and the deployment of DPC at the secondary transmitter, overlay spectrum sharing can achieve a significantly higher secondary rate than the proposed underlay spectrum sharing, and rate loss occurs with the deployment of linear precoding instead of DPC at the secondary transmitter.

When the secondary transmitter does not have non-causal knowledge of the primary message, it relays the primary message in an AF or a DF way in a two-phase transmission, while transmitting its own message. The primary link adapts its transmission strategy and cooperates with the secondary link to fulfill its rate requirement. The achievable secondary rate is maximized while satisfying the primary rate requirement and the primary and secondary power constraints. In the case of AF cooperative spectrum sharing, the primary transmitter employs MRT, and the primary receiver applies MRC to the received signals in the two phases; the secondary transmitter employs single-stream transmission for its own message, and MMSE receiver is deployed at the secondary receiver in the second phase. An iterative transceiver design algorithm is proposed, where in each iteration, an optimization problem is solved to obtain the optimal relaying matrix and beamforming vector, with respect to a given secondary receiver, by a bisection search through a sequence of second-order cone programming feasibility

problems. The iterative algorithm converges though is not guaranteed to achieve the global optimum. A good solution can be selected by several random initializations. For this setup, an alternative heuristic solution is proposed. Given the secondary receiver, the relaying matrix for the primary message is parametrized with two real-valued parameters, and has the structure of the outer product of two channel-related vectors. One is the MRC receiver for the primary signal with respect to the effective channel between the two transmitters. And the other is parametrized with one real-valued parameter, as the weighted sum of two channel-related vectors, which are the projections of the channel from the secondary transmitter to the primary receiver into the space and null space of the effective secondary channel, respectively. Moreover, given the secondary receiver and the relaying matrix for the primary message, the beamforming vector for the secondary message is parametrized with one real-valued parameter, as the weighted sum of two channel-related vectors, which are the projections of the effective secondary channel into the space and null space of the channel from the secondary transmitter to the primary receiver, respectively. An iterative transceiver design algorithm is proposed, where in each iteration, a grid search is performed to obtain the optimal relaying matrix and beamforming vector, with respect to a given secondary receiver. The iterative algorithm converges though is not guaranteed to achieve the global optimum. A good solution can be selected by several random initializations. Full power transmission is used at the secondary transmitter in the second phase.

In the case of DF cooperative spectrum sharing, the primary transmitter employs multiple-stream transmission in the first phase, to facilitate the decoding of the primary message at the secondary transmitter, and MRT in the second phase to facilitate its own transmission; the secondary transmitter employs DPC to obtain an interference-free secondary link in the second phase. A set of parameters are optimized, including relative duration of the two phases, primary transmission strategies in the two phases and secondary transmission strategy in the second phase, and properties of the parameters are studied to reduce the computational complexity of the optimization problem. A cubic search is required to obtain the optimal transmission strategies. Given the relative duration of the first phase and the power spent in the first phase by the primary transmitter, the primary transmit covariance matrix in the first phase is obtained, by balancing between the maximization of the received SNR at the primary receiver and that of the channel capacity from the primary transmitter to the secondary transmitter. After that, the secondary transmit covariance matrix in the second phase is obtained, by a line search over the power spent for the transmission of the primary message, while solving a corresponding convex optimization problem. The primary transmitter em-

employs full power transmission in the two phases. The secondary transmitter employs full power transmission in the second phase. The optimal choice of parameters is the one that yields the largest secondary rate. Numerical results show that with the cooperation from the secondary link, the primary link can avoid outage effectively, especially when the number of antennas at the secondary transceiver is large, while the secondary link can achieve a significant rate.

### 3.6. Proofs

#### 3.6.1. Proof of Proposition 5

It can be easily seen that the optimal  $\mathbf{w}_{21}$  is maximum ratio transmission, i.e.,  $\mathbf{w}_{21} = \frac{\mathbf{h}_{21}}{\|\mathbf{h}_{21}\|}$ , since it only exists in (3.9b). Given  $p_{22}$ , using the same approach as in the proof of Proposition 1 in Section 2.1.2,  $\mathbf{w}_{22}$  can be parametrized as in (3.11) and  $p_{21}$  is given by (3.14).

The optimal solution to (3.9) can be obtained by varying  $p_{22} \in [0, P_2]$  to achieve the maximum secondary rate.

#### 3.6.2. Proof of Proposition 6

Before the proof of Proposition 6, Lemma 3 is introduced.

**Lemma 3.** *To solve the multi-objective optimization problem*

$$\left( \min_{\mathbf{v}} |a + \mathbf{g}_1^H \mathbf{v}|^2, \max_{\mathbf{v}} |b + \mathbf{g}_2^H \mathbf{v}|^2 \right) \quad (3.77)$$

where  $\|\mathbf{v}\|^2 \leq \gamma$ ,  $\mathbf{v}, \mathbf{g}_1, \mathbf{g}_2 \in \mathbb{C}^N$ ,  $a, b \in \mathbb{C}$  and  $\gamma \in \mathbb{R}_+$ ,  $\mathbf{v}$  can be parametrized as

$$\mathbf{v}(\rho_1, \rho_2) = \rho_1 \frac{\Pi_{\mathbf{g}_1} \mathbf{g}_2}{\|\Pi_{\mathbf{g}_1} \mathbf{g}_2\|} + \rho_2 \frac{\Pi_{\mathbf{g}_1}^\perp \mathbf{g}_2}{\|\Pi_{\mathbf{g}_1}^\perp \mathbf{g}_2\|} \quad (3.78)$$

where  $\Pi_{\mathbf{g}_1} = \frac{\mathbf{g}_1 \mathbf{g}_1^H}{\|\mathbf{g}_1\|^2}$ ,  $\Pi_{\mathbf{g}_1}^\perp = \mathbf{I} - \Pi_{\mathbf{g}_1}$ ,  $|\rho_1|^2 + |\rho_2|^2 \leq \gamma$ , and  $\rho_1, \rho_2 \in \mathbb{C}$ .

*Proof.* Without loss of generality, assume that  $\mathbf{v}$  is parametrized as

$$\mathbf{v} = \xi_1 \frac{\Pi_{\mathbf{g}_1} \mathbf{g}_2}{\|\Pi_{\mathbf{g}_1} \mathbf{g}_2\|} + \xi_2 \frac{\Pi_{\mathbf{g}_1}^\perp \mathbf{g}_2}{\|\Pi_{\mathbf{g}_1}^\perp \mathbf{g}_2\|} + \sum_{l=3}^N \xi_l \mathbf{u}_l \quad (3.79)$$

where  $\Pi_{\mathbf{g}_1} = \frac{\mathbf{g}_1 \mathbf{g}_1^H}{\|\mathbf{g}_1\|^2}$ ,  $\Pi_{\mathbf{g}_1}^\perp = \mathbf{I} - \Pi_{\mathbf{g}_1}$ , the orthonormal set  $\left\{ \frac{\Pi_{\mathbf{g}_1} \mathbf{g}_2}{\|\Pi_{\mathbf{g}_1} \mathbf{g}_2\|}, \frac{\Pi_{\mathbf{g}_1}^\perp \mathbf{g}_2}{\|\Pi_{\mathbf{g}_1}^\perp \mathbf{g}_2\|}, \mathbf{u}_3, \dots, \mathbf{u}_N \right\}$  forms the orthonormal basis of space  $\mathbb{C}^N$ , and  $\sum_{l=1}^N |\xi_l|^2 \leq \gamma$ ,  $\xi_l \in \mathbb{C}$ ,  $l = 1, \dots, N$ .

Redistribute the power  $\delta = \sum_{l=3}^N |\xi_l|^2$  spent on span  $\{\mathbf{u}_3, \dots, \mathbf{u}_N\}$  to  $\frac{\Pi_{\mathbf{g}_1}^\perp \mathbf{g}_2}{\|\Pi_{\mathbf{g}_1}^\perp \mathbf{g}_2\|}$  as such

$$\mathbf{v} = \xi_1 \frac{\Pi_{\mathbf{g}_1} \mathbf{g}_2}{\|\Pi_{\mathbf{g}_1} \mathbf{g}_2\|} + (\xi_2 + e^{j\angle\phi} \sqrt{\delta}) \frac{\Pi_{\mathbf{g}_1}^\perp \mathbf{g}_2}{\|\Pi_{\mathbf{g}_1}^\perp \mathbf{g}_2\|} \quad (3.80)$$

with

$$\phi = b + \xi_1 \mathbf{g}_2^H \frac{\Pi_{\mathbf{g}_1} \mathbf{g}_2}{\|\Pi_{\mathbf{g}_1} \mathbf{g}_2\|} + \xi_2 \mathbf{g}_2^H \frac{\Pi_{\mathbf{g}_1}^\perp \mathbf{g}_2}{\|\Pi_{\mathbf{g}_1}^\perp \mathbf{g}_2\|} \quad (3.81)$$

that  $|b + \mathbf{g}_2^H \mathbf{v}|^2$  is increased while  $|a + \mathbf{g}_1^H \mathbf{v}|^2$  is unchanged, which means (3.80) gives a better solution to (3.77) than (3.79). Let  $\rho_1 = \xi_1$  and  $\rho_2 = \xi_2 + e^{j\angle\phi} \sqrt{\delta}$ , then  $|\rho_1|^2 + |\rho_2|^2 \leq \gamma$ , and  $\rho_1, \rho_2 \in \mathbb{C}$ .  $\square$

The denominator of the objective function in (3.20a) should be minimized and the numerator of the fraction in (3.20b) should be maximized with respect to  $\mathbf{w}_{21}$ ; the numerator of the objective function in (3.20a) should be maximized and the denominator of the fraction in (3.20b) should be minimized with respect to  $\mathbf{w}_{22}$ .

From Lemma 3, for the optimization problem  $\left(\min_{\mathbf{w}_{21}} \left| \frac{\sqrt{P_1}}{\|\mathbf{h}_{11}\|} \mathbf{h}_{12}^H \mathbf{h}_{11} + \sqrt{p_{21}} \mathbf{h}_{22}^H \mathbf{w}_{21} \right|^2, \max_{\mathbf{w}_{21}} \left| \sqrt{P_1} \|\mathbf{h}_{11}\| + \sqrt{p_{21}} \mathbf{h}_{21}^H \mathbf{w}_{21} \right|^2 \right)$ ,  $\mathbf{w}_{21}$  can be parametrized as in (3.21). With substitution of  $\mathbf{w}_{21}$  by (3.21), the numerator of the fraction in (3.20b) becomes  $\left| \varphi + e^{j\psi_2} \sqrt{1 - \lambda_1} \sqrt{p_{21}} \mathbf{h}_{21}^H \frac{\Pi_{\mathbf{h}_{22}}^\perp \mathbf{h}_{21}}{\|\Pi_{\mathbf{h}_{22}}^\perp \mathbf{h}_{21}\|} \right|^2$ , while the denominator of the objective function in (3.20a) becomes  $1 + \left| \frac{\sqrt{P_1}}{\|\mathbf{h}_{11}\|} \mathbf{h}_{12}^H \mathbf{h}_{11} + e^{j\psi_1} \sqrt{\lambda_1} \sqrt{p_{21}} \mathbf{h}_{22}^H \frac{\Pi_{\mathbf{h}_{22}} \mathbf{h}_{21}}{\|\Pi_{\mathbf{h}_{22}} \mathbf{h}_{21}\|} \right|^2$ , which is independent of  $\psi_2$ . Given  $\psi_1$ ,  $\lambda_1$  and  $p_{21}$ , the optimal  $\psi_2$  is given by (3.23) to maximize the numerator of the fraction in (3.20b). Given  $\psi_1$ ,  $\lambda_1$  and  $p_{21}$ , using the same approach as in the proof of Proposition 1 in Section 2.1.2,  $\mathbf{w}_{22}$  can be parametrized as in (3.22) and  $p_{22}$  is given by (3.26).

The optimal solution to (3.20) can be obtained by varying  $\psi_1 \in [0, 2\pi]$ ,  $\lambda_1 \in [0, 1]$  and  $p_{21} \in [0, P_2]$  to achieve the maximum secondary rate.

### 3.6.3. Proof of Proposition 7

It can be easily seen that the optimal  $\mathbf{w}_{21}$  is maximum ratio transmission, i.e.,  $\mathbf{w}_{21} = \frac{\mathbf{h}_{21}}{\|\mathbf{h}_{21}\|}$ , since it only exists in (3.33b). Let  $\mathbf{K} = p_{22} \mathbf{W}_{22} \mathbf{W}_{22}^H$  denote the transmit covariance matrix. Then (3.33) is equivalent to (3.35).

**Lemma 4.** *The optimal transmission strategy, namely, the solution to (3.35), uses full power, i.e.,  $p_{21} + \text{tr}(\mathbf{K}) = P_2$ .*

*Proof.* Assume  $p_{21} + \text{tr}(\mathbf{K}) < P_2$  at the optimum of (3.35), a new transmit covariance matrix can be constructed as  $\mathbf{K}' = \mathbf{K} + \frac{\delta}{\sqrt{N_{T,2}-1}} \Pi_{\mathbf{h}_{21}}^\perp$ , where  $\delta = P_2 - p_{21} - \text{tr}(\mathbf{K})$  and  $\Pi_{\mathbf{h}_{21}}^\perp = \mathbf{I} - \frac{\mathbf{h}_{21} \mathbf{h}_{21}^H}{\|\mathbf{h}_{21}\|^2}$ , such that the objective value in (3.35a) is nondecreasing while the constraint (3.35b) is still fulfilled.  $\square$

Given  $p_{21}$ , the objective function (3.35a) is concave in  $\mathbf{K}$ , and the constraints (3.35b) and (3.35c) are linear in  $\mathbf{K}$ , thus the optimization problem (3.35) is convex in  $\mathbf{K}$ . The optimal  $\mathbf{W}_{22} = \mathbf{K}^{\frac{1}{2}} / \sqrt{P_2 - p_{21}}$  can be obtained by a linear search over  $p_{21} \in [0, P_2]$  while solving (3.35) to achieve the maximum objective value.

### 3.6.4. Proof of Proposition 8

Before the proof of Proposition 8, Lemma 5 is introduced.

**Lemma 5.** *The function*

$$\beta \log_2 \left| \mathbf{I} + \frac{1}{\beta} \mathbf{B} \mathbf{C} \mathbf{B}^H \right| \quad (3.82)$$

defined for  $\beta \in (0, 1]$ , any  $\mathbf{B}$  and any  $\mathbf{C} \succeq \mathbf{0}$  (with appropriate dimensions) is strictly increasing in  $\beta$ .

*Proof.* It can be easily seen that

$$\beta \log_2 \left| \mathbf{I} + \frac{1}{\beta} \mathbf{B} \mathbf{C} \mathbf{B}^H \right| = \sum_{i=1}^r \beta \log_2 \left( 1 + \frac{\lambda_i}{\beta} \right), \quad (3.83)$$

where  $\lambda_i$  and  $r$  are the non-zero singular values and the rank of  $\mathbf{B} \mathbf{C} \mathbf{B}^H$ , respectively. The first derivative of each of the terms in the sum is positive for  $\beta > 0$ , thus (3.82) is strictly increasing in  $\beta$ .  $\square$

The proof of Proposition 8 follows. Statement 1 is proved by contradiction. Assume at the optimum

$$\alpha \operatorname{tr}(\mathbf{K}_1^{(1)}) + (1 - \alpha) P_1^{(2)} < P_1. \quad (3.84)$$

Define the matrix  $\widetilde{\mathbf{K}}_1^{(1)} = \gamma \mathbf{K}_1^{(1)}$  for some  $\gamma > 1$  such that

$$\alpha \operatorname{tr}(\widetilde{\mathbf{K}}_1^{(1)}) + (1 - \alpha) P_1^{(2)} \leq P_1. \quad (3.85)$$

This choice of matrix yields

$$\tilde{R}_1^{(1)} = \alpha \log_2 \left( 1 + \mathbf{h}_{11}^H \widetilde{\mathbf{K}}_1^{(1)} \mathbf{h}_{11} \right) \quad (3.86a)$$

$$= \alpha \log_2 \left( 1 + \gamma \mathbf{h}_{11}^H \mathbf{K}_1^{(1)} \mathbf{h}_{11} \right) \quad (3.86b)$$

$$> \alpha \log_2 \left( 1 + \mathbf{h}_{11}^H \mathbf{K}_1^{(1)} \mathbf{h}_{11} \right) \quad (3.86c)$$

$$= R_1^{(1)} \quad (3.86d)$$

and

$$\tilde{R}_t = \alpha \log_2 \left| \mathbf{I} + \mathbf{H}_t \widetilde{\mathbf{K}}_1^{(1)} \mathbf{H}_t^H \right| \quad (3.87a)$$

$$= \alpha \log_2 \left| \mathbf{I} + \gamma \mathbf{H}_t \mathbf{K}_1^{(1)} \mathbf{H}_t^H \right| \quad (3.87b)$$

$$= \alpha \sum_{i=1}^r \log_2(1 + \gamma \lambda_i) \quad (3.87c)$$

$$> \alpha \sum_{i=1}^r \log_2(1 + \lambda_i) \quad (3.87d)$$

$$= \alpha \log_2 \left| \mathbf{I} + \mathbf{H}_t \mathbf{K}_1^{(1)} \mathbf{H}_t^H \right| \quad (3.87e)$$

$$= R_t, \quad (3.87f)$$



where  $\lambda_i$  and  $r$  are the non-zero singular values and the rank of  $\mathbf{H}_t \mathbf{K}_1^{(1)} \mathbf{H}_t^H$ , respectively. Thus

$$\tilde{R}_1^{(1)} + R_1^{(2)} > R_1^* \quad (3.88)$$

$$\tilde{R}_t > R_1^*, \quad (3.89)$$

and a shorter duration of the first phase  $\tilde{\alpha} < \alpha$  can be found such that the rates, evaluated at  $\tilde{\alpha}$ , satisfy

$$\tilde{R}_1^{(1)}(\tilde{\alpha}) + R_1^{(2)}(\tilde{\alpha}) \geq R_1^*, \quad (3.90)$$

$$\tilde{R}_t(\tilde{\alpha}) \geq R_1^*. \quad (3.91)$$

At the same time, the secondary rate has been increased by Lemma 5, thus contradicting the assumption on the optimality of  $\mathbf{K}_1^{(1)}$  and  $P_1^{(2)}$ .

Statement 2 is also proved by contradiction. Assume at the optimum

$$p_{21} + p_{22} < P_2. \quad (3.92)$$

Consider two new powers

$$\tilde{p}_{21} = \gamma_{21} p_{21}, \quad (3.93)$$

$$\tilde{p}_{22} = \gamma_{22} p_{22}. \quad (3.94)$$

Since  $R_1^{(2)}$  is a continuous function of both  $p_{21}$  and  $p_{22}$ , sufficiently small  $\gamma_{21} > 1$  and  $\gamma_{22} > 1$  can be found such that the constraint (3.72e) is not violated and  $R_1^{(2)}$  evaluated for  $\tilde{p}_{21}$  and  $\tilde{p}_{22}$  remains unchanged (and hence (3.72c) is satisfied). However, using  $\tilde{p}_{22}$  yields a larger secondary rate  $R_2$ , which contradicts the assumption on the optimality of  $p_{21}$  and  $p_{22}$ .

### 3.6.5. Proof of Proposition 9

Assume at the optimum

$$R_1^{(1)}(\mathbf{K}_1^{(1)}) + R_1^{(2)} > R_1^*, \quad (3.95)$$

$$R_t(\mathbf{K}_1^{(1)}) \geq R_1^*. \quad (3.96)$$

The notation remarks the dependency of  $R_1^{(1)}$  and  $R_t$  on the covariance matrix  $\mathbf{K}_1^{(1)}$ . Let  $\sigma^*$  denote the power used by  $\mathbf{K}_1^{(1)}$ , i.e.,  $\sigma^* = \text{tr}(\mathbf{K}_1^{(1)})$ . The proof is divided into two cases.

First, consider the case  $\mathbf{K}_1^{(1)} \neq \mathbf{K}^{\text{WF}}(\sigma^*)$  with

$$\mathbf{K}^{\text{WF}}(\sigma^*) = \arg \max_{\Sigma \succeq \mathbf{0}: \text{tr}(\Sigma) \leq \sigma^*} \log_2 |\mathbf{I} + \mathbf{H}_t \Sigma \mathbf{H}_t^H|. \quad (3.97)$$

Both  $R_1^{(1)}$  and  $R_t$  are continuous functions of the entries of  $\mathbf{K}_1^{(1)}$ , and the log-det operator is concave on the set of Hermitian positive semi-definite matrices with bounded trace. Therefore, a Hermitian positive semi-definite covariance matrix  $\widetilde{\mathbf{K}}_1^{(1)}$  ( $\text{tr}(\widetilde{\mathbf{K}}_1^{(1)}) = \sigma^*$ ) can be found with  $\|\widetilde{\mathbf{K}}_1^{(1)} - \mathbf{K}_1^{(1)}\|$  small enough such that

$$R_1^{(1)}(\widetilde{\mathbf{K}}_1^{(1)}) + R_1^{(2)} > R_1^*, \quad (3.98)$$

$$R_t(\widetilde{\mathbf{K}}_1^{(1)}) > R_1^*. \quad (3.99)$$

Since  $R_1^{(1)}$ ,  $R_t$  and  $R_1^{(2)}$  are all continuous in  $\alpha$ , a shorter duration for the first phase can be found, i.e.,  $\tilde{\alpha} < \alpha$ , such that the two constraints are still satisfied. However, by Lemma 5 in Section 3.6.4, shortening the first phase strictly increases the secondary rate  $R_2$ , which contradicts the assumption on the optimality of the set of parameters.

In the case where  $\mathbf{K}_1^{(1)} = \mathbf{K}^{\text{WF}}(\sigma^*)$ , the rate  $R_t$  is already at maximum. In this case, if either  $P_1^{(2)} \neq 0$  or  $p_{21} \neq 0$ , similar arguments as those in the proof of Proposition 8 can be used to arrive at a contradiction. In contrast, if  $P_1^{(2)} = 0$  and  $p_{21} = 0$ ,  $R_1^{(2)} = 0$  and  $R_1^{(1)} \geq R_1^*$ , which indicates the primary receiver can decode the primary message after the first phase, and no cooperation from the secondary link is needed. This situation should be excluded in the system model of two-phase transmission.

### 3.6.6. Proof of Proposition 10

The first part of the proposition is proved by contradiction. Assume at the optimum

$$R_t = \alpha \log_2 \left| \mathbf{I} + \mathbf{H}_t \mathbf{K}_1^{(1)} \mathbf{H}_t^H \right| > R_1^*. \quad (3.100)$$

Note that

$$\mathbf{K}_1^{(1)} = \Pi_{\mathbf{h}_{11}} \mathbf{K}_1^{(1)} + \Pi_{\mathbf{h}_{11}}^\perp \mathbf{K}_1^{(1)} \quad (3.101)$$

$$= \beta_1 \boldsymbol{\Sigma}_1 + \beta_2 \boldsymbol{\Sigma}_2, \quad (3.102)$$

where  $\Pi_{\mathbf{h}_{11}} = \frac{\mathbf{h}_{11} \mathbf{h}_{11}^H}{\|\mathbf{h}_{11}\|^2}$ ,  $\Pi_{\mathbf{h}_{11}}^\perp = \mathbf{I} - \Pi_{\mathbf{h}_{11}}$ ,  $\beta_1 = \|\Pi_{\mathbf{h}_{11}} \mathbf{K}_1^{(1)}\|$ ,  $\beta_2 = \|\Pi_{\mathbf{h}_{11}}^\perp \mathbf{K}_1^{(1)}\|$ ,  $\boldsymbol{\Sigma}_1 = \beta_1^{-1} \Pi_{\mathbf{h}_{11}} \mathbf{K}_1^{(1)}$ , and  $\boldsymbol{\Sigma}_2 = \beta_2^{-1} \Pi_{\mathbf{h}_{11}}^\perp \mathbf{K}_1^{(1)}$  with  $\beta_i > 0$  for  $i \in \{1, 2\}$ . Otherwise, set  $\boldsymbol{\Sigma}_i = \mathbf{0}$  for  $i$  such that  $\beta_i = 0$ . Assuming  $\beta_i > 0$  for  $i \in \{1, 2\}$ , both  $\boldsymbol{\Sigma}_1$  and  $\boldsymbol{\Sigma}_2$  have unit norm. Now, let

$$\mathbf{K}_\parallel = \Pi_{\mathbf{h}_{11}}. \quad (3.103)$$

Thus,

$$\Pi_{\mathbf{h}_{11}} \mathbf{K}_\parallel = \mathbf{K}_\parallel, \quad (3.104)$$

$$\Pi_{\mathbf{h}_{11}}^\perp \mathbf{K}_\parallel = \mathbf{0}. \quad (3.105)$$

Now define a new matrix

$$\widetilde{\mathbf{K}}_1^{(1)} = \gamma \mathbf{K}_1^{(1)} + \epsilon \mathbf{K}_{\parallel} = \gamma \beta_1 \boldsymbol{\Sigma}_1 + \gamma \beta_2 \boldsymbol{\Sigma}_2 + \epsilon \mathbf{K}_{\parallel}, \quad (3.106)$$

where  $\epsilon = (1-\gamma)(\beta_1+\beta_2)$ . Note that  $\widetilde{\mathbf{K}}_1^{(1)}$  is a valid choice of covariance matrix because it is the sum of positive semi-definite Hermitian matrices and satisfies  $\text{tr}(\widetilde{\mathbf{K}}_1^{(1)}) = \text{tr}(\mathbf{K}_1^{(1)})$ . Since the determinant is a continuous function of the entries of the matrix, and the logarithm is a continuous function of its argument, there exists  $0 < \gamma < 1$  such that

$$\tilde{R}_t = \alpha \log_2 \left| \mathbf{I} + \mathbf{H}_t \widetilde{\mathbf{K}}_1^{(1)} \mathbf{H}_t^H \right| > R_1^*. \quad (3.107)$$

This choice of  $\widetilde{\mathbf{K}}_1^{(1)}$  yields

$$\tilde{R}_1^{(1)} = \alpha \log_2 \left( 1 + \mathbf{h}_{11}^H \widetilde{\mathbf{K}}_1^{(1)} \mathbf{h}_{11} \right) \quad (3.108a)$$

$$= \alpha \log_2 \left( 1 + \mathbf{h}_{11}^H (\gamma \beta_1 \boldsymbol{\Sigma}_1 + \epsilon \mathbf{K}_{\parallel}) \mathbf{h}_{11} \right) \quad (3.108b)$$

$$= \alpha \log_2 \left( 1 + \gamma \beta_1 \mathbf{h}_{11}^H \boldsymbol{\Sigma}_1 \mathbf{h}_{11} + \epsilon \mathbf{h}_{11}^H \mathbf{K}_{\parallel} \mathbf{h}_{11} \right) \quad (3.108c)$$

$$\geq \alpha \log_2 \left( 1 + \gamma \beta_1 \mathbf{h}_{11}^H \boldsymbol{\Sigma}_1 \mathbf{h}_{11} + \epsilon \mathbf{h}_{11}^H \boldsymbol{\Sigma}_1 \mathbf{h}_{11} \right) \quad (3.108d)$$

$$= \alpha \log_2 \left( 1 + (\beta_1 + \beta_2(1-\gamma)) \mathbf{h}_{11}^H \boldsymbol{\Sigma}_1 \mathbf{h}_{11} \right) \quad (3.108e)$$

$$> \alpha \log_2 \left( 1 + \beta_1 \mathbf{h}_{11}^H \boldsymbol{\Sigma}_1 \mathbf{h}_{11} \right) \quad (3.108f)$$

$$= R_1^{(1)}. \quad (3.108g)$$

The inequality in (3.108d) is due to the fact that

$$\mathbf{h}_{11}^H \mathbf{K}_{\parallel} \mathbf{h}_{11} \geq \mathbf{h}_{11}^H \boldsymbol{\Sigma}_1 \mathbf{h}_{11} \geq 0. \quad (3.109)$$

The inequality in (3.108f) follows if  $\beta_2 > 0$  by the fact that  $0 < \gamma < 1$ . Hence, for this new choice of  $\widetilde{\mathbf{K}}_1^{(1)}$ ,

$$\tilde{R}_1^{(1)} + R_1^{(2)} > R_1^*, \quad (3.110)$$

$$\tilde{R}_t > R_1^*. \quad (3.111)$$

Now, a shorter duration of the first phase  $\tilde{\alpha} < \alpha$  can be found such that the rates evaluated at  $\tilde{\alpha}$  satisfy

$$\tilde{R}_1^{(1)}(\tilde{\alpha}) + R_1^{(2)}(\tilde{\alpha}) \geq R_1^*, \quad (3.112)$$

$$\tilde{R}_t(\tilde{\alpha}) \geq R_1^*. \quad (3.113)$$

At the same time, the secondary rate has been increased by Lemma 5 in Section 3.6.4, thus contradicting the assumption on the optimality of  $\alpha$  and  $\mathbf{K}_1^{(1)}$ .

Finally, note that  $\beta_2 = 0$  implies that

$$\Pi_{\mathbf{h}_{11}} \mathbf{K}_1^{(1)} = \mathbf{K}_1^{(1)}, \quad (3.114)$$

so that  $\mathbf{K}_1^{(1)}$  is a Hermitian rank-one covariance matrix. Therefore,

$$\mathbf{K}_1^{(1)} = \rho \frac{\mathbf{h}_{11} \mathbf{h}_{11}^H}{\|\mathbf{h}_{11}\|^2}, \quad (3.115)$$

for some  $\rho \in \mathbb{R}$ . Thus concludes the proof.

### 3.6.7. Proof of Corollary 1

Assume that  $\mathbf{K}_1^{(1)}$  is the optimal covariance matrix in (3.72), and let  $\widehat{\mathbf{K}}_1^{(1)}$  be the output of Algorithm 4. Note that by construction of the algorithm  $\text{tr}(\widehat{\mathbf{K}}_1^{(1)}) = \text{tr}(\mathbf{K}_1^{(1)})$ . The proof is divided into two parts.

If  $\mathbf{K}_1^{(1)} = \rho \frac{\mathbf{h}_{11} \mathbf{h}_{11}^H}{\|\mathbf{h}_{11}\|^2}$  for some  $\rho \in \mathbb{R}^+$  (i.e., it corresponds to the MRT beamformer to the primary receiver), then trivially  $\widehat{\mathbf{K}}_1^{(1)} = \mathbf{K}_1^{(1)}$  as this is the initial guess of the algorithm (lines 2 and 3) and it satisfies

$$\alpha \log_2 \left| \mathbf{I} + \mathbf{H}_t \widehat{\mathbf{K}}_1^{(1)} \mathbf{H}_t^H \right| \geq R_1^*. \quad (3.116)$$

Thus, this is the output of the algorithm (lines 4 and 5).

For the case when  $\mathbf{K}_1^{(1)}$  does not correspond to the MRT beamformer, the optimality of the algorithm is proved by contradiction. Assume  $\widehat{\mathbf{K}}_1^{(1)} \neq \mathbf{K}_1^{(1)}$  and note that

$$\alpha \log_2 \left| \mathbf{I} + \mathbf{H}_t \mathbf{K}_1^{(1)} \mathbf{H}_t^H \right| = R_1^*, \quad (3.117)$$

$$\alpha \log_2 \left| \mathbf{I} + \mathbf{H}_t \widehat{\mathbf{K}}_1^{(1)} \mathbf{H}_t^H \right| = R_1^*. \quad (3.118)$$

The equality in (3.117) comes from Proposition 10 and the fact that  $\mathbf{K}_1^{(1)}$  is the optimal covariance matrix. The equality in (3.118) is ensured by construction of the algorithm in the limit of arbitrary numerical precision in the bisection method, i.e.,  $\epsilon \rightarrow 0$  (lines 9 to 17 in Algorithm 5). In addition,

$$\mathbf{h}_{11}^H \widehat{\mathbf{K}}_1^{(1)} \mathbf{h}_{11} > \mathbf{h}_{11}^H \mathbf{K}_1^{(1)} \mathbf{h}_{11} \quad (3.119)$$

because by construction, Algorithm 4 finds the matrix with the largest component in the direction of  $\mathbf{h}_{11}$  that satisfies (3.72b) with equality. Thus,

$$R_1^{(1)}(\widehat{\mathbf{K}}_1^{(1)}) + R_1^{(2)} > R_1^*, \quad (3.120)$$

$$R_t(\widehat{\mathbf{K}}_1^{(1)}) = R_1^*. \quad (3.121)$$

The same procedure as in Section 3.6.5 can be used to contradict the assumption on the optimality of  $\mathbf{K}_1^{(1)}$ . Thus,  $\widehat{\mathbf{K}}_1^{(1)} = \mathbf{K}_1^{(1)}$  in this case as well.

## Chapter 4.

# Energy-efficient Spectrum Sharing

Power is another precious resource besides spectrum. Different from the previous chapters which focus on the rate maximization of the secondary transmission, this chapter focuses on energy-efficient spectrum sharing, where the energy efficiency (EE) of the secondary transmission is optimized. The EE of the secondary transmission is defined as the ratio of the achievable secondary rate and the secondary power consumption, which includes both the transmit power and the circuit power at the secondary transmitter. For simplicity, the circuit power is modeled as a constant. Specifically, the EE of a MIMO secondary link in underlay spectrum sharing is optimized with the primary rate requirement and the secondary power constraint. Three transmission strategies are introduced based on the primary rate requirement and the channel conditions. Rate splitting and successive decoding are deployed at the secondary transmitter and receiver, respectively, when it is feasible, and otherwise single-user decoding is deployed at the secondary receiver. Based on this, an energy-efficient resource allocation algorithm is proposed. Moreover, the EE of a MIMO secondary link in overlay spectrum sharing is studied, where the secondary transmitter has non-causal knowledge of the primary message and employs DPC to obtain an interference-free secondary link. Energy-efficient precoding and power allocation is obtained to maximize the EE of the secondary transmission while satisfying the primary rate requirement and the secondary power constraint.

This chapter is partly based on the results reported in [LZJ14].



## 4.1. Energy-efficient Underlay Spectrum Sharing

### 4.1.1. System Model

The system considered is depicted in Figure 4.1 and consists of a MISO primary link with  $N_{T,1}$  transmit antennas and a MIMO secondary link with  $N_{T,2}$  transmit antennas and  $N_{R,2}$  receive antennas, assuming rate splitting at the secondary transmitter and successive decoding at the secondary receiver. The primary and secondary transmitters have power  $P_1$  and  $P_2$ , respectively. Moreover, assume that the secondary transmitter has a constant circuit power consumption of  $P_c$ . The channels from the primary transmitter to the primary and secondary receivers are denoted as  $\mathbf{h}_{11}$  and  $\mathbf{H}_{12}$ , respectively. The channels from the secondary transmitter to the primary and secondary receivers are denoted as  $\mathbf{h}_{21}$  and  $\mathbf{H}_{22}$ , respectively. The noises at the primary and secondary receivers are denoted as  $n_1$  and  $\mathbf{n}_2$ , respectively. The channels and noises are modeled as independent and identically distributed complex Gaussian random variables with zero mean and unit variance. Assume that the primary transmitter knows  $\mathbf{h}_{11}$ ; the secondary transmitter knows  $\mathbf{h}_{11}$ ,  $\mathbf{H}_{12}$ ,  $\mathbf{h}_{21}$  and  $\mathbf{H}_{22}$ .

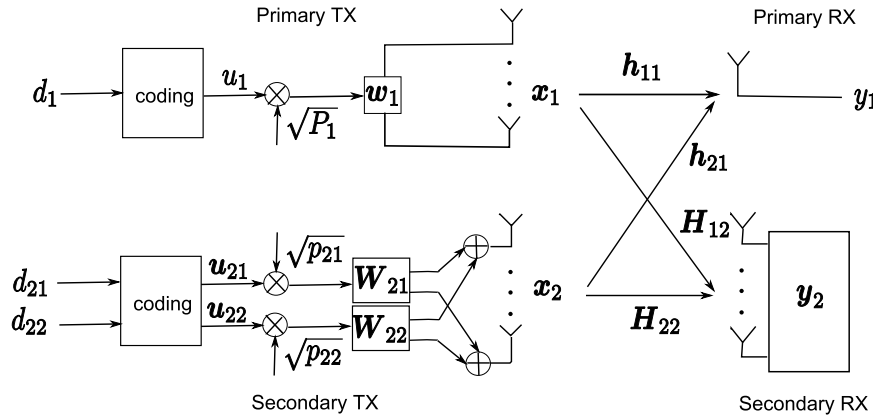


Figure 4.1.: System model consisting of a MISO primary link and a MIMO secondary link – rate splitting at the secondary transmitter and successive decoding at the secondary receiver.

The primary transmission strategy is normally given and fixed, with a rate requirement of  $R_1^*$ , and single-user decoding is deployed at the primary receiver. The primary transmitter employs an  $N_{T,1} \times 1$  beamforming vector  $\mathbf{w}_1$  ( $\|\mathbf{w}_1\| = 1$ ) and power  $P_1$  for message  $d_1$ . With maximum ratio transmission, i.e.,  $\mathbf{w}_1 = \frac{\mathbf{h}_{11}}{\|\mathbf{h}_{11}\|}$ , the signal from the primary transmitter is

$$\mathbf{x}_1 = \sqrt{P_1} \frac{\mathbf{h}_{11}}{\|\mathbf{h}_{11}\|} u_1(d_1), \quad (4.1)$$

where  $d_1$  is encoded into symbol  $u_1$  with unit average power, by a random Gaussian codebook with fixed information rate  $R_1^*$ . The transmit covariance matrix for  $d_1$  is  $\mathbf{K}_1 = \frac{P_1}{\|\mathbf{h}_{11}\|^2} \mathbf{h}_{11} \mathbf{h}_{11}^H$ . The primary receiver has knowledge of the codebook of  $d_1$ .

Assume that the interference from the primary transmitter to the secondary receiver is strong, and rate splitting and successive decoding are deployed at the secondary transmitter and receiver, respectively. At the secondary transmitter, the secondary message  $d_2$  is split into two sub-messages  $d_{21}$  and  $d_{22}$ .  $d_{21}$  ( $d_{22}$ ) is encoded into an  $M_1 \times 1$  ( $M_2 \times 1$ ) vector  $\mathbf{u}_{21}$  ( $\mathbf{u}_{22}$ ) of symbols with unit average power by a random Gaussian codebook.  $\mathbf{W}_{21}$  ( $\mathbf{W}_{22}$ ) is the normalized  $N_{T,2} \times M_1$  ( $N_{T,2} \times M_2$ ) precoding matrix and  $p_{21}$  ( $p_{22}$ ) is the power for the transmission of  $d_{21}$  ( $d_{22}$ ), where  $1 \leq M_1, M_2 \leq \min(N_{R,2}, N_{T,2})$ . The signal from the secondary transmitter is

$$\mathbf{x}_2 = \sqrt{p_{21}} \mathbf{W}_{21} \mathbf{u}_{21}(d_{21}) + \sqrt{p_{22}} \mathbf{W}_{22} \mathbf{u}_{22}(d_{22}). \quad (4.2)$$

The transmit covariance matrices for  $d_{21}$  and  $d_{22}$  are  $\mathbf{K}_{21} = p_{21} \mathbf{W}_{21} \mathbf{W}_{21}^H$  and  $\mathbf{K}_{22} = p_{22} \mathbf{W}_{22} \mathbf{W}_{22}^H$ , respectively. The secondary receiver has knowledge of the codebooks of  $d_{21}$ ,  $d_{22}$  and  $d_1$ .

The signals at the primary and secondary receivers are

$$y_1 = \sqrt{P_1} \|\mathbf{h}_{11}\| u_1(d_1) + \sqrt{p_{21}} \mathbf{h}_{21}^H \mathbf{W}_{21} \mathbf{u}_{21}(d_{21}) + \sqrt{p_{22}} \mathbf{h}_{21}^H \mathbf{W}_{22} \mathbf{u}_{22}(d_{22}) + n_1, \quad (4.3)$$

$$\mathbf{y}_2 = \sqrt{p_{21}} \mathbf{H}_{22} \mathbf{W}_{21} \mathbf{u}_{21}(d_{21}) + \sqrt{p_{22}} \mathbf{H}_{22} \mathbf{W}_{22} \mathbf{u}_{22}(d_{22}) + \frac{\sqrt{P_1}}{\|\mathbf{h}_{11}\|} \mathbf{H}_{12} \mathbf{h}_{11} u_1(d_1) + \mathbf{n}_2, \quad (4.4)$$

respectively.

At the secondary receiver,  $d_{21}$  is decoded first, then  $d_1$  (i.e., the interference), and finally  $d_{22}$ . This adds the constraint that the achievable rate of the primary message at the secondary receiver must be no less than  $R_1^*$  for the secondary receiver to successfully decode the primary message, i.e.,  $R_{12} \geq R_1^*$ , where

$$\begin{aligned} R_{12}(\mathbf{K}_{22}) &= \log_2 \frac{|\mathbf{I} + \mathbf{H}_{22} \mathbf{K}_{22} \mathbf{H}_{22}^H + \mathbf{H}_{12} \mathbf{K}_1 \mathbf{H}_{12}^H|}{|\mathbf{I} + \mathbf{H}_{22} \mathbf{K}_{22} \mathbf{H}_{22}^H|} \\ &= \log_2 \left| \mathbf{I} + (\mathbf{I} + \mathbf{H}_{22} \mathbf{K}_{22} \mathbf{H}_{22}^H)^{-1} \mathbf{M} \right| \end{aligned} \quad (4.5)$$

with  $\mathbf{M} = \mathbf{H}_{12} \mathbf{K}_1 \mathbf{H}_{12}^H$ , which is convex in  $\mathbf{K}_{22}$  [DC01, Lemma II.3] and matrix-decreasing in  $\mathbf{K}_{22}$  [MOA11, Ch 16, E.3.b.].

The achievable primary rate is

$$R_1(\mathbf{K}_{21}, \mathbf{K}_{22}) = \log_2 \left( 1 + \frac{\mathbf{h}_{11}^H \mathbf{K}_1 \mathbf{h}_{11}}{1 + \mathbf{h}_{21}^H (\mathbf{K}_{21} + \mathbf{K}_{22}) \mathbf{h}_{21}} \right), \quad (4.6)$$



and the achievable secondary rate is

$$\begin{aligned} R_2(\mathbf{K}_{21}, \mathbf{K}_{22}) &= \log_2 \frac{|\mathbf{I} + \mathbf{H}_{22}(\mathbf{K}_{21} + \mathbf{K}_{22})\mathbf{H}_{22}^H + \mathbf{M}|}{|\mathbf{I} + \mathbf{H}_{22}\mathbf{K}_{22}\mathbf{H}_{22}^H + \mathbf{M}|} + \log_2 |\mathbf{I} + \mathbf{H}_{22}\mathbf{K}_{22}\mathbf{H}_{22}^H| \\ &= \log_2 |\mathbf{I} + \mathbf{H}_{22}(\mathbf{K}_{21} + \mathbf{K}_{22})\mathbf{H}_{22}^H + \mathbf{M}| - R_{12}(\mathbf{K}_{22}), \end{aligned} \quad (4.7)$$

which is jointly concave in  $\mathbf{K}_{21}$  and  $\mathbf{K}_{22}$ . The first term in (4.7) corresponds to the part of the secondary message decoded in the presence of the interference (both from primary transmitter and self-interference). The second term in (4.7) corresponds to the part of the secondary message recovered after decoding and subtracting the primary message.

The two special cases, where the secondary receiver decodes the primary message at first (very strong interference) or does not decode it at all (weak interference), are included by setting  $\mathbf{K}_{21}$  and  $\mathbf{K}_{22}$  to the zero matrix, respectively.

The energy efficiency (EE) of the secondary transmission is defined as the ratio of the achievable rate and the power consumption, which includes both the transmit power and the circuit power, i.e.,

$$\text{EE}(\mathbf{K}_{21}, \mathbf{K}_{22}) = \frac{R_2(\mathbf{K}_{21}, \mathbf{K}_{22})}{\text{tr}(\mathbf{K}_{21} + \mathbf{K}_{22}) + P_c}. \quad (4.8)$$

To maximize the EE of the secondary transmission while satisfying the primary rate requirement  $R_1^*$  and the secondary power constraint  $P_2$ , the optimization problem can be formulated as

$$\max_{\mathbf{K}_{21}, \mathbf{K}_{22}} \text{EE}(\mathbf{K}_{21}, \mathbf{K}_{22}) \quad (4.9a)$$

$$\text{s.t. } R_1(\mathbf{K}_{21}, \mathbf{K}_{22}) \geq R_1^*, \quad (4.9b)$$

$$R_{12}(\mathbf{K}_{22}) \geq R_1^*, \quad (4.9c)$$

$$\text{tr}(\mathbf{K}_{21} + \mathbf{K}_{22}) \leq P_2, \quad (4.9d)$$

$$\mathbf{K}_{21} \succeq \mathbf{0}, \mathbf{K}_{22} \succeq \mathbf{0}, \quad (4.9e)$$

where it is implicitly assumed that (4.9c) applies only if  $\mathbf{K}_{22} \neq \mathbf{0}$ . The numerator and denominator of the objective function in (4.9a) are jointly concave and linear in  $\mathbf{K}_{21}$  and  $\mathbf{K}_{22}$ , respectively, i.e., the objective function is jointly pseudo-concave [Sch83]. (4.9b) and (4.9d) are jointly linear in  $\mathbf{K}_{21}$  and  $\mathbf{K}_{22}$ , respectively. Since  $R_{12}$  is convex in  $\mathbf{K}_{22}$ , (4.9c) is not convex. Overall, (4.9) is a non-convex fractional program. However, it is possible to solve it with limited computational complexity, as shown in the following sections.

### 4.1.2. Fractional Programming

A general nonlinear fractional program has the form

$$\max_{\mathbf{x} \in \mathcal{S}} \frac{f(\mathbf{x})}{g(\mathbf{x})} \quad (4.10)$$

where  $\mathcal{S} \subseteq \mathbb{R}^n$ ,  $f, g : \mathcal{S} \rightarrow \mathbb{R}$  and  $g(\mathbf{x}) > 0$ .  $f$  and  $g$  are differentiable. If  $f$  is concave,  $g$  is convex, and  $\mathcal{S}$  is a convex set, the objective function in (4.10) is pseudoconcave and (4.10) is called a concave fractional program; additionally  $f(\mathbf{x}) \geq 0$  is required, unless  $g$  is affine, implying that any stationary point is a global maximum and that the Karush-Kuhn-Tucker (KKT) conditions are sufficient if a constraint qualification is fulfilled [ICJF12]. Thus (4.10) can be solved directly by various convex programming algorithms [Sch83]. However, the concave fractional program can be transformed to an equivalent convex program and solved more efficiently.

Consider the function  $F(\lambda) = \max_{\mathbf{x} \in \mathcal{S}} f(\mathbf{x}) - \lambda g(\mathbf{x})$ . It can be shown that  $F(\lambda)$  is convex, continuous and strictly decreasing in  $\lambda$ , and that solving (4.10) is equivalent to finding the unique root of  $F(\lambda)$ , which can be accomplished by Dinkelbach's method with a super-linear convergence rate [Din67].

---

**Algorithm 7** Dinkelbach's method to solve (4.10)

---

1: **Initialize**  $\lambda_0$  with  $F(\lambda_0) \geq 0$ ,  $n = 0$ .

2: **while**  $F(\lambda_n) > \epsilon$  **do**

3:      $\mathbf{x}_n^* = \arg \max_{\mathbf{x} \in \mathcal{S}} f(\mathbf{x}) - \lambda_n g(\mathbf{x})$ ;

4:      $\lambda_{n+1} = \frac{f(\mathbf{x}_n^*)}{g(\mathbf{x}_n^*)}$ ;

5:      $n++$ ;

6: **end while**

7: **Output**  $\mathbf{x}_n^*$ ,  $\lambda_n$ .

---

### 4.1.3. Energy-efficient Precoding and Power Allocation

This section provides the solution to the non-convex fractional problem (4.9) in terms of concave fractional problems which can be efficiently solved by fractional programming. The two extreme cases in which either  $\mathbf{K}_{22} = \mathbf{0}$  or  $\mathbf{K}_{21} = \mathbf{0}$  and the intermediate case in which both  $\mathbf{K}_{21}$  and  $\mathbf{K}_{22}$  are non-zero matrices are treated separately. These three cases correspond to three distinct ranges of the primary rate requirement  $R_1^*$ .

**Case 1:  $\mathbf{K}_{22} = \mathbf{0}$ .** This case is obtained when  $R_1^* \geq \log_2 |\mathbf{I} + \mathbf{M}|$ , i.e., decoding the primary message at the secondary receiver is not possible at all. The secondary message

is decoded in the presence of the interference due to the primary message. The optimal  $\mathbf{K}_{21}$  is the solution to the problem

$$\max_{\mathbf{K}_{21}} \frac{\log_2 |\mathbf{I} + \mathbf{H}_{22} \mathbf{K}_{21} \mathbf{H}_{22}^H (\mathbf{I} + \mathbf{M})^{-1}|}{\text{tr}(\mathbf{K}_{21}) + P_c} \quad (4.11a)$$

$$\text{s.t. } \mathbf{h}_{21}^H \mathbf{K}_{21} \mathbf{h}_{21} \leq P_{\text{int}}, \quad (4.11b)$$

$$\text{tr}(\mathbf{K}_{21}) \leq P_2, \quad (4.11c)$$

$$\mathbf{K}_{21} \succeq \mathbf{0}, \quad (4.11d)$$

where

$$P_{\text{int}} = \frac{\mathbf{h}_{11}^H \mathbf{K}_1 \mathbf{h}_{11}}{2^{R_1^*} - 1} - 1 \geq 0. \quad (4.12)$$

The numerator and denominator of the objective function in (4.11a) are concave and linear in  $\mathbf{K}_{21}$ , respectively, i.e., the objective function is pseudo-concave. The constraints (4.11b) and (4.11c) are linear in  $\mathbf{K}_{21}$ , respectively. Overall, the optimization problem (4.11) is a concave fractional program.

**Case 2:  $\mathbf{K}_{21} = \mathbf{0}$ .** Proposition 11 shows that this case is obtained when

$$R_1^* \leq \log_2 \left| \mathbf{I} + (\mathbf{I} + \mathbf{H}_{22} \mathbf{\Sigma}^* \mathbf{H}_{22}^H)^{-1} \mathbf{M} \right|, \quad (4.13)$$

where  $\mathbf{\Sigma}^*$  is the solution to the problem

$$\max_{\mathbf{\Sigma}} \frac{\log_2 |\mathbf{I} + \mathbf{H}_{22} \mathbf{\Sigma} \mathbf{H}_{22}^H|}{\text{tr}(\mathbf{\Sigma}) + P_c} \quad (4.14a)$$

$$\text{s.t. } \mathbf{h}_{21}^H \mathbf{\Sigma} \mathbf{h}_{21} \leq P_{\text{int}}, \quad (4.14b)$$

$$\text{tr}(\mathbf{\Sigma}) \leq P_2, \quad (4.14c)$$

$$\mathbf{\Sigma} \succeq \mathbf{0}, \quad (4.14d)$$

and  $P_{\text{int}}$  is defined as in (4.12).

**Proposition 11.** Denote by  $(\mathbf{K}_{21}^*, \mathbf{K}_{22}^*)$  a solution of (4.9). If (4.13) holds, then  $\mathbf{K}_{21}^* = \mathbf{0}$ .

*Proof.* The proof is similar to that of Proposition 3 in Section 2.2.  $\square$

The primary message is decoded and subtracted before decoding the secondary message, and rate splitting is not required at the secondary transmitter. The optimal  $\mathbf{K}_{22} = \mathbf{\Sigma}^*$ .

The numerator and denominator of the objective function in (4.14a) are concave and linear in  $\mathbf{\Sigma}$ , respectively, i.e., the objective function is pseudo-concave. The constraints

(4.14b) and (4.14c) are linear in  $\Sigma$ , respectively. Overall, the optimization problem (4.14) is a concave fractional program.

**Case 3:**  $\mathbf{K}_{21} \neq \mathbf{0}$  and  $\mathbf{K}_{22} \neq \mathbf{0}$ . This case corresponds to the intermediate range of  $R_1^*$ , i.e.,

$$\log_2 \left| \mathbf{I} + (\mathbf{I} + \mathbf{H}_{22} \Sigma^* \mathbf{H}_{22}^H)^{-1} \mathbf{M} \right| < R_1^* < \log_2 |\mathbf{I} + \mathbf{M}|. \quad (4.15)$$

In this case, the solution of (4.9) is given by Proposition 12.

**Proposition 12.** *If (4.15) holds, then (4.9) is solved by  $\mathbf{K}_{21} = \widehat{\mathbf{K}}_{21} + (1 - \gamma)\widehat{\mathbf{K}}_{22}$  and  $\mathbf{K}_{22} = \gamma\widehat{\mathbf{K}}_{22}$ , where  $\gamma \in [0, 1]$  is chosen such that  $R_{12}(\mathbf{K}_{22}) = R_1^*$ , and  $\widehat{\mathbf{K}}_{21}$  and  $\widehat{\mathbf{K}}_{22}$  are the solution to the problem*

$$\max_{\mathbf{K}_{21}, \mathbf{K}_{22}} \frac{\log_2 \left| \mathbf{I} + \mathbf{H}_{22}(\mathbf{K}_{21} + \mathbf{K}_{22})\mathbf{H}_{22}^H + \mathbf{M} \right| - R_1^*}{\text{tr}(\mathbf{K}_{21} + \mathbf{K}_{22}) + P_c} \quad (4.16a)$$

$$\text{s.t. } \mathbf{h}_{21}^H(\mathbf{K}_{21} + \mathbf{K}_{22})\mathbf{h}_{21} \leq P_{\text{int}}, \quad (4.16b)$$

$$\log_2 \left| \mathbf{I} + (\mathbf{I} + \mathbf{H}_{22}\mathbf{K}_{22}\mathbf{H}_{22}^H)^{-1} \mathbf{M} \right| \leq R_1^*, \quad (4.16c)$$

$$\text{tr}(\mathbf{K}_{21} + \mathbf{K}_{22}) \leq P_2, \quad (4.16d)$$

$$\mathbf{K}_{21} \succeq \mathbf{0}, \mathbf{K}_{22} \succeq \mathbf{0}, \quad (4.16e)$$

where  $P_{\text{int}}$  is defined as in (4.12).

*Proof.* The proof is similar to that of Proposition 4 in Section 2.2.  $\square$

The numerator and denominator of the objective function in (4.16a) are jointly concave and linear in  $\mathbf{K}_{21}$  and  $\mathbf{K}_{22}$ , respectively, i.e., the objective function is jointly pseudo-concave. The constraints (4.16b) and (4.16d) are jointly linear in  $\mathbf{K}_{21}$  and  $\mathbf{K}_{22}$ , respectively, and the constraint (4.16c) is convex in  $\mathbf{K}_{22}$ . Overall, the optimization problem (4.16) is a jointly concave fractional program.

**Remark 22.** *The whole range of  $R_1^*$  is covered by these three cases, where in each case a corresponding concave fractional program is solved to obtain the optimal transmit covariance matrices. An additional line search is required in Case 3. The concave fractional programs can be solved by fractional programming, e.g., Dinkelbach's method as introduced in Section 4.1.2, which requires only the solutions of convex problems and has a super-linear convergence rate.*

**Remark 23.** *Comparing the two special cases, specifically (4.11) in Case 1 and (4.14) in Case 2, the solution to (4.11) is feasible for (4.14) and achieves a higher objective value for (4.14). It shows that rate splitting at the secondary transmitter and successive*

decoding at the secondary receiver does increase the achievable secondary EE when it is feasible, compared with single-user decoding at the secondary receiver.

The energy-efficient resource allocation is summarized in Algorithm 8.

---

**Algorithm 8** Energy-efficient resource allocation
 

---

```

1: if  $R_1^* \geq \log_2 |\mathbf{I} + \mathbf{H}_{12} \mathbf{K}_1 \mathbf{H}_{12}^H|$  then
2:    $\mathbf{K}_{22} = \mathbf{0}$ ;
3:   Solve (4.11) by Algorithm 7 to find  $\mathbf{K}_{21}$ ;
4: else
5:   Solve (4.14) by Algorithm 7 to find  $\Sigma^*$ ;
6:   if  $R_1^* \leq \log_2 |\mathbf{I} + \mathbf{H}_{12} \mathbf{K}_1 \mathbf{H}_{12}^H (\mathbf{I} + \mathbf{H}_{22} \Sigma^* \mathbf{H}_{22}^H)^{-1}|$  then
7:      $\mathbf{K}_{21} = \mathbf{0}, \mathbf{K}_{22} = \Sigma^*$ ;
8:   else
9:     Solve (4.16) by Algorithm 7 to find  $(\widehat{\mathbf{K}}_{21}, \widehat{\mathbf{K}}_{22})$ ;
10:    Perform a line search in  $\gamma \in [0, 1]$  such that  $R_{12}(\gamma \widehat{\mathbf{K}}_{22}) = R_1^*$ ;
11:     $\mathbf{K}_{21} = \widehat{\mathbf{K}}_{21} + (1 - \gamma) \widehat{\mathbf{K}}_{22}, \mathbf{K}_{22} = \gamma \widehat{\mathbf{K}}_{22}$ ;
12:  end if
13: end if
14: Output  $\mathbf{K}_{21}, \mathbf{K}_{22}$ .
    
```

---

#### 4.1.4. Numerical Simulations

Numerical simulations are performed to evaluate the performance of the proposed MIMO underlay spectrum sharing with energy efficiency optimization (*MIMO USS EE Opt*), and compare with that of MIMO underlay spectrum sharing with rate optimization (*MIMO USS Rate Opt*), as proposed in Section 2.2, in terms of secondary EE (in bit/Hz/Joule) or secondary rate (in bit/s/Hz) versus SNR of the secondary link (in dB). Moreover, the performance of *MIMO USS EE Opt* is compared with that of energy-efficient MIMO underlay spectrum sharing without rate splitting and successive decoding (*MIMO USS EE Opt w/o RS*), which corresponds to Case 1 in Section 4.1.3, in terms of secondary EE.

The primary rate requirement is set as a fraction of its instantaneous point-to-point channel capacity without secondary transmission, i.e.,

$$R_1^* = \rho \log_2 (1 + P_1 \|\mathbf{h}_{11}\|^2), \quad (4.17)$$

where  $0 < \rho \leq 1$  is the load factor of the primary link.

The system configuration is as follows. The primary transmitter has 2 antennas, and the secondary transmitter and receiver have 2 antennas each. The primary transmit power is fixed at 10 dB, and the secondary transmit power is varied from  $-20$  dB to 20 dB as the SNR of the secondary link, and the circuit power consumption at the secondary transmitter is set to 0 dB. The load factor of the primary link is varied from 25% to 100%. The simulation results are averaged over 1000 channel realizations.

As in Figure 4.2, at a certain primary link load, the secondary EE of both *MIMO USS EE Opt* and *MIMO USS Rate Opt* increase with the SNR, and are nearly the same at SNRs under 0 dB; the secondary EE of *MIMO USS EE Opt* saturates at SNRs over 0 dB, while that of *MIMO USS Rate Opt* decreases with the SNR. At the load factor of 75% and SNR of 10 dB, the EE gain of *MIMO USS EE Opt* over *MIMO USS Rate Opt* is about 0.5 bit/Hz/Joule.

As in Figure 4.3, at a certain primary link load, the secondary rate of both *MIMO USS EE Opt* and *MIMO USS Rate Opt* increase with the SNR, and are nearly the same at SNRs under 0 dB; the secondary power of *MIMO USS EE Opt* saturates at SNRs over 0 dB, while that of *MIMO USS Rate Opt* continues to increase with the SNR. At the load factor of 75% and SNR of 10 dB, the rate loss of *MIMO USS EE Opt* to *MIMO USS Rate Opt* is about 2.3 bits/s/Hz.

As in Figure 4.4, at a certain primary link load, the secondary power of both *MIMO USS EE Opt* and *MIMO USS Rate Opt* increase with the SNR, and are nearly the same at SNRs under 0 dB; the secondary power of *MIMO USS EE Opt* saturates at SNRs over 0 dB, while that of *MIMO USS Rate Opt* continues to increase with the SNR. At the load factor of 75% and SNR of 10 dB, the power saving of *MIMO USS EE Opt* over *MIMO USS Rate Opt* is about 7 dB.

As in Figure 4.5, at a certain primary link load, *MIMO USS EE Opt* can achieve a significantly higher EE than *MIMO USS EE Opt w/o RS*, and the EE gain becomes constant at SNRs over 0 dB, which is about 0.2 bit/Hz/Joule at the load factor of 75% and SNR of 10 dB.

Numerical results show that MIMO underlay spectrum sharing with EE optimization can achieve a significantly higher EE compared with MIMO underlay spectrum sharing with rate optimization, at certain SNRs and with certain circuit power, at the cost of the achievable secondary rate, while saving the transmit power. In MIMO underlay spectrum sharing with EE optimization, both the achievable secondary rate and EE increase as the SNR increases, until a point when the growth rate of the secondary power surpasses that of the secondary rate, and the secondary EE reaches its maximum and stays unchanged thereafter; while the secondary EE decreases after that point in

MIMO underlay spectrum sharing with rate optimization. It is also shown that with rate splitting at the secondary transmitter and successive decoding at the secondary receiver if feasible, a significantly higher EE can be achieved compared with the case when only single-user decoding is deployed at the secondary receiver.

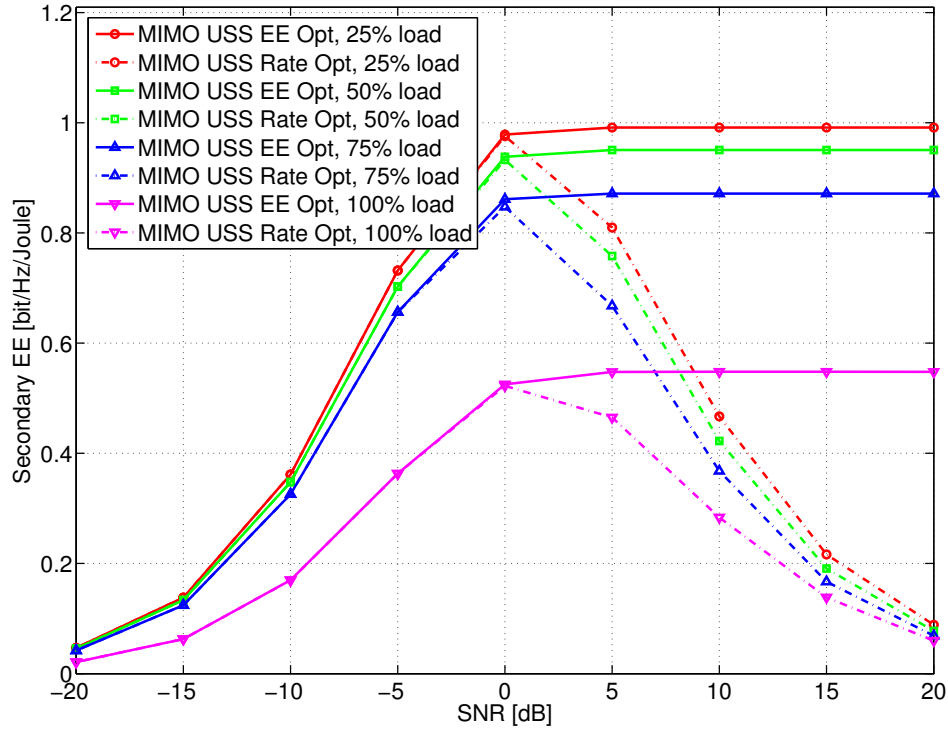


Figure 4.2.: Secondary EE versus SNR of the secondary link: *MIMO USS EE Opt* versus *MIMO USS Rate Opt* with different primary link loads.

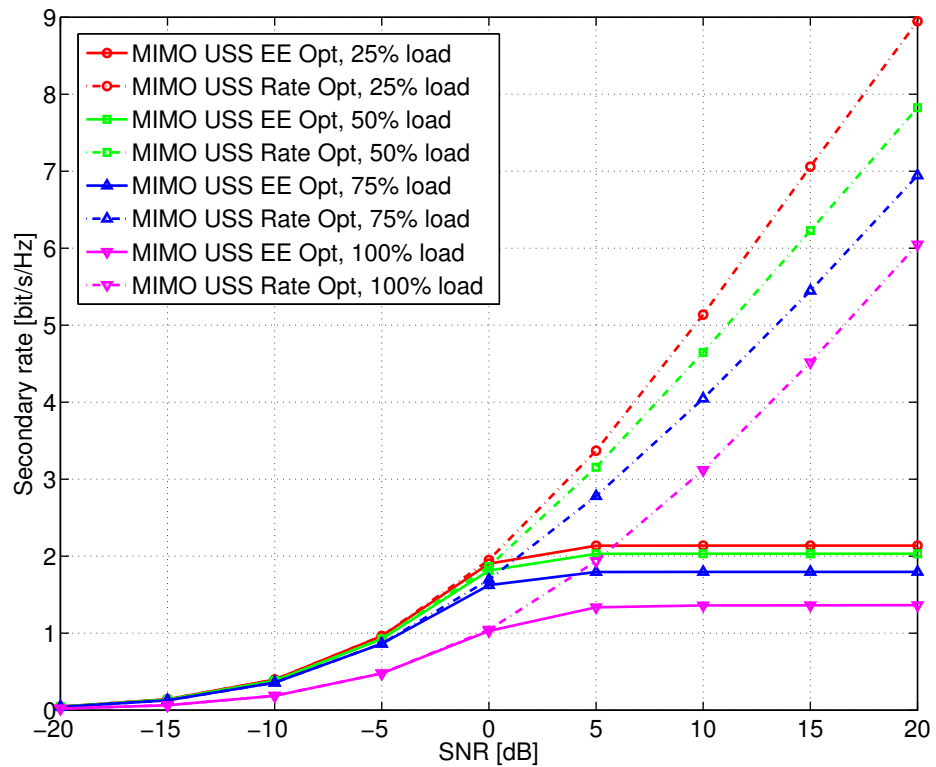


Figure 4.3.: Secondary rate versus SNR of the secondary link: *MIMO USS EE Opt* versus *MIMO USS Rate Opt* with different primary link loads.



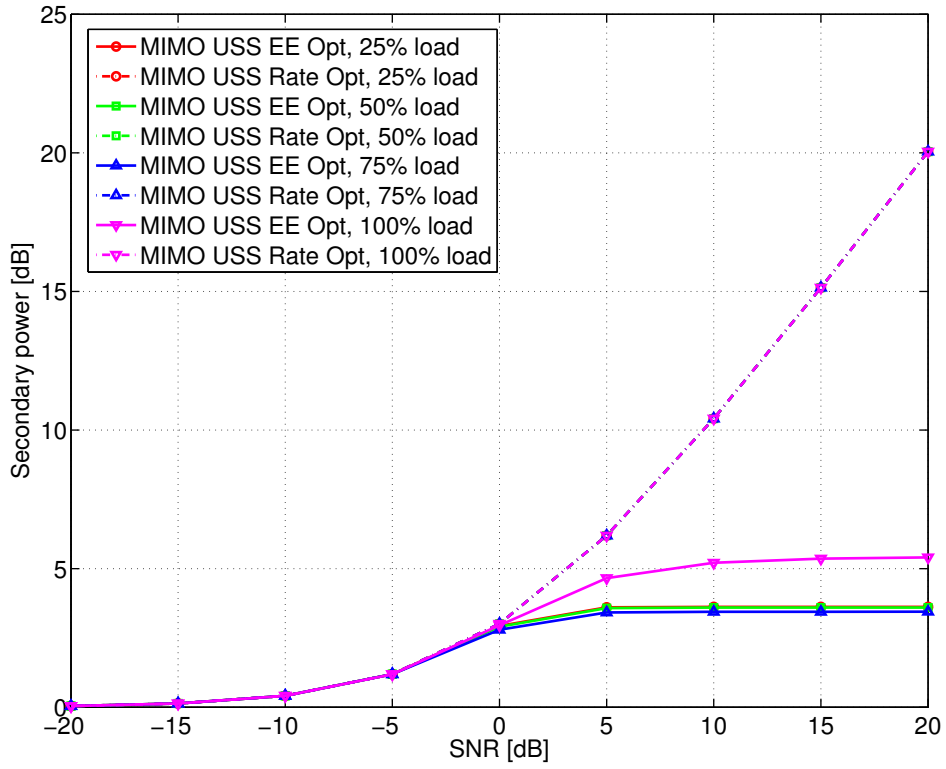


Figure 4.4.: Secondary power versus SNR of the secondary link: *MIMO USS EE Opt* versus *MIMO USS Rate Opt* with different primary link loads.

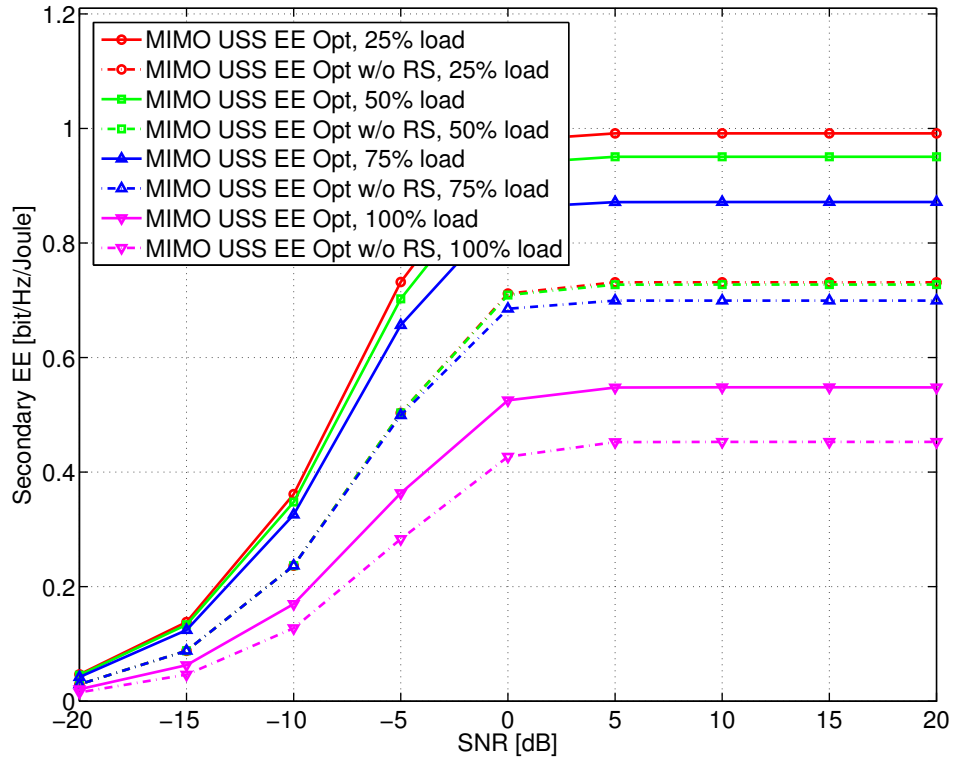


Figure 4.5.: Secondary EE versus SNR of the secondary link: *MIMO USS EE Opt* versus *MIMO USS EE Opt w/o RS* with different primary link loads.

## 4.2. Energy-efficient Overlay Spectrum Sharing

### 4.2.1. System Model

The system considered is depicted in Figure 4.6 and consists of a MISO primary link with  $N_{T,1}$  transmit antennas and a MIMO secondary link with  $N_{T,2}$  transmit antennas and  $N_{R,2}$  receive antennas. Assume that the secondary transmitter has non-causal knowledge of the primary message. The primary and secondary transmitters have power  $P_1$  and  $P_2$ , respectively. Moreover, assume that the secondary transmitter has a constant circuit power consumption of  $P_c$ . The channels from the primary transmitter to the primary and secondary receivers are denoted as  $\mathbf{h}_{11}$  and  $\mathbf{H}_{12}$ , respectively. The channels from the secondary transmitter to the primary and secondary receivers are denoted as  $\mathbf{h}_{21}$  and  $\mathbf{H}_{22}$ , respectively. The noises at the primary and secondary receivers are denoted as  $n_1$  and  $\mathbf{n}_2$ , respectively. The channels and noises are modeled as independent and identically distributed complex Gaussian random variables with zero mean and unit variance. Assume that the primary transmitter knows  $\mathbf{h}_{11}$ ; the secondary transmitter knows  $\mathbf{h}_{11}$ ,  $\mathbf{H}_{12}$ ,  $\mathbf{h}_{21}$  and  $\mathbf{H}_{22}$ .

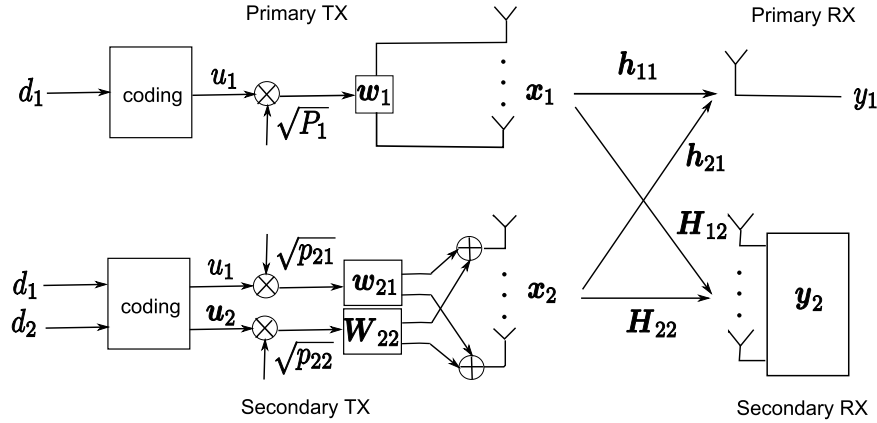


Figure 4.6.: System model consisting of a MISO primary link and a MIMO secondary link – non-causal primary message at the secondary transmitter.

The primary transmission strategy is normally given and fixed, with a rate requirement of  $R_1^*$ , and single-user decoding is deployed at the primary receiver. The primary transmitter employs an  $N_{T,1} \times 1$  beamforming vector  $\mathbf{w}_1$  ( $\|\mathbf{w}_1\| = 1$ ) and power  $P_1$  for message  $d_1$ . With maximum ratio transmission, i.e.,  $\mathbf{w}_1 = \frac{\mathbf{h}_{11}}{\|\mathbf{h}_{11}\|}$ , the signal from the primary transmitter is

$$\mathbf{x}_1 = \sqrt{P_1} \frac{\mathbf{h}_{11}}{\|\mathbf{h}_{11}\|} u_1(d_1), \quad (4.18)$$

where  $d_1$  is encoded into symbol  $u_1$  with unit average power, by a random Gaussian

codebook with fixed information rate  $R_1^*$ . The primary receiver has knowledge of the codebook of  $d_1$ .

Since the secondary transmitter has non-causal knowledge of  $d_1$ , it can transmit  $d_1$  to the primary receiver as a return for the access to the spectrum. The secondary transmitter has a total power of  $P_2$ . A fraction  $p_{21}$  of it is spent in a selfless manner to help the primary link achieve its rate requirement, and the remaining power  $p_{22}$  is used for the transmission of its own message  $d_2$ .

With knowledge of the primary message and codebook and perfect channel state information at the secondary transmitter, the interference (when decoding  $d_2$  at the secondary receiver) due to the transmission of  $d_1$  from both transmitters is known, and can be precanceled by DPC. With superposition coding in combination with DPC, the signal from the secondary transmitter is

$$\mathbf{x}_2 = \sqrt{p_{21}}\mathbf{w}_{21}u_1(d_1) + \sqrt{p_{22}}\mathbf{W}_{22}\mathbf{u}_2(d_1, d_2), \quad (4.19)$$

where  $d_1$  is encoded into symbol  $u_1$  with unit average power by the same codebook at the primary transmitter,  $d_2$  is encoded into an  $M \times 1$  vector  $\mathbf{u}_2$  of symbols with unit average power by DPC, and  $\mathbf{w}_{21}$  ( $\|\mathbf{w}_{21}\| = 1$ ) is the  $N_{T,2} \times 1$  beamforming vector and  $\mathbf{W}_{22}$  ( $\|\mathbf{W}_{22}\| = 1$ ) is the  $N_{T,2} \times M$  precoding matrix, where  $1 \leq M \leq \min(N_{R,2}, N_{T,2})$ . The secondary receiver has knowledge of the codebooks of  $d_1$  and  $d_2$ .

By the same arguments as in Section 3.1.2 and the results from [CS03] [WSS06], the achievable rates for the primary and secondary links are

$$R_1 = \log_2 \left( 1 + \frac{|\sqrt{P_1}|\|\mathbf{h}_{11}\| + \sqrt{p_{21}}\mathbf{h}_{21}^H\mathbf{w}_{21}|^2}{1 + p_{22}\|\mathbf{h}_{21}^H\mathbf{W}_{22}\|^2} \right), \quad (4.20)$$

$$R_2 = \log_2 |\mathbf{I} + p_{22}\mathbf{H}_{22}\mathbf{W}_{22}\mathbf{W}_{22}^H\mathbf{H}_{22}^H|, \quad (4.21)$$

for any feasible choice of beamforming vector  $\mathbf{w}_{21}$ , precoding matrix  $\mathbf{W}_{22}$  and powers  $p_{21}$  and  $p_{22}$ .

The EE of the secondary transmission is defined as the ratio of the achievable rate and the power consumption, which includes both the transmit power and the circuit power, i.e.,

$$\text{EE} = \frac{R_2}{p_{21} + p_{22} + P_c}. \quad (4.22)$$

To maximize the EE of the secondary transmission while satisfying the primary rate requirement  $R_1^*$  and the secondary power constraint  $P_2$ , the optimization problem can

be formulated as

$$\max_{\substack{\mathbf{w}_{21}, \mathbf{W}_{22} \\ p_{21}, p_{22}}} \text{EE} \quad (4.23\text{a})$$

$$\text{s.t. } \log_2 \left( 1 + \frac{|\sqrt{P_1} \|\mathbf{h}_{11}\| + \sqrt{p_{21}} \mathbf{h}_{21}^H \mathbf{w}_{21}|^2}{1 + p_{22} \|\mathbf{h}_{21}^H \mathbf{W}_{22}\|^2} \right) \geq R_1^*, \quad (4.23\text{b})$$

$$\|\mathbf{w}_{21}\| = \|\mathbf{W}_{22}\| = 1, \quad (4.23\text{c})$$

$$p_{21} + p_{22} \leq P_2, p_{21} \geq 0, p_{22} \geq 0. \quad (4.23\text{d})$$

### 4.2.2. Energy-efficient Precoding and Power Allocation

It can be easily seen that the optimal  $\mathbf{w}_{21}$  is maximum ratio transmission, i.e.,  $\mathbf{w}_{21} = \frac{\mathbf{h}_{21}}{\|\mathbf{h}_{21}\|}$ , since it only exists in (4.23b). Let  $\mathbf{K} = p_{22} \mathbf{W}_{22} \mathbf{W}_{22}^H$  denote the transmit covariance matrix, then (4.23) is equivalent to

$$\max_{\mathbf{K}, p_{21}} \frac{\log_2 |\mathbf{I} + \mathbf{H}_{22} \mathbf{K} \mathbf{H}_{22}^H|}{\text{tr}(\mathbf{K}) + p_{21} + P_c} \quad (4.24\text{a})$$

$$\text{s.t. } \mathbf{h}_{21}^H \mathbf{K} \mathbf{h}_{21} \leq P_{\text{int}}, \quad (4.24\text{b})$$

$$\text{tr}(\mathbf{K}) + p_{21} \leq P_2, \mathbf{K} \succeq \mathbf{0}, p_{21} \geq 0. \quad (4.24\text{c})$$

where  $P_{\text{int}} = \frac{(\sqrt{P_1} \|\mathbf{h}_{11}\| + \sqrt{p_{21}} \|\mathbf{h}_{21}\|)^2}{2^{R_1^*} - 1} - 1 \geq 0$ . The numerator and denominator of the objective function in (4.24a) are concave in  $\mathbf{K}$  and jointly linear in  $\mathbf{K}$  and  $p_{21}$ , respectively, i.e., the objective function is jointly pseudo-concave [Sch83]. The left-hand-side of the constraint (4.24b) is linear in  $\mathbf{K}$ , and the right-hand-side of (4.24b) is concave in  $p_{21}$ , i.e., (4.24b) is jointly convex in  $\mathbf{K}$  and  $p_{21}$ . The constraint (4.24c) is jointly linear in  $\mathbf{K}$  and  $p_{21}$ . Thus (4.24) is a jointly concave fractional program and can be solved by fractional programming, e.g., Dinkelbach's method as introduced in Section 4.1.2.

**Remark 24.** *The special case of  $p_{21} = 0$  in (4.23) corresponds to Case 2 of the energy-efficient MIMO underlay spectrum sharing in Section 4.1, with interference precancellation by DPC instead of interference cancellation by successive decoding. It shows that the proposed energy-efficient MIMO overlay spectrum sharing can achieve a higher EE than the energy-efficient MIMO underlay spectrum sharing in Section 4.1.*

### 4.2.3. Numerical Simulations

Numerical simulations are performed to evaluate the performance of the proposed MIMO overlay spectrum sharing with energy efficiency optimization (*MIMO OSS EE Opt*), and compare with that of MIMO overlay spectrum sharing with rate optimization (*MIMO*

*OSS Rate Opt*), as proposed in Section 3.2.2, in terms of secondary EE (in bit/Hz/Joule) or secondary rate (in bit/s/Hz) versus SNR of the secondary link (in dB). Moreover, the performance of *MIMO OSS EE Opt* is compared with that of energy-efficient MIMO underlay spectrum sharing (*MIMO USS EE Opt*), as proposed in Section 4.1, in terms of secondary EE.

The primary rate requirement is set as a fraction of its instantaneous point-to-point channel capacity without secondary transmission, i.e.,

$$R_1^* = \rho \log_2 (1 + P_1 \|\mathbf{h}_{11}\|^2), \quad (4.25)$$

where  $0 < \rho \leq 1$  is the load factor of the primary link.

The system configuration is as follows. The primary transmitter has 2 antennas, and the secondary transmitter and receiver have 2 antennas each. The primary transmit power is fixed at 10 dB, and the secondary transmit power is varied from  $-20$  dB to 20 dB as the SNR of the secondary link, and the circuit power consumption at the secondary transmitter is set to 0 dB. The load factor of the primary link is varied from 25% to 100%. The simulation results are averaged over 1000 channel realizations.

As in Figure 4.7, at a certain primary link load, the secondary EE of both *MIMO OSS EE Opt* and *MIMO OSS Rate Opt* increase with the SNR, and are nearly the same at SNRs under 0 dB; the secondary EE of *MIMO OSS EE Opt* saturates at SNRs over 0 dB, while that of *MIMO OSS Rate Opt* decreases with the SNR. At the load factor of 75% and SNR of 10 dB, the EE gain of *MIMO OSS EE Opt* over *MIMO OSS Rate Opt* is about 0.6 bit/Hz/Joule.

As in Figure 4.8, at a certain primary link load, the secondary rate of both *MIMO OSS EE Opt* and *MIMO OSS Rate Opt* increase with the SNR, and are nearly the same at SNRs under 0 dB; the secondary rate of *MIMO OSS EE Opt* saturates at SNRs over 0 dB, while that of *MIMO OSS Rate Opt* continues to increase with the SNR. At the load factor of 75% and SNR of 10 dB, the rate loss of *MIMO OSS EE Opt* to *MIMO OSS Rate Opt* is about 3 bits/s/Hz.

As in Figure 4.9, at a certain primary link load, the secondary power of both *MIMO OSS EE Opt* and *MIMO OSS Rate Opt* increase with the SNR, and are nearly the same at SNRs under 0 dB; the secondary power of *MIMO OSS EE Opt* saturates at SNRs over 0 dB, while that of *MIMO OSS Rate Opt* continues to increase with the SNR. At the load factor of 75% and SNR of 10 dB, the power saving of *MIMO OSS EE Opt* over *MIMO OSS Rate Opt* is about 7 dB.

As in Figure 4.10, at a certain primary link load, *MIMO OSS EE Opt* can achieve a higher EE than *MIMO USS EE Opt*, and the EE gain becomes constant at SNRs over

0 dB, which is about 0.1 bit/Hz/Joule at the load factor of 75% and SNR of 10 dB.

Numerical results show that MIMO overlay spectrum sharing with EE optimization can achieve a significantly higher EE compared with MIMO overlay spectrum sharing with rate optimization, at certain SNRs and with certain circuit power, at the cost of the achievable secondary rate, while saving the transmit power. In MIMO overlay spectrum sharing with EE optimization, both the achievable secondary rate and EE increase as the SNR increases, until a point when the growth rate of the secondary power surpasses that of the secondary rate, and the secondary EE reaches its maximum and stays unchanged thereafter; while the secondary EE decreases after that point in MIMO overlay spectrum sharing with rate optimization. It is also shown that MIMO overlay spectrum sharing with EE optimization can achieve a higher EE compared with MIMO underlay spectrum sharing with EE optimization.

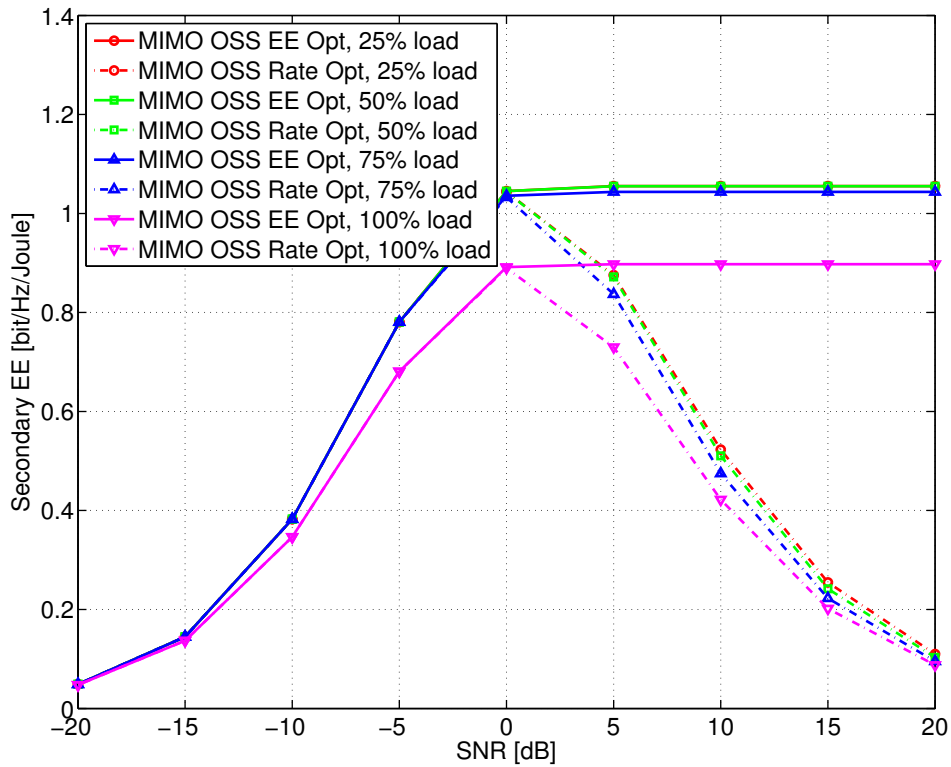


Figure 4.7.: Secondary EE versus SNR of the secondary link: *MIMO OSS EE Opt* versus *MIMO OSS Rate Opt* with different primary link loads.

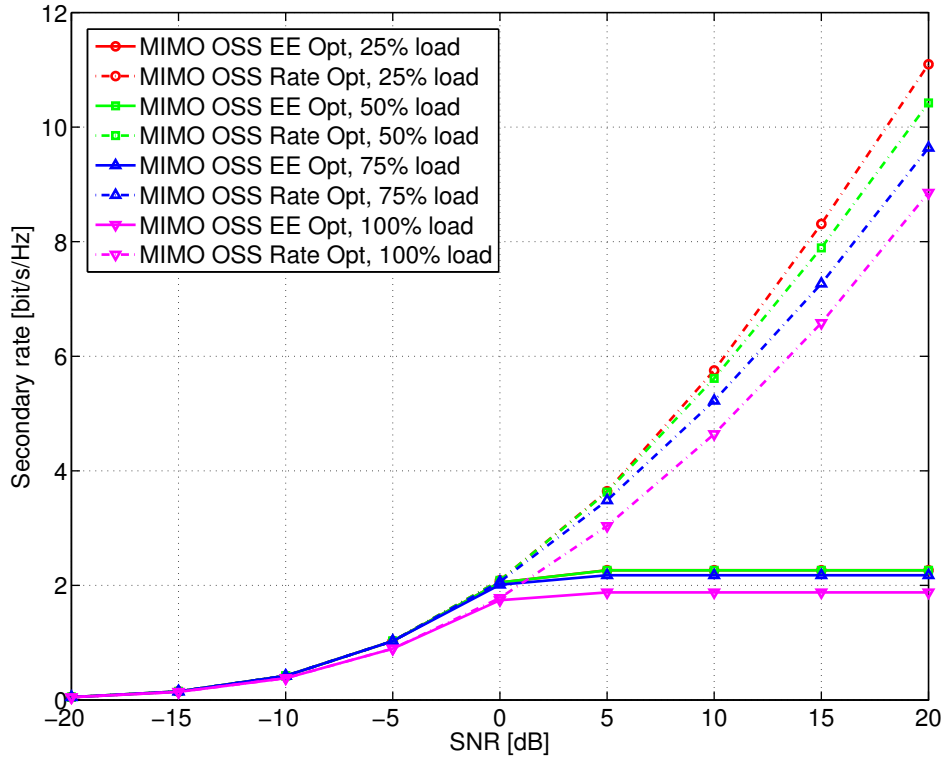


Figure 4.8.: Secondary rate versus SNR of the secondary link: *MIMO OSS EE Opt* versus *MIMO OSS Rate Opt* with different primary link loads.



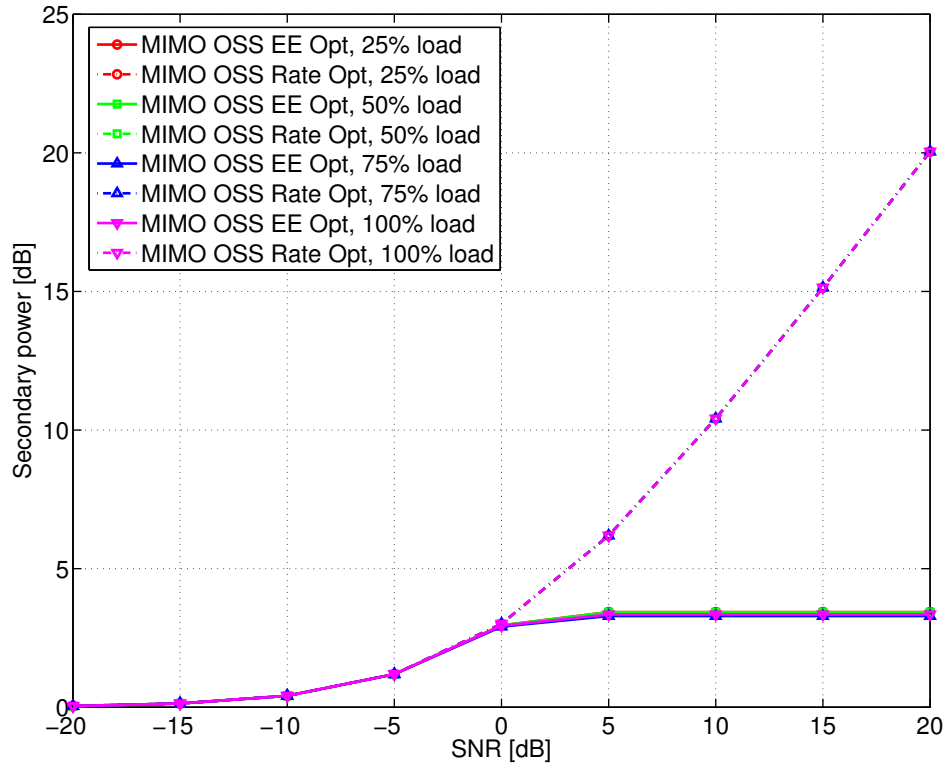


Figure 4.9.: Secondary power versus SNR of the secondary link: *MIMO OSS EE Opt* versus *MIMO OSS Rate Opt* with different primary link loads.

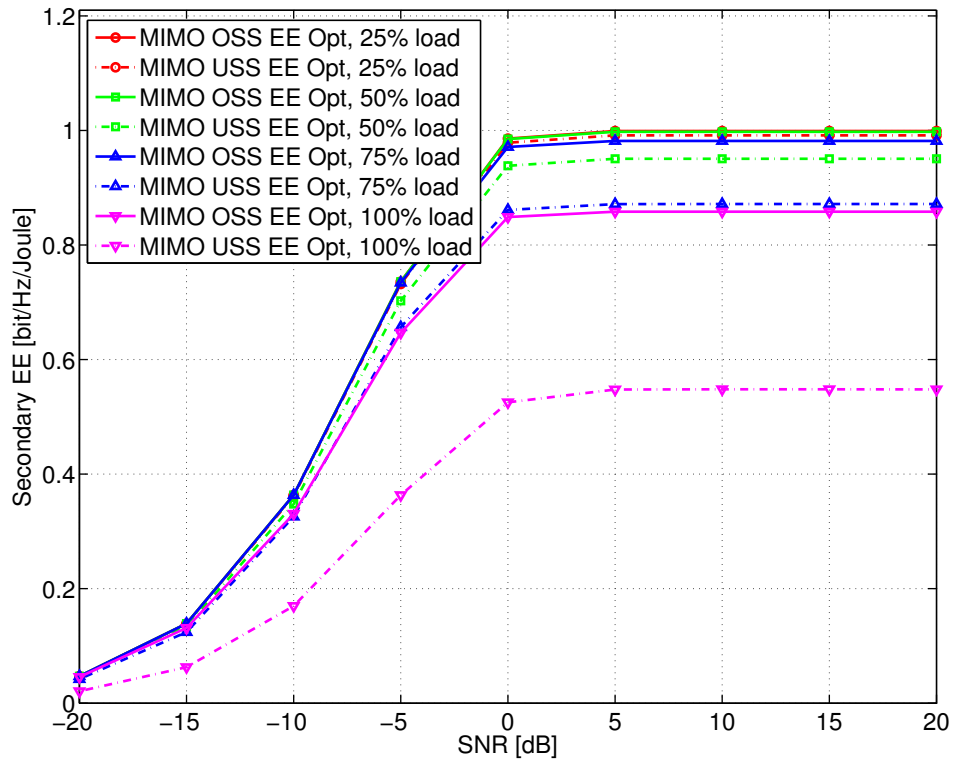


Figure 4.10.: Secondary EE versus SNR of the secondary link: *MIMO OSS EE Opt* versus *MIMO USS EE Opt* with different primary link loads.

### 4.3. Summary

The EE of a MIMO secondary link in underlay spectrum sharing is optimized with the primary rate requirement and the secondary power constraint. Three transmission strategies are introduced based on the primary rate requirement and the channel conditions. Rate splitting and successive decoding are deployed at the secondary transmitter and receiver, respectively, when it is feasible, and otherwise single-user decoding is deployed at the secondary receiver. For each case, a concave fractional program is solved by fractional programming, e.g., Dinkelbach's method, to obtain the optimal transmit covariance matrices. An additional line search is required for the case of intermediate primary rate requirement to obtain the optimal solution. Based on this, an energy-efficient resource allocation algorithm is proposed. Numerical results show that MIMO underlay spectrum sharing with EE optimization can achieve a significantly higher EE compared with MIMO underlay spectrum sharing with rate optimization, at certain SNRs and with certain circuit power, at the cost of the achievable secondary rate, while saving the transmit power. With rate splitting at the secondary transmitter and successive decoding at the secondary receiver if feasible, a significantly higher EE can be achieved compared with the case when only single-user decoding is deployed at the secondary receiver.

Moreover, the EE of a MIMO secondary link in overlay spectrum sharing is studied, where the secondary transmitter has non-causal knowledge of the primary message and employs DPC to obtain an interference-free secondary link. Energy-efficient precoding and power allocation is obtained to maximize the EE of the secondary transmission while satisfying the primary rate requirement and the secondary power constraint, through solving a concave fractional program by fractional programming. Numerical results show that MIMO overlay spectrum sharing with EE optimization can achieve a significantly higher EE compared with MIMO overlay spectrum sharing with rate optimization, at certain SNRs and with certain circuit power, at the cost of the achievable secondary rate, while saving the transmit power. MIMO overlay spectrum sharing with EE optimization can achieve a higher EE compared with the proposed MIMO underlay spectrum sharing with EE optimization.



# Chapter 5.

## Conclusions and Future Work

### 5.1. Conclusions

In this thesis, resource allocation in underlay and overlay spectrum sharing are investigated.

In underlay spectrum sharing, specifically, the coexistence of a MISO primary link and a MISO/MIMO secondary link is studied. The primary transmitter employs MRT, and single-user decoding is deployed at the primary receiver. Three scenarios are investigated, in terms of the interference from the primary transmitter to the secondary receiver, namely, weak interference, strong interference and very strong interference, or equivalently three ranges of primary rate requirement. Rate splitting and successive decoding are deployed at the secondary transmitter and receiver, respectively, when it is feasible, and otherwise single-user decoding is deployed at the secondary receiver. For each scenario, optimal beamforming/precoding and power allocation at the secondary transmitter is derived, to maximize the achievable secondary rate while satisfying the primary rate requirement and the secondary power constraint. In the case of MISO secondary channel, the beamforming vectors are parametrized with real-valued parameters, as the weighted sum of two channel-related vectors, which are the projections of the secondary channel into the space and null space of the channel from the secondary transmitter to the primary receiver, respectively; the secondary transmitter employs full power transmission. For the scenarios of weak and very strong interference, closed-form solutions are obtained; for the scenario of strong interference, a grid search is required to obtain the optimal solution. In the case of MIMO secondary channel, optimal transmit covariance matrices are obtained by solving corresponding convex optimization problems; the secondary transmitter employs full power transmission. An additional line search is required for the scenario of strong interference to obtain the optimal solution. Numerical results show that rate splitting at the secondary transmitter and successive decoding at the secondary receiver does significantly increase the achievable secondary

rate if feasible, compared with single-user decoding at the secondary receiver.

In overlay spectrum sharing, specifically, the coexistence of a MISO primary link and a MISO/MIMO secondary link is studied. The primary transmitter employs MRT, and single-user decoding is deployed at the primary receiver. When the secondary transmitter has non-causal knowledge of the primary message, DPC can be deployed at the secondary transmitter to precancel the interference (when decoding the secondary message at the secondary receiver), due to the transmission of the primary message from both transmitters. Optimal beamforming/precoding and power allocation at the secondary transmitter is obtained, to maximize the achievable secondary rate while satisfying the primary rate requirement and the secondary power constraint. In the case of MISO secondary channel, the beamforming vector for the primary message is MRT, and the beamforming vector for the secondary message has the same form of parametrization with one real-valued parameter, as those in the proposed MISO underlay spectrum sharing. The secondary transmitter employs full power transmission. A line search is required to obtain the optimal solution. In the case of MIMO secondary channel, the beamforming vector for the primary message is MRT, and the transmit covariance matrix for the secondary message is obtained by a line search while solving a convex optimization problem. The secondary transmitter employs full power transmission. Numerical results show that with non-causal knowledge of the primary message and the deployment of DPC at the secondary transmitter, overlay spectrum sharing can achieve a significantly higher secondary rate than the proposed underlay spectrum sharing.

Alternatively, due to the high implementation complexity of DPC, linear precoding can be deployed at the secondary transmitter. Optimal beamforming/precoding and power allocation at the secondary transmitter is obtained, to maximize the achievable secondary rate while satisfying the primary rate requirement and the secondary power constraint. In the case of MISO secondary channel, the beamforming vector for the primary message is parametrized with three real-valued parameters, as the weighted sum of two channel-related vectors, which are the projections of the channel from the secondary transmitter to the primary receiver in the space and null space of the secondary channel, respectively. The beamforming vector for the secondary message has the same form of parametrization with one real-valued parameter, as that when DPC is deployed at the secondary transmitter. The secondary transmitter employs full power transmission. A cubic search is required to obtain the optimal solution. In the case of MIMO secondary channel, an iterative transceiver design algorithm is proposed, where the secondary transmitter employs single-stream transmission for its own message and MMSE receiver is deployed at the secondary receiver. In each iteration, an optimiza-

tion problem is solved to obtain the optimal beamforming and power allocation at the secondary transmitter, with respect to a given secondary receiver, by the solution for the proposed MISO overlay spectrum sharing with linear precoding at the secondary transmitter. The iterative algorithm converges though not guaranteed to achieve the global optimum. A good solution can be selected by several random initializations. The secondary transmitter employs full power transmission. Numerical results show that rate loss occurs with the deployment of linear precoding instead of DPC at the secondary transmitter.

When the secondary transmitter does not have non-causal knowledge of the primary message, and still wants to help with the primary transmission in return for the access to the spectrum, it can relay the primary message in an AF or a DF way in a two-phase transmission, while transmitting its own message. The AF cooperative spectrum sharing between a MISO primary link and a MIMO secondary link is studied. To fulfill its rate requirement, the primary link has the incentive to adapt the transmission strategies in the two phases, namely, the primary transmitter employs MRT, and the primary receiver applies MRC to the received signals in the two phases. The secondary transmitter employs an AF relaying matrix for the primary message and single-stream transmission for its own message, and MMSE receiver is deployed at the secondary receiver in the second phase. An iterative transceiver design algorithm is proposed, to maximize the achievable secondary rate while satisfying the primary rate requirement and the secondary power constraint. In each iteration, an optimization problem is solved to obtain the optimal relaying matrix and beamforming vector, with respect to a given secondary receiver, by a bisection search through a sequence of second-order cone programming feasibility problems. The iterative algorithm converges though is not guaranteed to achieve the global optimum. A good solution can be selected by several random initializations. The secondary transmitter employs full power transmission in the second phase. For this setup, an alternative heuristic solution is proposed. Given the secondary receiver, the relaying matrix for the primary message is parametrized with two real-valued parameters, and has the structure of the outer product of two channel-related vectors. One is the MRC receiver for the primary signal with respect to the effective channel between the two transmitters. And the other is parametrized with one real-valued parameter, as the weighted sum of two channel-related vectors, which are the projections of the channel from the secondary transmitter to the primary receiver into the space and null space of the effective secondary channel, respectively. Moreover, given the secondary receiver and the relaying matrix for the primary message, the beamforming vector for the secondary message is parametrized with one real-valued parameter, as the weighted

sum of two channel-related vectors, which are the projections of the effective secondary channel into the space and null space of the channel from the secondary transmitter to the primary receiver, respectively. An iterative transceiver design algorithm is proposed, where in each iteration, a grid search is performed to obtain the optimal relaying matrix and beamforming vector, with respect to a given secondary receiver. The iterative algorithm converges though not guaranteed to achieve the global optimum. A good solution can be selected by several random initializations. The secondary transmitter employs full power transmission in the second phase. Numerical results show that with the cooperation from the secondary link, the primary link can avoid outage effectively, especially when the number of antennas at the secondary transceiver is large, while the secondary link can achieve a significant rate.

The DF cooperative spectrum sharing between a MISO primary link and a MIMO secondary link is studied, where the secondary transmitter tries to decode the primary message in the first phase, and if successful, helps transmit the primary message besides its own message in the second phase. To fulfill its rate requirement, the primary link has the incentive to adapt the transmission strategies in the two phases, namely, the primary transmitter employs multiple-stream transmission in the first phase, to facilitate the decoding of the primary message at the secondary transmitter, and MRT to facilitate its own transmission in the second phase. The secondary transmitter employs DPC to obtain an interference-free secondary link in the second phase. The achievable secondary rate is maximized while satisfying the decodability condition of the primary message at the secondary transmitter, the primary rate requirement and the primary and secondary power constraints. A set of parameters are optimized, including relative duration of the two phases, primary transmission strategies in the two phases and secondary transmission strategy in the second phase. Properties of the parameters are studied to reduce the computational complexity of the optimization problem. A cubic search is required to obtain the optimal transmission strategies. Given the relative duration of the first phase and the power spent in the first phase by the primary transmitter, the primary transmit covariance matrix in the first phase is obtained, by balancing between the maximization of the received SNR at the primary receiver and that of the channel capacity from the primary transmitter to the secondary transmitter. After that, the secondary transmit covariance matrix in the second phase is obtained, by a line search over the power spent for the transmission of the primary message, while solving a corresponding convex optimization problem. The primary transmitter employs full power transmission in the two phases. The secondary transmitter employs full power transmission in the second phase. The optimal choice of parameters is the one that yields the largest secondary



rate. Numerical results show that with the cooperation from the secondary link, the primary link can avoid outage effectively, especially when the number of antennas at the secondary transmitter is large, while the secondary link can achieve a significant rate.

Moreover, the EE of a MIMO secondary link in underlay spectrum sharing is optimized with the primary rate requirement and the secondary power constraint. Three transmission strategies are introduced based on the primary rate requirement and the channel conditions. Rate splitting and successive decoding are deployed at the secondary transmitter and receiver, respectively, when it is feasible, and otherwise single-user decoding is deployed at the secondary receiver. For each case, the original non-convex fractional problem is reformulated into a concave fractional program, which can be efficiently solved by fractional programming, e.g., Dinkelbach's method, to obtain the optimal transmit covariance matrices. An additional line search is required for the case of intermediate primary rate requirement to obtain the optimal solution. Based on this, an energy-efficient resource allocation algorithm is proposed. Numerical results show that MIMO underlay spectrum sharing with EE optimization can achieve a significantly higher EE compared with MIMO underlay spectrum sharing with rate optimization, at certain SNRs and with certain circuit power, at the cost of the achievable secondary rate, while saving the transmit power. With rate splitting at the secondary transmitter and successive decoding at the secondary receiver if feasible, a significantly higher EE can be achieved compared with the case when only single-user decoding is deployed at the secondary receiver.

Furthermore, the EE of a MIMO secondary link in overlay spectrum sharing is maximized with the primary rate requirement and the secondary power constraint. The secondary transmitter has non-causal knowledge of the primary message and employs DPC to obtain an interference-free secondary link. The beamforming vector for the primary message is MRT, and the transmit covariance matrix for the secondary message is obtained through solving a concave fractional program by fractional programming. Numerical results show that MIMO overlay spectrum sharing with EE optimization can achieve a significantly higher EE compared with MIMO overlay spectrum sharing with rate optimization, at certain SNRs and with certain circuit power, at the cost of the achievable secondary rate, while saving the transmit power. MIMO overlay spectrum sharing with EE optimization can achieve a higher EE compared with the proposed MIMO underlay spectrum sharing with EE optimization.

## 5.2. Future Work

In this thesis, the system models in underlay and overlay spectrum sharing with rate or EE optimization involve a MISO primary link, and the related results apply to the scenarios of a MIMO primary link with a fixed receiver. Nevertheless, the extension to the scenario of a MIMO primary link with a general receiver is interesting and challenging for future work. In the case of a MISO primary link, the primary interference constraint or the primary rate requirement can be imposed, and both are convex constraints. In the case of a MIMO primary link, the primary interference constraint can be total or peak interference constraint [SPPF09], which is convex; while the primary rate requirement is nonconvex, which makes the optimization problem difficult to solve.

In this thesis, full channel state information is assumed in the system models, which is difficult to obtain in practice, especially the channel from the secondary transmitter to the primary receiver, since the primary link is usually assumed to be oblivious of the existence of the secondary link. It is necessary to discuss about the channel acquisition, e.g., using channel feedback or channel reciprocity/calibration in time division duplexing mode, and investigate the scenarios with partial or imperfect channel state information.

In this thesis, the coexistence of one primary link and one secondary link is considered. The extensions to the scenario of multiple secondary links and/or multiple primary links and the scenario of multi-carrier transmission are potential future work. The EE optimization of the secondary transmission in these scenarios can be further investigated.

# Appendix A.

## Further Contributions

During my Ph.D. studies, I have contributed to other publications which have not been included in this thesis. The reason for not including the corresponding contributions is to focus on the system models of the coexistence of a MISO primary link and a MISO/MIMO secondary link. The further contributions are listed below.

In [JL11], the coexistence of a SISO primary link and a secondary MIMO multiple access channel is studied. The primary rate requirement is transformed into an interference constraint profile with individual interference constraints for the secondary users. By spatial shaping (linear precoding), an iterative algorithm is proposed to optimize the sum capacity of the secondary MIMO multiple access channel, in which each secondary user updates its transmit strategy while the transmit strategies of the other secondary users are fixed. The optimal single-user transmit strategy is obtained by comparing the achievable rate of two iterative algorithms, where transmit covariance matrix with either rank-one or rank-larger-than-one is optimized.

In [KSL<sup>+</sup>12], the sum-rate maximization of two-user MIMO secondary interference channel in the presence of a MIMO primary link is studied. The maximum interference induced at the primary receiver is limited by a spectrum mask or an interference constraint at the secondary transmitters. The Vickrey-Clarke-Groves theory is applied to find the so-called correlated equilibrium that corresponds to the playing strategies for the two secondary users. The regret-matching algorithm is implemented to find the optimal playing strategies for the two secondary users. A new cost function is proposed that allows the fast convergence of the developed solutions to the optimal or sub-optimal point.

In [BSLT<sup>+</sup>12], the cooperative spectrum sharing of a SISO primary link and a MISO secondary link is studied. The secondary transmitter relays the primary message in a DF way in a two-phase transmission, while transmitting its own message. The primary link adapts its transmission strategy and cooperates with the secondary link to fulfill

its rate requirement. To maximize the achievable secondary rate while satisfying the primary rate requirement and the primary and secondary power constraints, a set of parameters are optimized, including relative duration of the two phases, primary power allocation in the two phases and secondary beamforming and power allocation in the second phase. Different from [BSLT<sup>+</sup>12], where DPC is deployed at the secondary transmitter in the secondary phase to obtain an interference-free secondary link, linear precoding is deployed with lower complexity in [LBSJT12].

- [BSLT<sup>+</sup>12] R. Blasco-Serrano, J. Lv, R. Thobaben, E. Jorswieck, A. Kliks, and M. Skoglund, “Comparison of underlay and overlay spectrum sharing strategies in MISO cognitive channels,” in *International ICST Conference on Cognitive Radio Oriented Wireless Networks and Communications (CROWNCOM)*, Jun. 2012.
- [JL11] E. Jorswieck and J. Lv, “Spatial shaping in cognitive MIMO MAC with coded legacy transmission,” in *IEEE International Workshop on Signal Processing Advances in Wireless Communications (SPAWC)*, Jun. 2011.
- [KSL<sup>+</sup>12] A. Kliks, P. Sroka, J. Lv, E. Jorswieck, R. Blasco-Serrano, and R. Thobaben, “Crystallized rate regions in the secondary interference channels,” in *International ITG Workshop on Smart Antennas (WSA)*, Mar. 2012.
- [LBSJT12] J. Lv, R. Blasco-Serrano, E. Jorswieck, and R. Thobaben, “Linear precoding in MISO cognitive channels with causal primary message,” in *International Symposium on Wireless Communication Systems (ISWCS)*, Aug. 2012.

# Bibliography

- [ASW12] H. Al-Shatri and T. Weber, “Achieving the maximum sum rate using D.C. programming in cellular networks,” *IEEE Transactions on Signal Processing*, vol. 60, no. 3, pp. 1331–1341, Mar. 2012.
- [BH02] J. C. Bezdek and R. J. Hathaway, “Some notes on alternating optimization,” in *Advances in Soft Computing – AFSS 2002*, ser. Lecture Notes in Computer Science. Springer Berlin Heidelberg, 2002, vol. 2275, pp. 288–300.
- [BL11] E.-V. Belmega and S. Lasaulce, “Energy-efficient precoding for multiple-antenna terminals,” *IEEE Transactions on Signal Processing*, vol. 59, no. 1, pp. 329–340, Jan. 2011.
- [BOO<sup>+</sup>10] L. Bixio, G. Oliveri, M. Ottonello, M. Raffetto, and C. S. Regazzoni, “Cognitive radios with multiple antennas exploiting spatial opportunities,” *IEEE Transactions on Signal Processing*, vol. 58, no. 8, pp. 4453–4459, Aug. 2010.
- [BSLT<sup>+</sup>13] R. Blasco-Serrano, J. Lv, R. Thobaben, E. A. Jorswieck, and M. Skoglund, “Multi-antenna transmission for underlay and overlay cognitive radio with explicit message learning phase,” *EURASIP Journal on Wireless Communications and Networking (JWCN)*, special issue on Cooperative Cognitive Networks, 2013.
- [BV04] S. Boyd and L. Vandenberghe, *Convex Optimization*. Cambridge University Press, Mar. 2004.
- [Car78] A. Carleial, “Interference channels,” *IEEE Transactions on Information Theory*, vol. 24, no. 1, pp. 60–70, Jan. 1978.
- [CG79] T. Cover and A. Gamal, “Capacity theorems for the relay channel,” *IEEE Transactions on Information Theory*, vol. 25, no. 5, pp. 572–584, Sep. 1979.

## Bibliography

- [CJ08] V. Cadambe and S. Jafar, “Interference alignment and degrees of freedom of the K -user interference channel,” *IEEE Transactions on Information Theory*, vol. 54, no. 8, pp. 3425–3441, Aug. 2008.
- [CJC09] S. W. Choi, S. Jafar, and S.-Y. Chung, “On the beamforming design for efficient interference alignment,” *IEEE Communications Letters*, vol. 13, no. 11, pp. 847–849, Nov. 2009.
- [CJS13] P. Cao, E. Jorswieck, and S. Shi, “Pareto boundary of the rate region for single-stream MIMO interference channels: Linear transceiver design,” *IEEE Transactions on Signal Processing*, vol. 61, no. 20, pp. 4907–4922, Oct. 2013.
- [Cos83] M. Costa, “Writing on dirty paper (corresp.),” *IEEE Transactions on Information Theory*, vol. 29, no. 3, pp. 439–441, May 1983.
- [Cov72] T. Cover, “Broadcast channels,” *IEEE Transactions on Information Theory*, vol. 18, no. 1, pp. 2–14, Jan. 1972.
- [CS03] G. Caire and S. Shamai (Shitz), “On the achievable throughput of a multi-antenna Gaussian broadcast channel,” *IEEE Transactions on Information Theory*, vol. 49, no. 7, pp. 1691–1706, Jul. 2003.
- [CT06] T. M. Cover and J. A. Thomas, *Elements of Information Theory*. Wiley, 2006.
- [CTKS14] M. Cardone, D. Tuninetti, R. Knopp, and U. Salim, “On the gaussian interference channel with half-duplex causal cognition,” *IEEE Journal on Selected Areas in Communications*, vol. 32, no. 11, Nov. 2014.
- [CWO10] D. Chatterjee, T. Wong, and O. Oyman, “On achievable rate regions for half-duplex causal cognitive radio channels,” in *IEEE International Symposium on Information Theory (ISIT)*, Jun. 2010.
- [DC01] S. Diggavi and T. Cover, “The worst additive noise under a covariance constraint,” *IEEE Transactions on Information Theory*, vol. 47, no. 7, pp. 3072–3081, Nov. 2001.
- [Din67] W. Dinkelbach, “On nonlinear fractional programming,” *Management Science*, vol. 13, no. 7, pp. 492–498, 1967.

- [DMT06] N. Devroye, P. Mitran, and V. Tarokh, “Achievable rates in cognitive radio channels,” *IEEE Transactions on Information Theory*, vol. 52, no. 5, pp. 1813–1827, May 2006.
- [DWA09] S. Deng, T. Weber, and A. Ahrens, “Capacity optimizing power allocation in interference channels,” *AEÜ - International Journal of Electronics and Communications*, vol. 63, no. 2, pp. 139–147, 2009.
- [ETW08] R. Etkin, D. Tse, and H. Wang, “Gaussian interference channel capacity to within one bit,” *IEEE Transactions on Information Theory*, vol. 54, no. 12, pp. 5534–5562, Dec. 2008.
- [FAAEBP14] Y. Fadlallah, K. Amis, A. Aïssa-El-Bey, and R. Pyndiah, “Interference alignment for a multi-user SISO interference channel,” *EURASIP Journal on Wireless Communications and Networking*, 2014.
- [Fed02] Federal Communications Commission, “Spectrum policy task force,” Tech. Rep. ET Docket no. 02-135, Nov. 2002.
- [FJL<sup>+</sup>13] D. Feng, C. Jiang, G. Lim, J. Cimini, L.J., G. Feng, and G. Li, “A survey of energy-efficient wireless communications,” *IEEE Communications Surveys & Tutorials*, vol. 15, no. 1, pp. 167–178, 2013.
- [GJMS09] A. Goldsmith, S. Jafar, I. Maric, and S. Srinivasa, “Breaking spectrum gridlock with cognitive radios: An information theoretic perspective,” *Proceedings of the IEEE*, vol. 97, no. 5, pp. 894–914, May 2009.
- [Hay05] S. Haykin, “Cognitive radio: Brain-empowered wireless communications,” *IEEE Journal on Selected Areas in Communications*, vol. 23, no. 2, pp. 201–220, Feb. 2005.
- [HHYO14] S. He, Y. Huang, L. Yang, and B. Ottersten, “Coordinated multicell multiuser precoding for maximizing weighted sum energy efficiency,” *IEEE Transactions on Signal Processing*, vol. 62, no. 3, pp. 741–751, Feb. 2014.
- [HK81] T. Han and K. Kobayashi, “A new achievable rate region for the interference channel,” *IEEE Transactions on Information Theory*, vol. 27, no. 1, pp. 49–60, Jan. 1981.
- [HLDV09] E. Hossain, L. Le, N. Devroye, and M. Vu, “*Cognitive radio: from theory to practical network engineering*” in *New directions in wireless communications research*. Springer, 2009, ch. 10, pp. 251–289.

## Bibliography

- [HMZ05] A. Host-Madsen and J. Zhang, “Capacity bounds and power allocation for wireless relay channels,” *IEEE Transactions on Information Theory*, vol. 51, no. 6, pp. 2020–2040, Jun. 2005.
- [HPT09] Y. Han, A. Pandharipande, and S. H. Ting, “Cooperative decode-and-forward relaying for secondary spectrum access,” *IEEE Transactions on Wireless Communications*, vol. 8, no. 10, pp. 4945–4950, Oct. 2009.
- [HT13a] G. Huang and J. Tugnait, “On energy efficient MIMO-assisted spectrum sharing for cognitive radio networks,” in *IEEE International Conference on Communications (ICC)*, Jun. 2013.
- [HT13b] —, “On precoding for maximum weighted energy efficiency of MIMO cognitive multiple access channels,” in *IEEE Global Communications Conference (GLOBECOM)*, Dec. 2013.
- [HZBLG11] K. Hamdi, K. Zarifi, K. Ben Letaief, and A. Ghrayeb, “Beamforming in relay-assisted cognitive radio systems: A convex optimization approach,” in *IEEE International Conference on Communications (ICC)*, Jun. 2011.
- [ICJF12] C. Isheden, Z. Chong, E. Jorswieck, and G. Fettweis, “Framework for link-level energy efficiency optimization with informed transmitter,” *IEEE Transactions on Wireless Communications*, vol. 11, no. 8, pp. 2946–2957, 2012.
- [JC13] —, “Energy-efficient transmission for MIMO interference channels,” *IEEE Transactions on Wireless Communications*, vol. 12, no. 6, pp. 2988–2999, Jun. 2013.
- [JDI<sup>+</sup>13] J. Jiang, M. Dianati, M. Imran, R. Tafazolli, and Y. Chen, “On the relation between energy efficiency and spectral efficiency of multiple-antenna systems,” *IEEE Transactions on Vehicular Technology*, vol. 62, no. 7, pp. 3463–3469, Sep. 2013.
- [JL10] E. Jorswieck and E. Larsson, “Monotonic optimization framework for the two-user MISO interference channel,” *IEEE Transactions on Communications*, vol. 58, no. 7, pp. 2159–2168, Jul. 2010.
- [JLD08] E. A. Jorswieck, E. G. Larsson, and D. Danev, “Complete characterization of the Pareto boundary for the MISO interference channel,” *IEEE*



*Transactions on Signal Processing*, vol. 56, no. 10, pp. 5292–5296, Oct. 2008.

- [JV09] A. Jovicic and P. Viswanath, “Cognitive radio: An information-theoretic perspective,” *IEEE Transactions on Information Theory*, vol. 55, no. 9, pp. 3945–3958, Sep. 2009.
- [JX08] J. Jiang and Y. Xin, “On the achievable rate regions for interference channels with degraded message sets,” *IEEE Transactions on Information Theory*, vol. 54, no. 10, pp. 4707–4712, Oct. 2008.
- [KGG05] G. Kramer, M. Gastpar, and P. Gupta, “Cooperative strategies and capacity theorems for relay networks,” *IEEE Transactions on Information Theory*, vol. 51, no. 9, pp. 3037–3063, Sep. 2005.
- [KL10] E. Karipidis and E. Larsson, “Efficient computation of the Pareto boundary for the MISO interference channel with perfect CSI,” in *International Symposium on Modeling and Optimization in Mobile, Ad Hoc and Wireless Networks (WiOpt)*, May 2010.
- [LBSJ<sup>+</sup>12] J. Lv, R. Blasco-Serrano, E. Jorswieck, R. Thobaben, and A. Kliks, “Optimal beamforming in MISO cognitive channels with degraded message sets,” in *IEEE Wireless Communications and Networking Conference (WCNC)*, Apr. 2012.
- [LJ11] J. Lv and E. A. Jorswieck, “Spatial shaping in cognitive system with coded legacy transmission,” in *International ITG Workshop on Smart Antennas (WSA)*, Feb. 2011.
- [LJ14] —, “Transmission strategies for MIMO overlay spectrum sharing,” in *International ITG Workshop on Smart Antennas (WSA)*, Mar. 2014.
- [LJBS<sup>+</sup>12] J. Lv, E. Jorswieck, R. Blasco-Serrano, R. Thobaben, and A. Kliks, “Linear precoding in MISO cognitive channels with degraded message sets,” in *International ITG Workshop on Smart Antennas (WSA)*, Mar. 2012.
- [LKL11] J. Lindblom, E. Karipidis, and E. Larsson, “Closed-form parameterization of the Pareto boundary for the two-user MISO interference channel,” in *IEEE International Conference on Acoustics, Speech and Signal Processing (ICASSP)*, May 2011.

## Bibliography

- [LKL13] —, “Efficient computation of Pareto optimal beamforming vectors for the MISO interference channel with successive interference cancellation,” *IEEE Transactions on Signal Processing*, vol. 61, no. 19, pp. 4782–4795, Oct. 2013.
- [LKPR11] L. Li, F. Khan, M. Pesavento, and T. Ratnarajah, “Power allocation and beamforming in overlay cognitive radio systems,” in *IEEE Vehicular Technology Conference (VTC Spring)*, May 2011.
- [LTW04] J. Laneman, D. Tse, and G. W. Wornell, “Cooperative diversity in wireless networks: Efficient protocols and outage behavior,” *IEEE Transactions on Information Theory*, vol. 50, no. 12, pp. 3062–3080, Dec. 2004.
- [LWZ<sup>+</sup>12] J. Li, D. Wang, P. Zhu, L. Tang, and X. You, “Closed-form solutions to the Pareto boundary and optimal distributed strategy for the two-user MISO interference channel,” in *International Conference on Wireless Communications Signal Processing (WCSP)*, Oct. 2012.
- [LZJ14] J. Lv, A. Zappone, and E. A. Jorswieck, “Energy-efficient MIMO underlay spectrum sharing with rate splitting,” in *IEEE International Workshop on Signal Processing Advances in Wireless Communications (SPAWC)*, Jun. 2014.
- [MCJ14] R. Mochaourab, P. Cao, and E. Jorswieck, “Alternating rate profile optimization in single stream MIMO interference channels,” *IEEE Signal Processing Letters*, vol. 21, no. 2, pp. 221–224, Feb. 2014.
- [MGKS08] I. Marić, A. Goldsmith, G. Kramer, and S. Shamai (Shitz), “On the capacity of interference channels with one cooperating transmitter,” *European Transactions on Telecommunications*, vol. 19, no. 4, pp. 405–420, Apr. 2008.
- [Mia13] G. Miao, “Energy-efficient uplink multi-user MIMO,” *IEEE Transactions on Wireless Communications*, vol. 12, no. 5, pp. 2302–2313, May 2013.
- [Mit00] J. Mitola, “Cognitive radio: An integrated agent architecture for software defined radio,” Ph.D. dissertation, KTH Royal Institute of Technology, Sweden, May 2000.
- [MJ11] R. Mochaourab and E. Jorswieck, “Optimal beamforming in interference

- networks with perfect local channel information,” *IEEE Transactions on Signal Processing*, vol. 59, no. 3, pp. 1128–1141, Mar. 2011.
- [MJ12] ———, “Exchange economy in two-user multiple-input single-output interference channels,” *IEEE Journal of Selected Topics in Signal Processing*, vol. 6, no. 2, pp. 151–164, Apr. 2012.
- [MLLV11] R. Manna, R. H. Y. Louie, Y. Li, and B. Vucetic, “Cooperative spectrum sharing in cognitive radio networks with multiple antennas,” *IEEE Transactions on Signal Processing*, vol. 59, no. 11, pp. 5509–5522, Nov. 2011.
- [MOA11] A. W. Marshall, I. Olkin, and B. C. Arnold, *Inequalities: Theory of Majorization and Its Application*. Springer, 2011.
- [MYK07] I. Maric, R. Yates, and G. Kramer, “Capacity of interference channels with partial transmitter cooperation,” *IEEE Transactions on Information Theory*, vol. 53, no. 10, pp. 3536–3548, Oct. 2007.
- [PS13] J. Park and Y. Sung, “On the Pareto-optimal beam structure and design for multi-user MIMO interference channels,” *IEEE Transactions on Signal Processing*, vol. 61, no. 23, pp. 5932–5946, Dec. 2013.
- [QZH09] L. P. Qian, Y. Zhang, and J. Huang, “MAPEL: Achieving global optimality for a non-convex wireless power control problem,” *IEEE Transactions on Wireless Communications*, vol. 8, no. 3, pp. 1553–1563, Mar. 2009.
- [QZLC11] J. Qiu, R. Zhang, Z.-Q. Luo, and S. Cui, “Optimal distributed beamforming for miso interference channels,” *IEEE Transactions on Signal Processing*, vol. 59, no. 11, pp. 5638–5643, Nov. 2011.
- [RG13] S. Rini and A. Goldsmith, “On the capacity of the MIMO cognitive interference channel,” in *IEEE International Symposium on Information Theory (ISIT)*, Jul. 2013.
- [RTD11] S. Rini, D. Tuninetti, and N. Devroye, “New inner and outer bounds for the memoryless cognitive interference channel and some new capacity results,” *IEEE Transactions on Information Theory*, vol. 57, no. 7, pp. 4087–4109, Jul. 2011.

## Bibliography

- [RTD12] —, “Inner and outer bounds for the gaussian cognitive interference channel and new capacity results,” *IEEE Transactions on Information Theory*, vol. 58, no. 2, pp. 820–848, Feb. 2012.
- [Sch83] S. Schaible, “Fractional programming,” *Zeitschrift für Operations Research*, vol. 27, no. 1, pp. 39–54, 1983.
- [SHL13] S. Song, M. Hasna, and K. Letaief, “Prior zero forcing for cognitive relaying,” *IEEE Transactions on Wireless Communications*, vol. 12, no. 2, pp. 938–947, Feb. 2013.
- [SJXW09] S. Seyedmehdi, J. Jiang, Y. Xin, and X. Wang, “An improved achievable rate region for causal cognitive radio,” in *IEEE International Symposium on Information Theory (ISIT)*, Jun. 2009.
- [SK11] E.-H. Shin and D. Kim, “Time and power allocation for collaborative primary-secondary transmission using superposition coding,” *IEEE Communications Letters*, vol. 15, no. 2, pp. 196–198, Feb. 2011.
- [SPPF09] G. Scutari, D. Palomar, J.-S. Pang, and F. Facchinei, “Flexible design of cognitive radio wireless systems,” *IEEE Signal Processing Magazine*, vol. 26, no. 5, pp. 107–123, Sep. 2009.
- [SV08] S. Sridharan and S. Vishwanath, “On the capacity of a class of MIMO cognitive radios,” *IEEE Journal of Selected Topics in Signal Processing*, vol. 2, no. 1, pp. 103–117, Feb. 2008.
- [SY04] S. Serbetli and A. Yener, “Transceiver optimization for multiuser MIMO systems,” *IEEE Transactions on Signal Processing*, vol. 52, no. 1, Jan. 2004.
- [TV05] D. Tse and P. Viswanath, *Fundamentals of Wireless Communication*. Cambridge University Press, 2005.
- [VLDE13] V. Varma, S. Lasaulce, M. Debbah, and S. Elayoubi, “An energy-efficient framework for the analysis of MIMO slow fading channels,” *IEEE Transactions on Signal Processing*, vol. 61, no. 10, pp. 2647–2659, May 2013.
- [WSS06] H. Weingarten, Y. Steinberg, and S. Shamai (Shitz), “The capacity region of the Gaussian multiple-input multiple-output broadcast channel,” *IEEE Transactions on Information Theory*, vol. 52, no. 9, pp. 3936–3964, Sep. 2006.

- [WV13] Z. Wu and M. Vu, “A half-duplex transmission scheme for the gaussian causal cognitive interference channel,” in *IEEE International Conference on Communications (ICC)*, Jun. 2013.
- [WVA07] W. Wu, S. Vishwanath, and A. Arapostathis, “Capacity of a class of cognitive radio channels: Interference channels with degraded message sets,” *IEEE Transactions on Information Theory*, vol. 53, no. 11, pp. 4391–4399, Nov. 2007.
- [XQ13] J. Xu and L. Qiu, “Energy efficiency optimization for MIMO broadcast channels,” *IEEE Transactions on Wireless Communications*, vol. 12, no. 2, pp. 690–701, Feb. 2013.
- [ZC10] R. Zhang and S. Cui, “Cooperative interference management with MISO beamforming,” *IEEE Transactions on Signal Processing*, vol. 58, no. 10, pp. 5450–5458, Oct. 2010.
- [ZJZ09] Q. Zhang, J. Jia, and J. Zhang, “Cooperative relay to improve diversity in cognitive radio networks,” *IEEE Communications Magazine*, vol. 47, no. 2, pp. 111–117, Feb. 2009.
- [ZL08] R. Zhang and Y.-C. Liang, “Exploiting multi-antennas for opportunistic spectrum sharing in cognitive radio networks,” *IEEE Journal on Selected Topics in Signal Processing*, vol. 2, no. 1, pp. 88–102, Feb. 2008.
- [ZLC10] R. Zhang, Y.-C. Liang, and S. Cui, “Dynamic resource allocation in cognitive radio networks,” *IEEE Signal Processing Magazine*, vol. 27, no. 3, pp. 102–114, May 2010.
- [ZM10] W. Zhang and U. Mitra, “Spectrum shaping: a new perspective on cognitive radio-part I: coexistence with coded legacy transmission,” *IEEE Transactions on Communications*, vol. 58, no. 6, pp. 1857–1867, Jun. 2010.
- [ZSWO13] G. Zheng, S. Song, K.-K. Wong, and B. Ottersten, “Cooperative cognitive networks: Optimal, distributed and low-complexity algorithms,” *IEEE Transactions on Signal Processing*, vol. 61, no. 11, pp. 2778–2790, Jun. 2013.